MSc. Thesis

RTC strategy reducing the ecological impact of an urban drainage system

By

Sophie Brevoord

July 2022

This page is intentionally left blank

RTC strategy reducing the ecological impact of an urban drainage system

By

Sophie Louise Brevoord

In partial fulfillment of the requirements for the degree of

Master of Science
in Water Management

at the Delft University of Technology,
to be defended publicly on Thursday, July 14, 2022, at 09:00 AM.

Student number: 4737199
Supervisors:
Dr. Ir. Jeroen Langeveld   TU Delft, Sanitary Engineering
Ir. Job van der Werf   TU Delft, Sanitary Engineering

Thesis committee:
Dr. Ir. Edo Abraham   TU Delft, Water Resource Management
Prof. Dr. Zoran Kapelan   TU Delft, Sanitary Engineering
Dr. Ir. Petra van Daal-Rombouts Waterschap De Dommel

This page is intentionally left blank

Abstract

Urban wastewater systems can impact the urban ecology by untreated wastewater discharges through combined sewer overflow (CSO) events, or by partial treatment of the wastewater at the wastewater treatment plant (WWTP). CSO events can cause oxygen depletion, eutrophication, and the discharge of pathogens. The partial treatment of the wastewater causes an increased concentration of ammonium in the WWTP effluent, which can lead to toxic ammonium levels in the receiving river water. These problems can be (partially) mitigated by optimizing the existing infrastructure. Optimization of the available storage will help handle the increased pressure on the urban drainage system (UDS) and the stricter environmental regulations simultaneously.

A method to control the dynamic performance of the combined sewer system is Real-Time Control (RTC). A RTC strategy controls the combined sewer system dynamically based on real-time information about the system state. This research aims to develop a RTC strategy that decreases the negative ecological impact of the combined sewer system on the river by optimizing the available in-sewer volume. By doing so, the objectives to reduce the total amount of spilled CSO volume and to decrease the ammonium peaks towards the WWTP should be met. This research is applied to the case study of Geldrop-Mierlo, this is a municipality located in the UDS of Eindhoven. The trade-off between those two objectives was explored in the Wastewater Process simulator WEST. Rainfall events with a maximum intensity of 3.1 mm/hr and higher or rainfall events with maximum intensity < 3 mm/hr and total rainfall depth of > 4.8 mm, were found to be more likely to cause DO dips. The objective function which is used in the optimization process is dependent on the forecasted rainfall and the trade-off described above.

The UDS is modeled in a full-hydrodynamic (FH) model and a simplified conceptual model. The conceptual model is made to reduce the computation time. The catchment of the FH model is split up into 3 different catchments, that each are modelled as a reservoir in the conceptual model. The characteristics of each reservoir are dependent on the characteristics of these catchments in the FH model. The characteristics that are included are: storage curve, outflow dynamics, and CSO dynamics. Both models are calibrated and validated.
The UDS is controlled with the Model Predictive Control (MPC) methodology using a Genetic Algorithm (GA) to find the optimal solution to minimize the negative ecological impact of the UDS on the river. Both the FH model and simplified model are used in the MPC optimization.

Based on the analysis of the case study, the optimization results show that the impact of the MPC procedure on the receiving river is not significant. The reasons for this are location specific, but the main findings are that 1) the hydraulic constraints of the catchments restrict the MPC procedure from working, 2) although the calibration results of the conceptual model indicated accurate results, this does no guarantee that the model is also accurate enough to use in the MPC procedure. The required accuracy is location-specific.

This page is intentionally left blank

Table of contents

List of figures

List of tables

1. Introduction

1.1 Literature Review

The underground system of urban areas is crowded with pipelines that are necessary to let the urban area function properly. From an urban water management perspective, this infrastructure is needed to ensure the drinking water and sanitation demand, the control of infiltration and stormwater runoff, and the maintenance of urban ecosystems and recreational parks (Loucks & van Beek, 2017). The functions above ensure public health in urban areas. The sewer system underneath the urban area can be divided into a combined sewer system and a separated sewer system. A combined sewer system transports dry weather flow: water that originates from household use, and wet weather flow: stormwater. Roughly 68% of the houses in the Netherlands are connected to the combined sewer system (Gastkemper, 2013). A separated sewer system transports the dry weather flow and the wet weather flow separately.

When the capacity of the combined system is reached, water is discharged through combined sewer overflow (CSO) structures, to avoid flooding the system. During these events, untreated wastewater is discharged into receiving water bodies. This can cause oxygen depletion, eutrophication, and discharge of pathogens, which can have adverse impacts on the river ecology (Quijano et al., 2017; Soriano et al., 2019; Wang, 2014, Owolabi et al., 2022; Sojobi & Zayed, 2022). The Water Framework Directive (WFD) mandates the EU member States to ensure good ecological quality of their natural waters, implying reduction or mitigation against CSO events (Commission Report, 2009).

Increased impervious areas and high-intensity rainfall due to climate change might increase the occurrence of CSO events (Frehmann et al., 2002). Hereby, the urgency to decrease the amount of CSO events becomes more urgent over time, since the impacts of climate change are expected to increase over time. Another problem that could arise from peak inflow, is the increased ammonium concentration in the wastewater treatment plant (WWTP) effluent caused by peak inflow to the WWTP. An increased amount of ammonium concentration in the effluent can be toxic for fish and other aquatic animals in the water body (Du, et al., 2019).

These problems can be mitigated with multiple solutions. Possible solutions are (1) to increase the in-sewer storage by expanding the sewer network, (2) to expand the WWTP facility in such a way that the WWTP can handle higher loads, and (3) to disconnect stormwater runoff and reduce the impervious fraction of landcover. All these solutions are costly and require construction activities and available space, which can be impractical in urbanized areas (Frehmann et al. 2002).

Optimization of the existing infrastructure before considering additional measures is therefore advisable. Currently, the combined sewer system is predominantly statically operated. Since the input in the sewer system is dynamic over time, the full capacity of a system might not be reached. Optimization of the available storage might help handle the increased pressure and the increased environmental regulations simultaneously (Neugebauer et al., 1991). A method to control the dynamic performance of the sewer system is Real-Time Control (RTC). RTC described the technique through which the sewer system is dynamically controlled based on real-time information about the system state (Schütze et al., 2002). Process variables are monitored and, at the same time, used to operate actuators during the flow process. Controllers influence the process by adjusting actuators (e.g. pumps, valves, movable weirs, gates, etc.) to achieve minimum deviations of the controlled process variable from its desired value (Schütze et al., 2014).

1.1.1 RTC: strategies based on objective

The first step in designing a RTC strategy is devising the objective function. The objectives can be roughly categorized into three control strategies: volume-based (VB), quality-based (QB), or impact-based (IB) strategies (Garcia, et al., 2015).

Volume-based control

Volume-based control aims to minimize the spilled volume out of the system and is therefore considered the simplest strategy, considering only the hydrodynamics of the UDS system. Previous research indicated that volume-based control is the most representative type of control to minimize different sorts of impacts on the receiving water (Engelhard et al., 2008). Information regarding water quantities is required, e.g. water level measurement and possibly flows. This makes it the control type that requires the least input information (Bachmann et al., 2016). Volume-based control is useful for systems with available idle system capacity.

Quality based control

In the quality-based (QB) control type, the difference in water pollution levels is considered to optimize the available storage. This type ensures that the most polluted water gets priority to be transported to the wastewater treatment plant (WWTP). The potential of the QB control is dependent on the Mass-Volume (MV) curve that describes the dynamics of the pollutants and CSO volume during an event (Bertrand-Krajewski et al., 1998). High pollutant loads during the beginning of an event indicate a decrease in RTC potential compared to relatively high pollutant loads during the middle/ last part of the event, this implicates that the RTC potential decreases during a first flush effect. Another pollutant that can be included is an increased ammonium load in the WWTP effluent caused by a peak inflow towards the WWTP (van Daal-Rombouts et al. 2017). It requires information regarding water quantities, and water quality of the wastewater. Most RTC systems do not take water quality into account, since available continuous quality measurement devices are lacking. In the case that there are data measurements, the quality of the available data impacts the outcome of the RTC. The quality of the available data is dependent on the accuracy, availability of accepted data, and the measuring frequency. Besides that, the predictive effect of quality models is weak (Kanso et al., 2005).

Impact based control

The impact-based (IB) control takes, besides the water quantity and quality, the differences in vulnerability of the environment into account. The quality of the receiving water body is used as the optimization function, in which dissolved oxygen (Rauch & Harremoës, 1999) and/ or ammonium (Langeveld et al., 2013) are commonly used parameters. IB control requires knowledge of water quantity, quality, and sensitivities of the receiving water. The latter can be determined by the response of environmental parameters to the actuator operation. Vezzaro & Grum (2014) added a simple cost function to different CSOs based on the sensitivity difference of the receiving waters. A consequence of this could be that additional overflows in one part of the catchments are caused to ensure that other overflows are prevented. Concluding, that a minimization objective focusing on the impact of CSO events might cause additional overflow volume or frequency (Rauch & Harremoës, 1999). This consequence of the IB control strategy could require legislative changes (Meng et al., 2020). As described above, next to the spilled pollutants during a CSO event, the dynamics at the WWTP become necessary to include if considering the impact of an UDS on the receiving water body. A reduction of the inflow towards the WWTP during wet weather flow (WWF) conditions, reduces the ammonium peaks in the WWTP effluent (van Daal-Rombouts et al., 2017). By reducing the flow towards the WWTP, additional CSO events might occur. This balance is relevant for a multi-criteria RTC strategy because the ecological impact might decrease by causing a CSO event rather than overloading the WWTP (Frehmann et al., 2002). The impact-based control type requires the most information. The potential

of IB is the highest if there are differences in the vulnerability of the receiving water. Common issues regarding IB control are: (1) the lack of data for calibration and (2) the application of locally calibrated model data to complex sewer and river systems (Erbe & Schütze, 2005). Comparison of the IB control and PB control to VB control performance is impossible because of the difference in expressing the RTC potential (Rauch & Harremoës, 1996).

1.1.2. Multi-objective function

An objective function can consist of multiple individual objectives: a multi-objective function. There are several ways to comply with the conflicting nature of the multiple objectives considered in a multi-objective function. The multi-objective function can be converted to a single-objective function by scalarization in which every objective function is assigned a weight/ penalty (Ocampo-Martinez et al., 2008). Weights are determined through a trial-and-error process, which can be a time-consuming process. Besides that, adapting penalties to changes in the system might be difficult.

An alternative to scalarization is the use of a multi-objective optimization algorithm based on Pareto dominance. The main advantage of using Pareto dominance is that it is not necessary to specify the preferred objective. Instead, one can choose a preferred solution among the Pareto optimal solutions. Disadvantages of the Pareto dominance are the computational requirement and the interpretation of the Pareto solution. The latter is especially a drawback during RTC (Lund et al., 2018).

1.1.3 RTC: control level

The next decision that can be made by the designer, is the level of control of the system. The system can be controlled on a local or a global level (or a decentralized control) (García et al., 2015). If a system is locally controlled, the actuator is controlled solely based on the controller with which it is paired. This means that there is no information exchange with controllers at other sites. However, there is indirect communication through dynamics influenced by the actuators. The sensor and actuator are located close to each other. The limited information exchange throughout the system causes that local control utilizes mainly heuristic procedures such as if-then rules and fuzzy logic (García et al., 2015). The number of actuators used in a local control system is usually limited, therefore it is a better solution for smaller systems (Eulogi et al., 2020). The advantage of local control is that it consists of lesser effort and expense for data transfer, which makes it a better solution for smaller urban drainage systems (UDS) (Mounce et al., 2020). In a system that is globally controlled a central unit receives information from different sensors located over different locations in the system. This makes it possible for a system to react to events occurring in other parts of the system. The control decision can be made by one central unit, or several controllers share information and make joint decisions. The central unit determines the actuator settings through either heuristics procedures or using real-time optimization. This type of control has the possibility of including rainfall forecasts. This form of control outperforms the other forms of control (Gelormino & Ricker 1994; Giraldo et al., 2010), however, the difference in performance is not always significant (Sun, et al., 2020). A disadvantage of global control is that the wireless telecommunication network is expensive. Another disadvantage regarding the telecommunication network is, that whenever there is a fault in one of the sensors/ actuators, the global control needs to stop immediately and move to local control (Ocampo-Martinez et al., 2013). Although this is not desirable, the overall reduction in CSO frequency and volume respectively, might decrease (Weyand, 2002). Global control appears to have the largest potential for larger, complicated UDS with a high (>5) number of actuators (Van der Werf et al., 2022). The choice on control level is dependent on the preferences of the operator. The choice should be made based on the systems' characteristics: size, actuator numbers and loading. Literature shows an ongoing discussion on the preference for global or local control (Kroll, 2019).

1.1.4 RTC: heuristic or optimization control

RTC strategies can be divided into two distinct procedures: Heuristics and real-time optimization-based RTC (Garcia et al., 2015). The main difference between both procedures is that heuristics are based on extensive knowledge of the system, whereas the optimization-based control procedure computes the best actuator setting based on a model of the system. Both of the procedures are explained below.

Heuristic control

Heuristic control is based on experience and knowledge of the system behavior (Garcia, et al., 2015). This control can be appealing since the resulting control seems rational. It is usually developed to have low implementation complexity, therefore this control is used in systems that are complex to model. The disadvantage of heuristic control is that it can be difficult to obtain an optimal solution (Cen & Xi, 2007; García et al., 2015; Mollerup et al., 2013). A heuristic control is typically based on rules, following a so-called Rule-Based Control (RBC) procedure, which requires extensive knowledge of the system behavior. RBC is a set of control rules in the form of 'if-then-else' rules. These rules are developed by experts and can be used in combination with other methodologies such as fuzzy logic (Fuchs & Beeneken, 2005). A fuzzy set contains membership functions, that represent the degree of truth as an extension of valuation. The membership functions can be optimized using a genetic algorithm (Mounce, et al., 2020). RBC requires less computational power than needed in the optimized strategies and therefore can use a full hydrodynamic (FH) model for the computation (Kroll, 2019).

The main critique of RBC is that system states that are not foreseen by the designer, will not be used as an input in the model. Therefore the modeled system will not be capable of adapting to such states. Another limitation concerning input data is that RBC only uses current system states. The performance might be limited by decisions based on this information. This might result in a decline in optimal use of the wastewater system control potential. RBC is compared to other control procedures, more transparent, and easier to reproduce. This makes communication with authorities and stakeholders easier (Kroll, 2019).

Model-based predictive control

Model Predictive Control (MPC) contains of 3 main parts: internal MPC model, optimizer and full hydraulic model (Figure 1). MPC is a type of model-based, optimal control where at each time step, *k*, an optimal control input sequence $\bar{u}_k = [u_k, u_{k+1}, \ldots., u_{k+N-1}]$ is computed. This sequence is computed over a finite future time horizon, the prediction horizon *N*. This input sequence is obtained by solving an optimization problem using the internal MPC model (Lund et al., 2018). The first control input in the optimal control input sequence u_k is applied to the FH model. At the next time step, there is a shift of a step in the prediction horizon, to *k+1*, and the next optimal control input sequence $\bar{u}_{k+1} = [u_{k+1}, u_{k+2}, \ldots., u_{k+N}]$ can be computed. The optimization makes use of the current state of the FH model as an initial state of the internal MPC model that is used to compute future states along the prediction horizon in order to optimize the objective function (Fiorelli et al., 2013). MPC makes use of an internal MPC model to ensure that the computation time will not take longer than the evaluation rate (Verzarro et al., 2014). Since the internal MPC model is a simplified version of the real system, the applicability of the model outcome to the real system is reduced, causing uncertainty of the applicability of the model outcome.
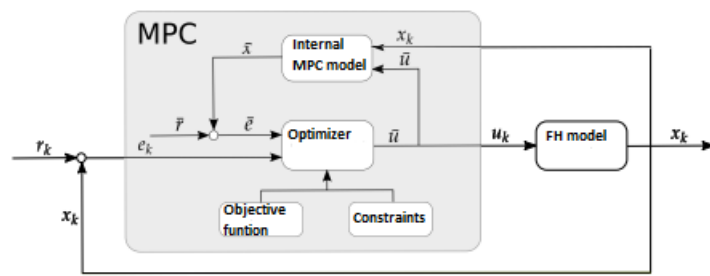
Figure 1: MPC main components (Kassem & Hassan, 2012)

Implementing MPC induces multiple uncertainties in the model performance. According to Heusch (2011), the impact of an internal MPC model on the applicability to small catchments is acceptable. Contrary to this, Mollerup et al. (2016) argue that MPC might not be suitable for small catchments. Another uncertainty that is introduced by MPC is created by the forecasted data. The quality of the input data will determine the quality of the generated output (Mollerup et al., 2016). However, Löwe et al. (2016) found that MPC simulations demonstrated improvements in control efficiency if forecast information, and its corresponding uncertainty, are included. This is found because the high optimization frequency overcomes drifts in the simulation. However there are multiple uncertainties, the exact effect of these uncertainties on the model performance remain uncertain.

Comparison of different types of control and strategies

There are different opinions and findings in research comparing the efficiency of RBC and MPC procedures. It is up to the modeler to determine which type of model will be used. Since all case studies and corresponding system characteristics are different, there is no single best control algorithm that is applicable for all different scenarios possible (Schütze et al., 2017). Therefore, only general findings regarding the pro and cons of the different model types are discussed above.

Mollerup et al. (2016) found that for small catchments (here: 320 ha impervious area) the application of RBC has the preference over MPC. The small improvement of performance comparing MPC to RBC, does not weigh up to the high investment costs of MPC. The German guideline for the planning of RTC of sewer networks (DWA 2005) agrees that the potential of RBC should not be underestimated, especially in smaller catchments. The main advantage of RBC over MPC is that it can be implemented with less effort. Regarding implementation, it is dependent on which type of control can be implemented based on the available software and the background of the people in charge of a project (Pleau et al., 2005). Currently implemented type of control is of importance. In an uncontrolled system, the introduction should be done stepwise, beginning with simple control and extending to a more complex system whenever the simpler control is understood well by the people in charge (Weyand, 2002). The best practice doesn't need to contain the most complex algorithm. It appears that the systems' performance improvement (defined by the set objectives) of simple control algorithms can be similar to the performance improvement of complex algorithms. This outcome is of importance and shifts the focus of the preference of creation of a very complex algorithm to creating an algorithm that suits the case study based on a thorough determination of data available and the set objective.

1.1.5 Performance evaluation

RTC potential

The magnitude of improvement of the system performance caused by the implementation of a RTC strategy, is dependent on the RTC potential. This potential can, before the selection of RTC, be roughly estimated by the management tool: Planning Aid for Sewer System in Real-Time Control (PASST) (Schütze et al., 2004). The outcome of PASST will be an indicator of whether including RTC in an UDS, will give sufficient improvement in system performance. The PASST tool is used as a pre-assessment of the RTC potential of a given system. This tool applies readily available information of the system on a scoring table, which makes it possible to evaluate the RTC potential. The sum of the scores indicate the potential of RTC, and hereby the feasibility of further RTC studies. The outcome of this test is indicative, and should only be used to answer the question whether implementation of RTC in a case study area is promising and whether further studies should continue. If not, the RTC design should terminate here and the focus on the improvement of the system should be based on conventional measures/ solutions. The questionnaire includes information on the catchment, wastewater production, sewer system, operational system behavior, receiving water, and WWTP (Dirckx et al., 2007).

Evaluation of the RTC performance

Van Daal-Rombouts (2017) defined general steps that can be followed for the evaluation of RTC performance. The RTC performance is measured by first stating a clear objective function that need to be obtained by implementing the RTC. By clearly defining the objective function, the assessment of the RTC performance can be executed more precisely and more targeted. The definition of the objective function will help to define the assessment parameters, which are the parameters that will assess whether the goals are obtained. Afterward, the range of conditions in the evaluation period should be defined. The sensitivity to the current system functioning, however, might give a skewed idea of the potential of RTC. A common baseline should therefore be used to allow for better inter-catchment analysis (Van der Werf et al., 2021).

The further assessment is different for model-driven and data-driven evaluations. The data-driven evaluation focuses on setting up and using a reliable measurement station. The model-driven evaluation focuses on setting up a model and subsequently calibrating and validating it. Uncertainties in model results (Deletic, et al., 2012) and monitoring results (Bertrand-Krajewski et al., 2003) influence both evaluation methods. A benefit of the data-driven method over the model-driven method is that the data driven method is able to include uncertainties and common system failures in the assessment procedure. The model based method only includes theoretical RTC performance, which is the ideal functioning of the RTC. The model based method gives an indication of the upper-bound of the practical RTC performance (Van der Werf et al., 2022). However, the performance of the RTC might increase due to the adaptability of the RTC for unanticipated events in practice. This effect cannot be included in the performance analyses (Pleau et al. 2005). This concludes that data driven and model driven methods to evaluate RTC performance cannot be compared.

Finally, for both the model-driven and data-driven system, the system performance with and without RTC is compared, by determining the impact of RTC, including an uncertainty analysis (Van Daal-Rombouts, 2017). This should ideally be done for multi-years datasets, to adequately assert the performance of the RTC procedure, however, this is still not frequently done (Van der Werf et al., 2022).

1.2 Problem Statement

As set out throughout the introduction, the urban wastewater system can negatively impact urban ecology and public health through combined sewer overflow and overloading of WWTPs leading to partially untreated effluent entering the urban water ways. Both events impact the water quality of receiving river water. Real Time Control (RTC) has been shown to effectively minimize these adverse effects. However, the lack of quality data for calibration of the model can complicate the implementation of the RTC strategy. Therefore, it is proposed to express impact quantitatively by exploring the relation between impact on the receiving river and discharged WWTP effluent/ CSO volume in available measurement data. Hereby, an impact-based problem is solved by a volume based RTC strategy.

Next to that, the design of a multi-objective function can lead to various problems. Scalarized optimization problems require the assignment of weights to each objective. The weights are determined through trial-and-error process, which is time-consuming. Another way of solving a multi-objective optimization problem is an optimization algorithm. However, the interpretation of the Pareto front during the optimization is a disadvantage. Since both of these methods cause drawbacks while using in a RTC strategy, this research proposes a method to describe a multi-objective optimization problem in a dynamic single-objective function that dynamically switches between objectives based on a pre-defined threshold. The dynamic character of the optimization strategy makes it possible to distinguish the two objectives, being able to consider the objective with the most impact in the optimization process.

Thus, the problem in this thesis can be described as the need for improvement of the water quality of receiving waters that are connected to an UDS by including both the objective to minimize ammonium peaks in the WWTP effluent as well as reducing the total amount of CSO events that cause DO dips. This problem will be solved by implementing a dynamic RTC optimization strategy.

1.3 Research question and sub-questions

This research aims to reduce the negative impact on the ecological quality of rivers that receive water from combined sewer systems, by taking into account the variable origin of ecological impacts. The corresponding research question will be: *Is a dynamic RTC strategy capable of reducing the ecological impact caused by a combined sewer system?*

Sub questions:

• Can the trade-offs between ammonium loading and dissolved oxygen (DO) concentration be linked to rainfall characteristics?

• Is it possible to capture the performance of a sewer system in both a full hydraulic model and a simplified (conceptual) model?

• What is the environmental impact of a RTC strategy that dynamically optimizes the system for both dissolved oxygen and ammonium concentrations?

1.4 Thesis Outline

The rest of this thesis is outlined as follows. In Chapter 2, the methodology used to answer the research questions is set out. Chapter 3 describes the case study area that is used in this research, by explaining geographical and system characteristics. Chapter 4 presents the results obtained. Chapter 5 gives a discussion of the results and the findings during this study. The main conclusions are presented in chapter 6, and finally the ideas for future research are described in chapter 7.

2. Methodology

The main goal of this research is to investigate whether a multi-objective RTC strategy would be capable of reducing the ecological impact caused by the wastewater system. Optimization is used to find the optimal actuator settings, to reduce the negative impact on the ecology caused by ammonium peaks in the WWTP effluent and dips in DO concentration caused by CSO events. For this thesis, we have developed and applied a methodology that coupled hydrodynamic model SWMM version 5.1 (Ngamalieu-Nengoue et al., 2019) and Genetic Algorithm (GA) as an optimization algorithm. The usage of a hydrodynamic model such as SWMM to evaluate UDS performance subject to different actuator settings is done in multiple studies (Sun et al., 2020; Troutman et al., 2020; Abdel-Aal et al., 2020; Krol et al., 2018) and many more.

This chapter will cover the trade-off between DO dips and ammonium peaks (Chapter 2.1), the optimization process (Chapter 2.2.), and the method of UDS simulation, creation & calibration of the conceptual model (Chapter 2.3).

2.1 Impact of pollutant trade-off in the urban water system

To be able to decrease the overall ecological impact of a wastewater system, it is important to first understand the current ecological impact and which factors play a part in this. As described in the introduction (Chapter 1) ammonium peaks and DO dips have both a negative ecological impact and therefore have the focus in this study.

Answering the sub-question: ***Can the trade-offs between ammonium loading and DO be linked to rainfall characteristics?*** gives insight into the cause of DO dips and ammonium loading, and whether there is a relation between rainfall characteristics and the occurrence of these events. The rainfall characteristics that are included are the duration of a rain event, maximum intensity of a rain event, and total sum of rain during a rain event. If the trade-off between ammonium loading and DO dips can be linked to rainfall characteristics, then the outcome of this sub-question can be used in the objective function that is used in the optimization of the UDS.

Here, a model-based approach, using an integrated model of the catchment, is proposed to first evaluate the impacts the urban wastewater system has on the urban waters and then find correlations within the dataset based on precipitation characteristics.

2.1.1 WEST model

To answer this sub-question, the first step was to create an integrated model of the catchment, including the sewer, treatment plant, and receiving waters. This was modeled with the WEST simulator (www.mikepoweredbydhi.com) using a modified activated sludge model No. 2D biokinetic model (Gernaey, 2004). WEST is a 0-dimensional simulation tool from which water quality parameters can be obtained, and is therefore suitable for answering this sub-question. The UDS was for previous research already modeled in the WEST simulator. It is beyond the scope of this research to further explain the details of the model setup, calibration, and validation. The details considering model setup and calibration can be found in Amerlinck (2015). To improve the reliability during wet weather conditions (e.g. peak of effluent solids and sludge buffering), a specific secondary settling model was applied which was created by Benedetti (2011) and afterwards successfully used by Langeveld et al. (2013) and Moreno-Rodenas et al. (2017).

The rest of the UDS is simulated in a simplified form since WEST is a 0-dimensional model focusing on the simulation of water quality parameters (e.g. the WWTP) instead of the hydrodynamics in the UDS. The UDS is subdivided into multiple catchments, that each represents a part of the UDS. The output of the catchment is a sum of the DWF and the runoff that is generated by the received rainfall in that catchment. Catchments are connected to each other or connected to storage tanks. The storage tanks are either connected to other storage tanks, pumps, or a CSO location. If the latter is the case, the storage tank is connected to the river reach that receives the water during a CSO event. The rivers are simulated in multiple river reaches. The river reaches receive water from upstream river reaches, runoff from the catchments, and if applicable from CSO's (figure 2). In appendix 1, an overview of the full layout of the system can be found.
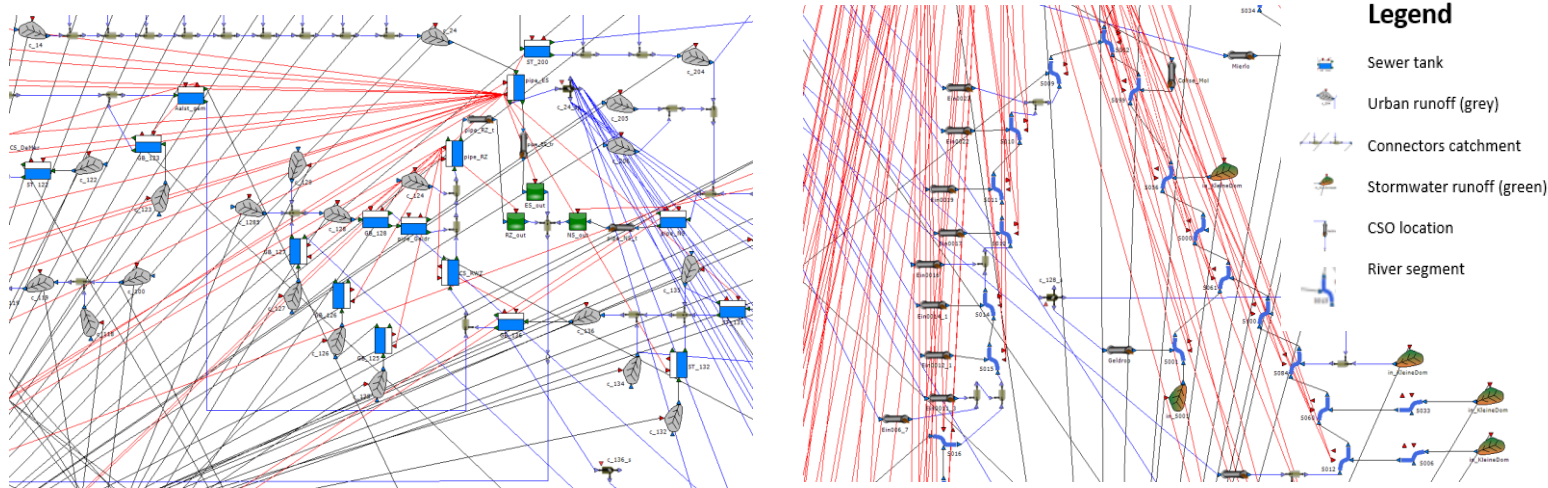
Figure 2: Layout UDS Eindhoven in WEST (left), connection CSO to river segments (right)

The following outputs are obtained from WEST:

1. DO concentration [mg/L]
2. NH_4^+ concentration [mg/L]

Information concerning the DO concentration is obtained at multiple locations. The selected locations are either directly downstream of a CSO location or are directly downstream of a river convergence. The latter makes it possible to monitor the influence of a CSO event over a longer distance. Rain data was obtained to link the DO and NH_4^+ concentrations to the rainfall characteristics at that moment in time.

2.1.2 Analysis of output WEST model

A clear definition of an ammonium peak and DO dip is necessary. Besides that, it is necessary to define the characteristics of the beginning and the end of a rain event to ensure that the oxygen/ ammonium concentrations can be linked to a certain event.

Therefore the following definitions are determined:

- An ammonium peak is characterized by an ammonium concentration that is higher than 3 mg/L
- An oxygen dip is characterized by an oxygen concentration that is lower than 4 mg/L
- A rainfall event is characterized by a dry spell of 12 hours before and after the actual rain, to ensure that the flow in the systems returns to DWF.

10

The UDS performance is simulated in WEST for the year 2019. The rain events are divided into rain events that did and did not cause a DO dip. A total of 185 rain events were considered. From each rain event the following characteristics were extracted: duration, maximum rainfall intensity [mm/hr], and the total depth of a rain event. These characteristics are selected since these are most defining for UDS dynamics. These characteristics are plotted in boxplots for both rain events that cause a DO dip and for rain events that do not cause a DO dip. These boxplots give an indication about the relation between rainfall characteristics and the DO/ ammonium events. To further determine the trade-off between the two events, a decision tree is made using the decision tree module from the scikit learn library in Python. This module is a non-parametric supervised learning method used for classification and regression. By learning simple decision rules based on imported data by the user, the model can predict the value of a target variable. In this research, the target variable is whether the objective should be focusing on preventing DO dips or ammonium peaks. The data in the decision tree is split based on the entropy, which is an information theory metric that measures the impurity of observations. A high entropy indicates a high level of impurity in the decision. If the decision tree gives diluted results, e.g. the decisions are specific for certain events instead applicable to a wide range of events, then it can be concluded that the tradeoff between ammonium peaks and DO dips cannot be linked to rainfall characteristics. The rainfall data is provided by the Royal Netherlands Meteorological Institute. The data has a five-minute interval and pixel size of 1x1 km.

2.2 Methodology MPC

In this study, an MPC scheme was used to optimize the system. In chapter 1, MPC is explained. The three main components of MPC are: the internal MPC model, the optimizer which is dependent on the constraints and an objective function, and the FH model. In this Chapter, the implementation of the MPC concept and the different design choices are described. Chapter 2.3 describes further details on the used hydraulic models.

2.2.1 Implementation MPC concept

Figure 3 gives an overview of the optimization process used in this research.
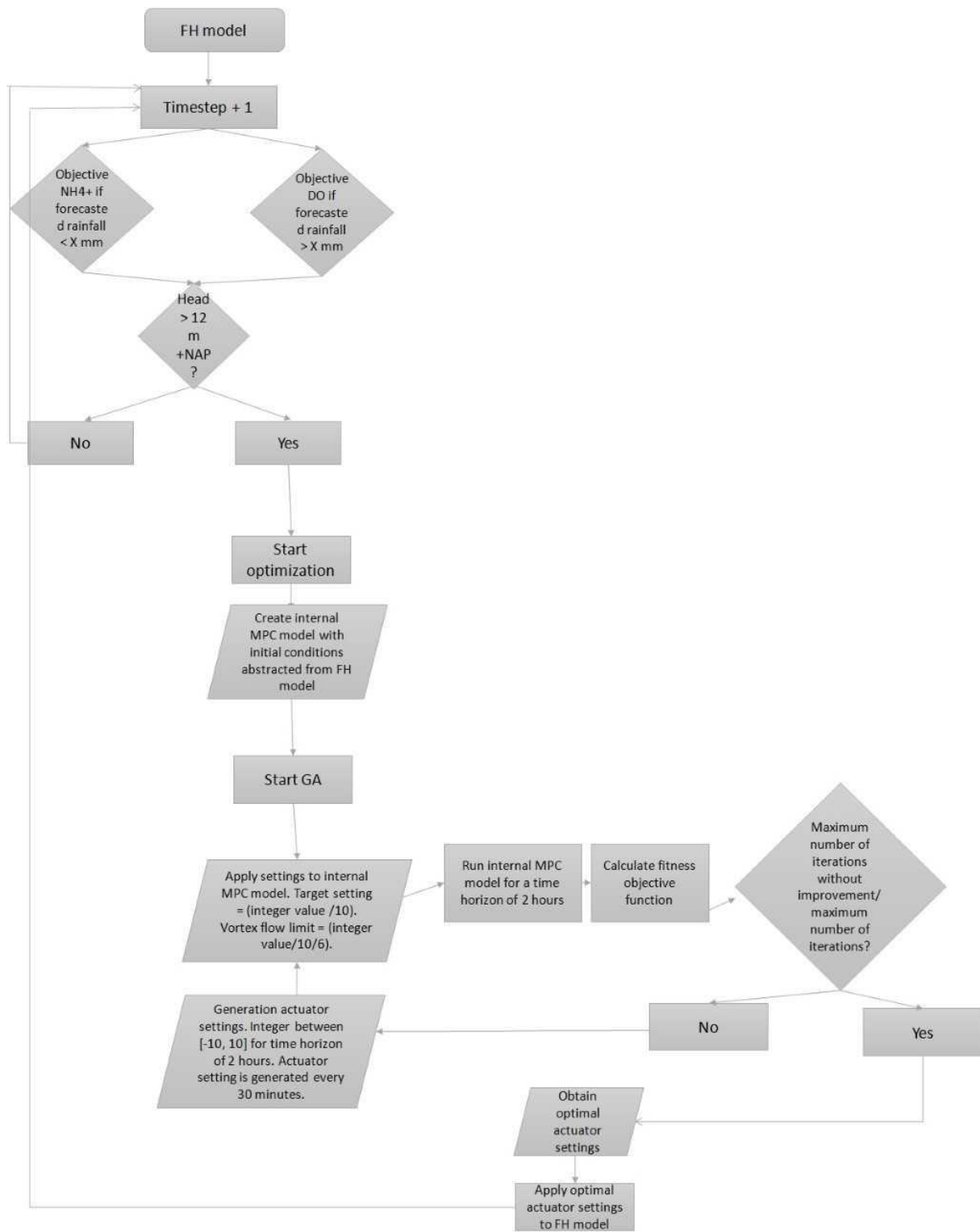
Figure 3: Overview optimization process

The set objective function is the most defining component in the final optimal output in the MPC algorithm. The objective function should correspond with the objective of the physical system to control. The optimal actuator settings are determined by solving the optimization problem which consists of two objectives: reducing DO dips caused by CSO events and reducing the NH_4^+ peaks in WWTP effluent. The optimization problem can be solved using a multi-objective function, however as described in the literature review, this can cause problems. Therefore, in this study, a new method is tested by considering the two objective functions separately. The rainfall forecast determines which objective function is selected during the optimization process. The DO objective could be reached by maximizing the flow towards the WWTP. Whereas the occurrence of NH_4^+ peaks can be prevented by a moderate increase of discharge towards the WWTP during the start of WWF.

Since the objectives are contrary to each other, this optimization problem considers only 1 objective function during the optimization process. The objective that will be considered in the optimization problem is dependent on the forecasted rainfall. The outcome of research question 1 will give insight into the exact triggering threshold (e.g. total forecasted rainfall amount in mm) that determines which objective function will be used.

The optimization problem consists of two objective functions: $Objective$ 1: is an indirect objective that indirectly aims to reduce the ammonium peaks. , and $Objective$ 2: aims to reduce the oxygen dips in the receiving river water, caused by CSO events.

$$H = \min\left[\sum_{k=1}^{P} Q_{WWTP_k}(t) - Q_{target_k}(t)\right] \; if \; sum \; forecasted \; rainfall \; is \; < threshold \; \; (Objective \; 1)$$

$$F = \min\left[\sum_{i=1}^{N} G_i * Q_{CSO_i}(t)\right] \; if \; sum \; forecasted \; rainfall \; i \; \geq threshold \; (Objective \; 2)$$

Where Q_{target} stands for a predefined maximum discharge towards the WWTP that does not cause an ammonium peak. Q_{wwtp} stands for the total inflow in the WWTP per time step. By taking the difference between Q_{target} and Q_{wwtp} it is ensured that during the optimization process, the pumps do not completely shut down but keep pumping at a pumping rate that does not cause an ammonium peak. P stands for the pumps that are connected to the WWTP. These are the pumps that connect RZ to the WWTP and the pump that connects ES to the WWTP.

N is the total amount of CSO locations. The parameter G is a weight parameter that is dependent on the importance of the CSO location. Q_{cso} stands for the total volume of water that is spilled at each time step.

The FH model is the model that applies the optimization results. Jupyter Notebook with Python is used to link the model in SWMM to the MPC process. To enable Python to access SWMM 5.1 data model, the PySWMM package (McDonnell et al., 2020) will be used, along with the SWMMToolbox package. In Chapter 2.3.1. further details of the FH model are explained.

This research aims to minimize the occurrence of DO dips and NH4+ peaks. Every simulation step the forecasted rainfall is evaluated against the NH4+/DO threshold which is determined in research question 1. It is not necessary to optimize every simulation time step, since the system is in some cases able to respond accurately to the incoming rainfall because of available in-sewer volume. Therefore, after the evaluation of the forecasted rainfall, it is determined whether the head in the node just upstream of the WWTP is higher than the head above the 95% confidence interval of the DWF pattern.

It is chosen to apply the constraint to the most downstream node in the system because the head in this node gives the best indication of the system state. By starting the optimization process only after this threshold, there is sufficient time for the actuators to respond to the WWF according to the optimization outcome.

The optimization does not start if the simulation time step is less than 2 hours before the end time of the simulation. This requirement is set, since the systems' transport time to the WWTP is longer than 2 hours, therefore optimization in (at least) the last 2 hours does not impact the peaks at the WWTP. If these two requirements are met, the optimization process can start.

Internal MPC model

The internal MPC model is used to optimize the system settings for a finite time horizon. Jupyter Notebook with Python will link the internal MPC model in SWMM to the optimization process. In Chapter 2.3.2. further details of the internal MPC model are presented.

The initial conditions of the internal MPC model are adapted to the current condition in the FH model. The following initial conditions are adapted: start date and time of the model and end date and time of the model, the initial node depth, and the initial flow in conduits. The start data are changed to the current time in the FH model. The end date is changed to the current time in the FH model plus two hours. By doing so, the internal model will optimize the actuator settings for the coming two hours. The choice for the prediction horizon is a trade-off between computation time and performance. The prediction horizon must be large enough to be able to anticipate on future events, such as violations of the constraints. The choice to set the prediction horizon at 2 hours, is made based on the fact that a simulation step is 5 minutes, the horizon is hereby large enough to anticipate future events. Besides that, the prediction horizon of 2 hours has a reasonable simulation time.

The rainfall that is used in the internal MPC model is observed rainfall data. By not using predicted rainfall data, it is expected that the optimization outcome is more precise, although previous research has shown little sensitivity in RTC performance to rainfall uncertainty comparted to model uncertainties (van der Werf, under review). Besides that, this research is determining the theoretical/ model based potential of the RTC strategy, in which the practical uncertainties such as rainfall forecast and actuator settings, are not considered (as explained in the literature review).

Optimization

The optimization problem and algorithm are key aspects of the MPC since it is responsible for finding the optimal model control inputs. The Genetic Algorithm (GA) is chosen as the used optimization algorithm to find the optimal model control inputs because a GA is capable of handling large, complex, discrete, and non-linear systems like a UDS (Baek et al., 2015). GA have been established as an optimization method in the literature for over two decades (Rauch & Harremoës, 1999).

Jupyter Notebook with Python will link the internal MPC model to the GA, using the Python package: PySWMM (McDonnell et al., 2020). A pre-made GA package, developed by Ryan Mohammad Solgi (Hassanat et al., 2019) will be used as the optimization algorithm. The source code of the GA package is adapted, in such a way that it is possible to add function variables or parameters (that do not need to be optimized) to the function that will be optimized.

GA is a popular evolutionary algorithm that works based on Charles Darwin's theory of natural evolution. GA reflects the process of natural selection in which the fittest individuals are selected for reproduction to produce new individuals for the next generation and follows as set of predefined stages (Figure 4). Which are further described in Appendix 2. The overall principle of the GA is

controlled by crossover probability, mutation probability, population size, and the stopping criteria (Goldberg & Holland, 1988).
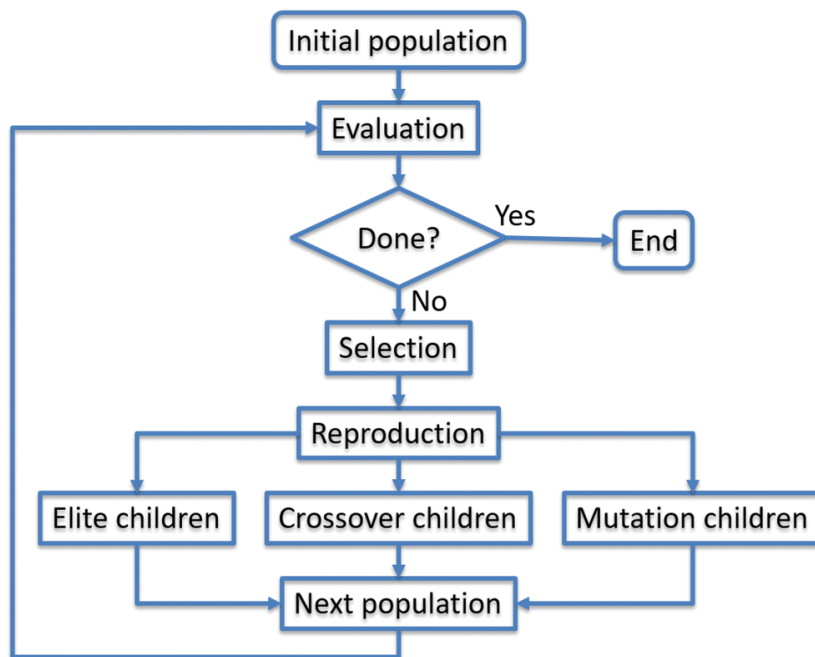
Figure 4: Overview Genetic Algorithm

The optimization parameters that are used in the GA optimization can be found in table 1.

Table 1: GA parameters

GA parameters	Value [-]
Population size	10
Elite ratio	0.05
Cross-over probability	0.5
Mutation probability	0.1
Max number of iterations	25
Max number iterations without improvement	20

Constraints

SWMM is subject to implicit constraints that are described in the model itself. Examples of implicit constraints are:
- the lower and upper limit pumping capacity
- lower and upper limit flowrate through conduit vortex

2.3 Hydraulic Simulation

The properties and the behavior of the real UDS must be replicated in a hydrologic and hydraulic model to be able to adequately evaluate the performance of the UDS. Established software packages for hydrodynamic modelling can be used for this, such as: InfoWorks, Mouse (DHI, 2009) or SWMM (Rossman, 2005). All three of these packages support the possibility of data export to text-based files in a node-link-notation or use similar formats as data storage through which access for external software is made easy. As the hydrodynamic modelling environment InfoWorks ICM does not allow for the exchange of information with the model during simulations, it is chosen to work with SWMM. The Storm Water Management Model (SWMM) is developed by the United States Environmental Protection Agency (US-EPA). SWMM is a well-known model that can be used as a dynamic simulation engine to simulate and replicate the hydraulic behavior of water runoff and sewer systems. SWMM makes use of the 1D Saint-Venant equations. This thesis focuses only on 1D flow in the sewer system, whereas 2D flow, like floodings, is not considered in this research. Thus, SWMM is a suitable tool for this research, which is supported by previous research executed (Sadler et al. (2019); Garcia et al., (2015)). SWMM makes use of the following objects to model and operate the rainfall-runoff and water transport processes: Links (e.g. conduits, pumps, orifices, weirs, and outlets), nodes (e.g. junctions, outfalls, flow dividers, storage units), rain gages, sub-catchments, climate parameters, control rules (e.g. for pumps/ orifice settings), pollutant information, curves (e.g. for pump or storage) and time-series (e.g. temperature, evaporation, rainfall, inflows).

In this research multiple models are used to optimize the performance of UDS. An overview of the used models can be found in figure 3.
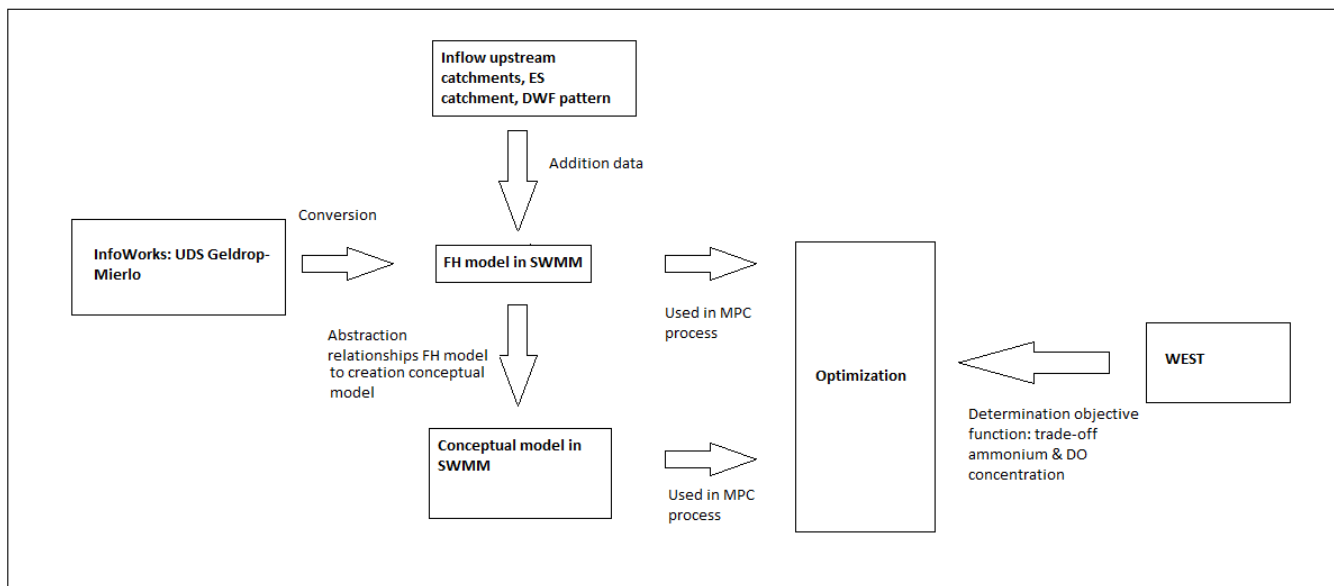
Figure 5: Overview used models

2.3.1 Full Hydraulic model in SWMM

The FH model is a 1 D-model that takes hydrodynamic processes into account. The FH model is used during the optimization process and for the creation of the conceptual model the key relationships between variables are obtained through FH model simulations. As explained above, the FH model is created in SWMM. The FH model is applied in this study for three purposes: 1) The FH model is used during the optimization process, 2) The FH model is used to obtain the key relationships between variables of simulations which are consecutively used in the creation of the conceptual model 3) The performance of the conceptual model is compared to the performance of the FH model.

Calibration FH model

To be able to use the FH model in SWMM5, the model must be calibrated against existing measurement data, to ensure the accuracy of the model. The calibration is evaluated based on available measurement data and different rainfall events. The calibration of the FH model was performed based on manually modifying different calibration parameters in a trial-and-error manner. The calibration parameters are conduit roughness and the initial loss due to infiltration in the catchment (table 2). These calibration parameters are chosen since these parameters are not fixed and not measurable, therefore the tuning of the FH model should be based on these parameters. The modification of the calibration parameters in the trial-and-error procedure is executed based on maintaining the existing water balance in a certain part of the system. During the calibration process, the system is strategically divided in smaller parts based on the available measurement data. Hereby, the impact of the alterations of calibration parameters should impact the dynamics in the therefore designated area.

Table 2: Calibration parameters FH model

Parameter	Bounds
Conduit roughness	0-1
% Impervious subcatchment	0-100

The aim of the calibration was to ensure that the dynamics in the sewer catchments and the connected CSO's represented the UDS as per the measurement data. The model settings were adjusted in such a way that the timing of peaks (e.g. flow/ head) and the magnitude of the peaks correspond to the measurement data. In this research, the focus is on the WWF. Therefore, the focus during the calibration was on the conditions during WWF. The outputs from the SWMM simulations can be post-processed using python and the SWMMtoolbox package. The calibration involved a detailed check of the measured and modeled parameter data at four different locations. The FH model simulation outcome contains information every 5 min timestep and include information concerning: stored volume, water level and flows in manholes, pumps, CSOs, and conduits. The measured parameter data is plotted together with the modeled parameter data. During calibration, this helped to give insights into what parameters changes could potentially lead to better results and a successful calibration. Resulting from the calibration, the calibration outcome is evaluated by the Nash-Sutcliffe Efficiency (NSE) coefficient. This coefficient determines the relative magnitude of the residual variance compared to the measured data variance (Nash & Sutcliffe, 1970). This coefficient makes it possible to compare calibration results and evaluate the fit with the measured data.

The NSE coefficient is calculated with the following formula:

$$NSE = 1 - \frac{\sum_{t=1}^{T} \left(Q_o^t - Q_m^t\right)^2}{\sum_{t=1}^{T} \left(Q_o^t - \overline{Q}_o\right)^2}$$

Where Q_m is the modeled parameter and Q_o is the observed/ measurement parameter at time t.

An NSE outcome of 1 indicates that the modeled data is a perfect fit with the measured data. An NSE outcome of 0 indicates that the model outcome is as accurate as the mean of the measured data. Inf < NSE < 0 indicates that the measured mean is a better predictor than the model (Nash & Sutcliffe, 1970).

At least three rain events, not all causing CSO events but including a spread of characteristics, should be chosen for the calibration and validation. The model is calibrated on single event calibration. Literature proves that this might be insufficient. The definition of a rain event allows the system to fully drain all the water out of the system and fill it up again. A rainfall event is defined in the same way as in sub-question 1: the beginning and end of a rain event are defined by a dry spell of 12 hours before and after a rainfall event. Therefore, in this case, a single calibration event is assumed to be sufficient to work with.

For SWMM to be able to calculate the exact runoff, it is required to implement the daily evaporation data in the model. The daily evaporation data that is used in this research, is provided by the Royal Netherlands Meteorological Institute.

2.3.2 Conceptual model in SWMM

As the computational time associated with the aforementioned FH model is very large, a conceptual model is made to emulate the dynamics of the FH model. The conceptual model aimed to replicate the dynamics of the FH model in as few relationships/ characteristics as possible. It is key to find a balance between the complexity, that can simulate the dynamics in the FH model, and the simplicity, which reduces the simulation time. The conceptual model will be used in the optimization process as the internal MPC model, to obtain quick simulation results.

Creation of the conceptual model

A linear reservoir model is a model that emulates the dynamics of an FH model by a simple linear relation between discharge and storage in a reservoir. The conceptual model is based on a linear reservoir model. Since the simple linear relation between storage and discharge does not capture the more complex dynamics caused by pumps/ CSOs, it is important to consider other process descriptions separately in order to simulate the flow behavior from the FH model correctly (Van Daal-Rombouts et al., 2016). The exact components that are included in the linear reservoir model and the components that need to be added separately, were iteratively determined dependent on the catchments characteristics. Additional key relationships/ geometrical information are obtained through FH model simulations. To maintain the simplicity of the conceptual model, only process descriptions that cannot be included in the linear reservoir model and that are key for the flow dynamics, are taken separately. The simplified catchments were modelled in SWMM.

The relationships that are included in the model are described below. These relations are obtained using the SWMMtoolbox package in python.

Storage curve sewer

The relationship between storage volume and water level is referred to as storage curve. The sewer tank in the conceptual model should follow the same storage curve as the sewer in the FH model. The storage curve of the FH model was calculated by grouping the water volume in the sewer in 10 cm intervals of the corresponding water level. The grouped volumes were averaged and smoothed to obtain the storage-level curve. By smoothing the grouped volumes, instabilities within the simulation were not considered.

The water volumes in the FH model were calculated by:

$$\Sigma \, Filling \, degree \, conduit * maximum \, volume \, conduit$$

<u>Discharge through connection</u>

The connection between the sewer tank and the transport pipeline indicates the relation between the discharge rate under multiple heads in the sewer tank. The relation between the water level at the upstream end of the connection and the discharge through the connection is obtained from the FH model.

<u>Discharge through CSO</u>

Discharge through CSOs can be calculated by the standard weir equation for transverse weirs:

$$Q = C_w * L * h^{3/2}$$

In which: Q = discharge [m³/s], C_w = discharge coefficient [-], L = length [m], h = height [m]

During the calibration process of the conceptual model, the following parameters can be adapted: invert level, weir height, weir width to obtain a good fit with the relationship between the discharge through the CSO and the water level in the FH model.

Aside from the relationship described above, the parameters of the catchments from the FH model are used to calculate the weighted average for the same parameters for the sewer tanks in the conceptual model. The parameters from the FH model of which the weighted average is used in the design of the sewer tank are stated in table 3.

Table 3: SWMM parameters for sewer tanks

Group parameters SWMM	Parameters
Area	total impervious area, total width, total slope
Subarea	impervious total area, perv tot area, s imperv tot area, s perv tot area, pctzerotot area
Infiltration	max rate tot, min rate tot, decay tot, dry time tot, max infiltot
DWF	Baseline
Rain	weighted average of all rain gages in the selected area

Calibration conceptual model

The calibration of the conceptual model is based on modifying influential parameters by manually adjusting them in a trial-and-error manner, with the aim of simulating the dynamics from the FH model captured in the relationship described in chapter 2.3.1. The calibration outcome is evaluated by the node head, stored volume, and the occurrence and total volume of CSO events. The influential calibration parameters are conduit roughness, the CSO weir dimensions, and infiltration. The modification of the influential parameters in the trial-and-error procedure is executed based on maintaining the water balance and replicating the relationship obtained from the FH model.

This study aims to meet the objective, which is to reduce the polluting impact of the WWTP and UDS on the environment. This includes reducing the impact of CSO events. The impact of CSO events depends on the occurrence of these events and the total spilled CSO volume during these events. The primary calibration criterion is to correctly determine the total discharged volume during CSO events, which is dependent on the stored volume in the system. This is the primary calibration criterion because a part of the objective function is to reduce the total spilled volume from CSO locations. The second calibration criterion is to correctly simulate the occurrence of a CSO event. This occurrence is

dependent on the head in the system. The calibration was evaluated with the NSE value for easy comparison and evaluation.

Hysteresis

Storage curves give an insight into the relationship between the total volume (stored volume in nodes, conduit, and storage units) and the corresponding head. This curve is a key source of information for multiple applications, such as calibration and validation of the modeling of sewer catchments, rainfall-runoff models, etc. but it is also a useful relationship for the creation of a conceptual model that pursues to replicate a complex hydrodynamic model (Wolfs et al., 2013).

Backwater effects can affect the storage curve resulting in looped trajectories, denoted as hysteretic behavior (Figure 6). A backwater effect is defined by the introduction of water storage upstream from a flow disturbance (in the case of a sewer system this could be upstream of a conduit junction) (Castelltort et al., 2020). Practically, this means that during high peak inflows, the head in the system will depend on whether the total stored volume is increasing or decreasing. As the volume increase, the conduit slope becomes greater than the slope for steady flow at the same stage. Hence, the volume in the sewer is greater than the steady storage curve would suggest. The size and the form of hysteresis are different for each peak inflow.

Hysteresis can have a significant impact on the storage curve. The conceptual model is created based on a single steady storage curve. This curve links the measured head to the volume in one singular relationship, which means that unsteadiness and backwater are not included. To be able to calibrate the conceptual model to the FH model, either the rising or the falling branch of the storage curve of the FH model is replicated in the singular storage curve for the conceptual model.
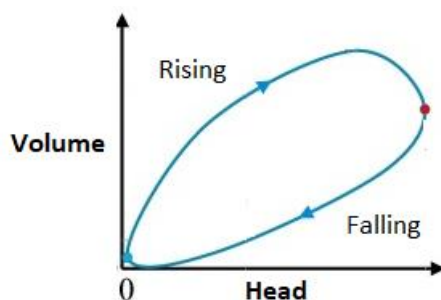
Figure 6: Hysteresis

3. Case study

Throughout this research, a part of the UDS connected to the WWTP of Eindhoven, the Netherlands has served as a case study. In this chapter, details about the case study will be discussed. Chapter 3.1 discusses the water system to which the UDS is connected. Chapter 3.2 describes the UDS of Eindhoven. In this chapter, the different elements and the global operation of the UDS will be discussed and the municipality that will be used for the application of the RTC strategy will be presented. In Chapter 3.3, the ecological issues that are originating from the UDS will be explained. Lastly, Chapter 3.4 describes the RTC potential of the case study area.

3.1 Surface water system

The WWTP of Eindhoven is located within the boundaries of water board De Dommel, encompassing nearly 30 different natural water bodies (Figure 7). Within the catchment, studied, the Dommel and the Kleine Dommel are the receiving water bodies, and their physical and ecological details are discussed below.

Figure 7: Map water board De Dommel (Waterschap de Dommel)

3.1.1. Dommel

The Dommel has a total length of 120 km, divided over Belgium (35 km) and the Netherlands (85 km) where it crosses the catchment of UDS Eindhoven (Figure 7). The effluent of WWTP Eindhoven is discharged on the Dommel. The source of the Dommel is located at 77 m+ NAP at the Kempens Plateau, which is in the municipality Peer in Limburg. By following the river downstream, the Dommel merges with the Aa in 's Hertogenbosch. The river flows further as the river Dieze that flows eventually into the Meuse. Therefore, the catchment of the Dommel is part of the catchment of the Meuse. The Dommel is a lowland river, which is characterized by a wide valley and irregular discharge.

The discharge of the Dommel is irregular because it depends on the amount of rainfall in the river basin. The Dommel is a relatively small river: the baseflow of the river just upstream of the WWTP is between 1 and 10 m^3/s, with an estimated mean effluent during dry weather flow at 1.25 m^3/s. The effluent during wet weather flow is estimated at 9.75 m^3/s. Therefore, the share of the WWTP effluent on the river can increase up to 90% of the total flow. The high share of the effluent in the total flow of the river causes that the Dommel is sensitive to the WWTP outflow. The main problems that can be found due to WWTP effluent in the Dommel are DO depletion, ammonium peaks, and seasonal average nutrient concentration levels (Langeveld et al., 2017). The Dommel is part of the Natura 2000, which is the European network of core breeding and resting sites for rare and threatened species, because of the existence of floating water plantain.

Afwateringskanaal (drainage canal) Eindhoven connects the Dommel with the Beatrixkanaal. This canal is constructed to prevent high water levels, and associated problems, in Eindhoven. After the construction of the canal, it became possible to discharge abundant water from the Dommel and the river Gender on the Beatrixkanaal and consequently on the Wilhelminakanaal. By doing so, the water level in Eindhoven decreases.

The Dommel is located in an area that is under the supervision of the water board *de Dommel*. The water board was founded in 1863, to counteract floodings. To prevent floodings, the water board decided to improve the ability of discharge through the Dommel by normalizing/ canalizing parts of it. However, severe flooding happened in 1995. This event initiated the start of the implementation of other measures, among others the designation of areas that can be flooded during extreme rainfall. At the beginning of the 21st century, the water board shifted the applied methodology from canalizing the Dommel to bringing the natural character of the Dommel back. Meaning that the canalization of certain parts of the Dommel became undone. Eventually, the water storage capacity was improved by these plans.

3.1.2. De Kleine Dommel

A large part of the municipalities of Leende, Heeze, and Geldrop is part of the catchment of the Kleine Dommel. The total area of the catchment consists of 210 km2 and the total length of the Kleine Dommel is 11 km. The Kleine Dommel is a lowland river with a strong meandering character. The Kleine Dommel originated because of the confluence of the Grote Aa and the Sterkselse Aa in Heeze. The river crosses Geldrop and flows into the Dommel on the West side of Nuenen. CSO locations of UDS Eindhoven (in catchment Geldrop) discharge on the Kleine Dommel. Because of the low flow of the Kleine Dommel, the river is very sensitive to CSO events and the ecological impact is significant.

Between Heeze and Geldrop, the valley of the Kleine Dommel is located next to the Strabrechtse Heide (moorland). This moorland is part of the Natura 2000, therefore the Kleine Dommel is of ecological value.

3.2 Wastewater system Eindhoven

The whole wastewater system of Eindhoven consists of the WWTP of Eindhoven and 10 municipalities. These municipalities are divided into three different sewer catchments, that all have their own size and characteristics. The three sewer catchments are: Nuenen -Son, Eindhoven Stad (ES) and Riool Zuid (RZ) (Figure 8). Every sewer catchment has a separate inflow to the WWTP. Under normal dry weather flow conditions, the inflow from ES accounts for 50% of the daily hydraulic loading to the WWTP. The remaining 9 municipalities are each connected to one of the two wastewater transport mains. The transport main of Nuenen-Son, located to the North of the WWTP, collects water from two municipalities. The transport main is 7 km in length and accounts for 7% of the hydraulic capacity. The other transport main, Riool Zuid, is located in the south and collects wastewater from 7 municipalities. Transport main Riool Zuid is 32 km in length and accounts for 43% of the hydraulic capacity of the WWTP. The WWTP of Eindhoven discharges to the river Dommel as main receiving water body (Langeveld et al., 2017).
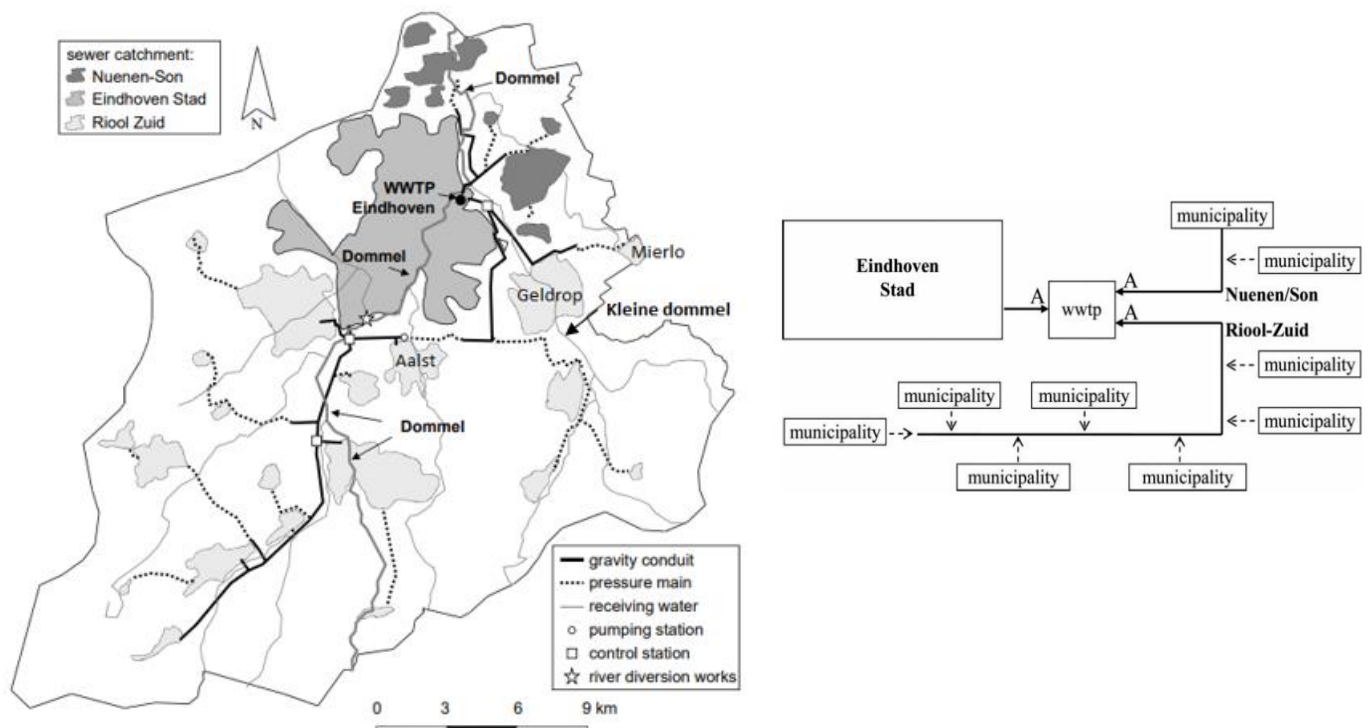
Figure 8: WWTP Eindhoven with corresponding sewer catchments (**Left**) receiving streams and schematic lay out of the wastewater system (**Right**) (**Van Daal-Rombouts, 2017**)

The UDS contains 223 km gravity-flow pipelines, 36 km pressurized pipelines, 196 pressure sewage pumping stations, 32 main pumping stations, and over 200 CSO locations (van Riel, 2017). The maximum load of the biological treatment of the WWTP is 26.250 m^3/h. After the influent is pumped into the WWTP, bar screens will remove the large solid particles (Figure 9). The water will be pumped via sand traps, into 3 primary clarifiers. In parallel to the treatment lines, there is a stormwater settling tank located that can treat up to 8750 m^3/h. This results in a total hydraulic capacity of 35.000 m^3/h. Water will be discharged to the stormwater settling tank whenever the capacity of the plant up to the primary clarifiers is reached and the in-sewer storage for ES is used. If the capacity of the stormwater settling tank is reached as well, the water will be discharged into the Dommel. After the primary clarifiers, the biological treatment process will start: the system consists of 3 activated sludge tanks

(30300 m³) with anaerobic, aerated, and denitrification zones. Each tank is connected through a cascade system to 4 secondary clarifiers with each a volume of 6300 m³. Then the effluent of the secondary clarifier is discharged into the river Dommel.
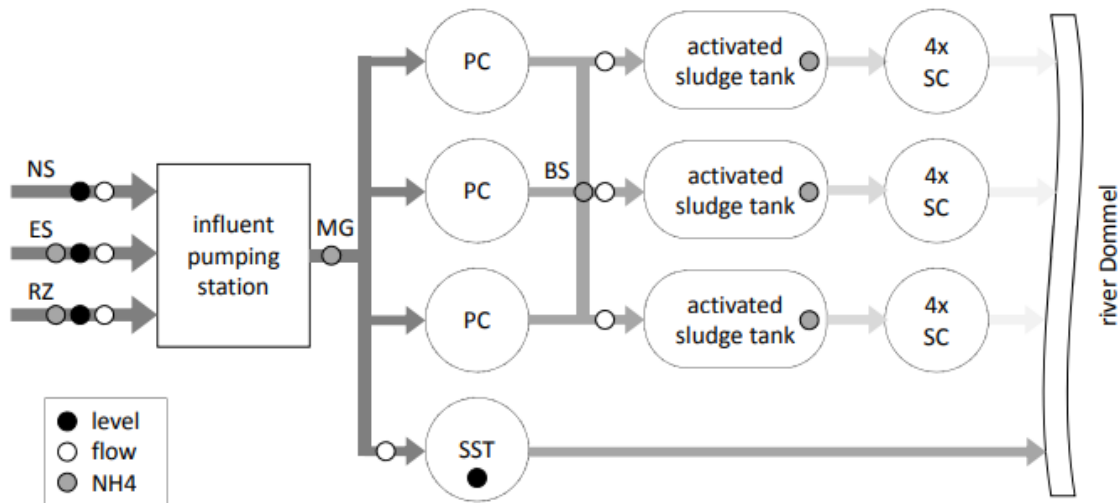
Figure 9: Schematic layout WWTP Eindhoven (Van Daal-Rombouts, 2017)

The case study that will be used in this research is the wastewater system of the municipality Geldrop-Mierlo, in which roughly 39600 people are living. This municipality contains the villages: Geldrop, Mierlo, and Hoog Geldrop, with a total area of 31,39 km². Generally, it is a flat area with a ground level of approximately 18.5-19.5 m above sea level (ASL) (van Riel, 2017). Geldrop-Mierlo is one out of the seven municipalities that discharge on the transport line RZ. It is the most downstream located municipality that is connected to RZ. Pumping station Aalst is located upstream of the connection of the municipality to RZ. At pumping station Aalst, wastewater is pumped into two parallel pressure mains using 4 parallel pumps (3.000 m³/h per pump). The pressure mains transport the wastewater over approximately 3 km. Afterward, the wastewater in RZ is transported in free-flow pipes, this is the part where the municipality Geldrop-Mierlo is connected to RZ. The municipality can be divided into three parts: Geldrop West (GW), Geldrop East (GE), and Mierlo (Figure 10). The connections are described below.

The flow from GW– RZ is influenced by the head in RZ, which is dependent on the upstream pumping rate of pumping station Aalst.

Figure 10 shows that catchment GE is connected to both catchment GW and Mierlo. Therefore, the outflow of GE is distributed over both connection points to RZ. The exact proportion of outflow to one connection point is dependent on the head levels within the catchment at the 3 connection points of GW and GE, and the head level downstream of pump Mierlo. GE mainly discharges via the connection point with Mierlo to RZ. The outflow of catchment Mierlo is pumped.

Figure 10: Layout system with focus on catchment Geldrop-Mierlo

The rainfall data used in this research is the rain gauge adjusted radar data with a 1 km x 1 km resolution at a five-minute interval provided by the Royal Netherlands Meteorological Institute (Overeem et al., 2009). The rainfall predictions are obtained from the output of the HARMONIE model. This model provides every 6 hours, the predicted hourly rainfall (2.5 km x 2.5 km grid) for a time horizon of 48 hours (Hirlam Aladin Regional Mesosclae Operational NWP in Europe). The average amount of precipitation in the case study is 763 mm per year, in which April is the driest month and July is the wettest month (World Weather & Climate information, 2020).

3.2.1 FH model
Catchment Geldrop-Mierlo was first modeled in InfoWorks ICM 10.0. This model was made for the water board and the municipalities. For this research, the FH model was transferred to SWMM5.1.

Although the conversion process from InfoWorks to SWMM is automated, several issues tend to arise during the process that needs to be sorted. These issues end up causing invalid parameters resulting in failure to simulate the system. Particular issues around the node depth, invert level, geometrical data, and DWF parameters arose and had to be sorted. The erroneous input parameters are replaced by values that are based on the InfoWorks ICM model and had to be extracted manually. Appendix 3 & 4 shows the adjustment of parameter information during the conversion process from InfoWorks to SWMM.

Addition of data to FH model
The available model contained model data for the catchment Geldrop East, Geldrop West, and Mierlo. Hereby, the model missed data concerning: catchment Eindhoven Stad, the DWF pattern, and the inflow from the area connected upstream of municipality Geldrop-Mierlo. A description of the added data is given below.

Catchment Eindhoven Stad

The UDS that is converted from InfoWorks only includes the UDS of Geldrop-Mierlo. However, for this study, the total inflow to the WWTP is important because the total inflow towards the WWTP determines whether an ammonium peak will occur. The total inflow includes the inflow from RZ, ES, and Nuenen-Son. For this study, the inflow from Nuenen-Son is neglected because the share of this catchment in the total WWTP inflow is relatively small. The total pumping capacity from the WWTP is compensated for this. Besides that, the current control gives priority during WWF conditions to RZ over ES, since the CSO location the Collse Molen is located in RZ. This causes, during WWF conditions, more pressure on the sewer system in ES, which might result in CSO events. The total inflow from Nuenen-Son during WWF conditions is not reduced. Therefore, Nuenen-Son is not included in the optimization problem in this research.

The optimization process will optimize the available in-sewer volume in catchment ES, but except for the pump, the actuators in the system are not optimized. Therefore, this system is added to the model in a simplified form. The sewer network of ES is simulated in one sewer tank, with a CSO location and a pump that pumps the water from the sewer tank to the WWTP. The characteristics of the sewer tank: sub-catchment information, rainfall, and total in sewer volume are obtained from the WEST simulator. Figure 11 shows the relation between the in-sewer volume and the total amount of spilled CSO volume. This relationship is based on a run of 300 days. It shows that CSO events occur if the in–sewer volume exceeds the amount of 165.000 m^3. Based on this information and the implemented storage curve in SWMM, it is possible to calculate the invert level of the CSO weir. The dimensions of the CSO weir (length and height) are determined by manually adjusting these dimensions in a trial-and-error manner. The eventual dimensions are a weir length of 10 m and a weir height of 10 meters. The pump characteristics are based on reality, with a maximum pump capacity of 8.3 m^3/s.
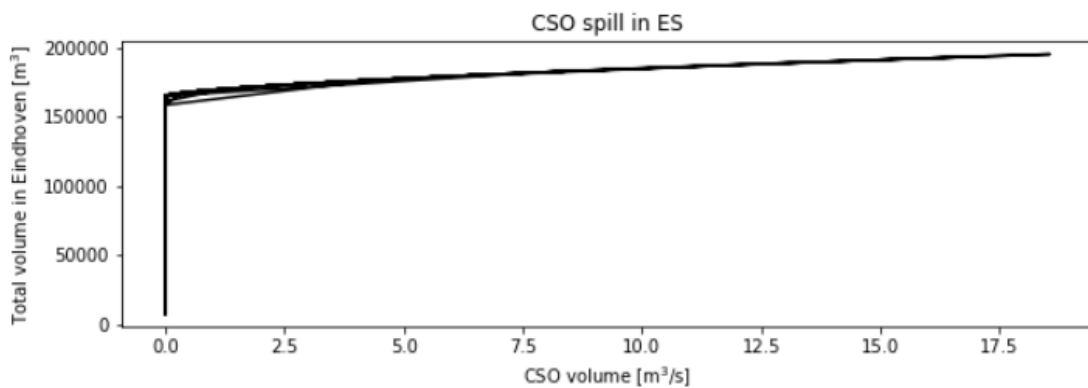

Figure 11: Relation CSO discharge and stored volume for catchment Eindhoven

Inflow upstream catchment

The total inflow from RZ to the WWTP is the sum of the inflow from UDS Geldrop-Mierlo and the inflow from the upstream area of Geldrop-Mierlo. The inflow from the upstream area is pumped by the pumps in Aalst and Heeze towards Geldrop-Mierlo. The time series of these pumps are added to the most upstream node in the case study area, to replicate the dynamics in the transport line RZ. By adding these pumps, the dynamics of the upstream part of the UDS are taken into account as well. The pump data was analyzed on incorrect outliers by checking whether both pumps are active during WWF conditions. Pump Aalst has 4 pumps and 2 pressure pipelines. It is assumed that during WWF conditions, both pumps (connected to the pressure pipeline) are operational. If one pump is not operational during WWF conditions, the flow rate of the other pump is copied and used as a proxy.

DWF pattern

The DWF pattern in SWMM consists of a baseline value, which is an indicator of the size of the catchments, and the DWF pattern. This DWF pattern was missing and is therefore manually added. This pattern is based on a Bachelor Project that focused on the sewer system of Eindhoven. Table 4 shows the used DWF pattern. The baseline value is abstracted from the InfoWorks model.

Table 4: DWF pattern SWMM

Name	Multipliers					
Hourly_pop_1	Hourly	1.12	1.00	0.91	0.81	0.72	0.64
		0.60	0.59	0.64	0.79	0.96	1.08
		1.17	1.21	1.23	1.23	1.21	1.17
		1.15	1.15	1.18	1.18	1.16	1.13
Monthly_pop_1	Monthly	0.99	1.05	1.12	1.18	1.06	0.94
		0.88	0.92	0.94	1.05	1.02	

Evaporation data

For SWMM to be able to calculate the exact runoff, it is required to implement the daily evaporation data in the model. The daily evaporation data that is used in this research, is provided by the Royal Netherlands Meteorological Institute.

Calibration FH model

The calibration of the FH model was evaluated based on available measurement data and multiple rainfall events with different characteristics (Table 5) (Figure 12).

Table 5: Available data for calibration

Measurement data	Parameter
Aalst_1	Pump rate pump Aalst_1 [m^3/hr]
Aalst_2:	Pump rate pump Aalst_2 [m^3/hr]
Heeze_1	Pump rate pump Heeze [m^3/hr]
RG_Mierlo_Q	Pump rate pump Mierlo
RG_Mierlo_H	Head directly upstream of pump Mierlo
WWTP_1	Pump rate pump_1 WWTP
WWTP_2	Pump rate pump_2 WWTP
Collse_Molen	Height measurements at CSO Collse Molen
Dom_008	Head node Geldrop West
Dom_009	Head node Geldrop West
Dom_042	Head control station Riool Zuid
GO1	Head Geldrop East
GO2	Geldrop East water height

The calibration of the locations GO1, GO2, and Mierlo was taken separately since the available measurement data was limited. Therefore, the preferred calibration events, which are described below, could not be used for the calibration of these locations. The measurement data for GO1 and GO2 was corrected by correction factors that were proposed by the data collectors. Details on this correction procedure can be found in appendix 5.
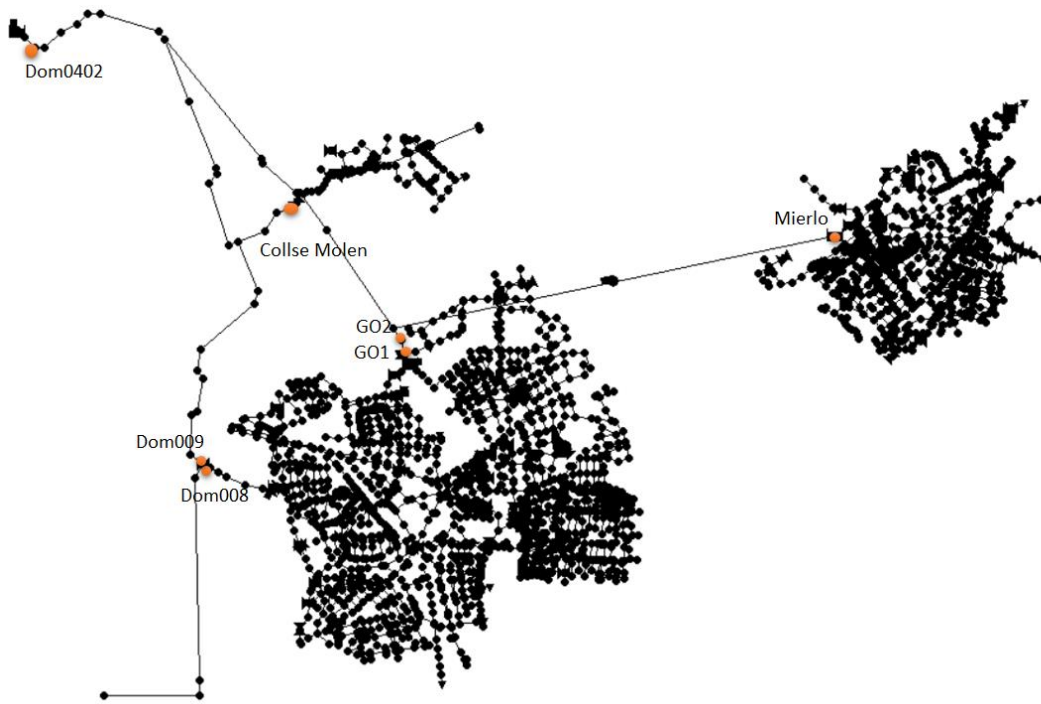
Figure 12: Locations available measurement data

For the calibration & validation, three rainfall events are used that have different characteristics. The events led to a significant rise in water levels in the sewer system and CSO event(s). The selected events and the corresponding characteristics are summarized in table 6. These rain events are selected because the characteristics of the events are different from each other, which induces different system states. Event 1, the calibration event, distinguishes from events 2 and 3 because the rainfall falls continuously throughout the whole calibration period. Event 2 (validation event) is characteristic of the high peak rainfall. Event 3 (validation event) consists of 2 single events which are both considered in the calibration process.

Table 6: Selected rain events with key characteristics

Event [dd-mm-yyyy]	Rainfall depth [mm]	Max rain intensity [mm/hr]
Event 1: 02/20/2020-02/24/2020	22.7	8.8
Event 2: 06/15/2020-06/18/2020	47.9	43.4
Event 3: 06/27/2020-07/01/2020	16.9	9.3

The rain events that were used to calibrate & validate Geldrop East and Mierlo are presented in table 7. These two additional events are used to calibrate the FH model since the available measurement data for Mierlo and Geldrop East were incomplete for the events described in table 7. The events in table 5 were selected because of the high maximum rainfall intensities and the difference in duration of peak rainfall. Event 4 is used during calibration and event 5 is used during validation of the FH model.

Table 7: Selected rain events with key characteristics used for calibration Geldrop East

Event [dd-mm-yyyy]	Rainfall depth [mm]	Max rain intensity [mm/hr]
Event 4: 02/22/2020 - 02/23/2020	18.6	13.5
Event 5: 02/09/2020 – 02/12/2020	23.5	20.5

3.2.2 Conceptual model

The FH model is divided into 3 catchments (Figure 13) respectively Geldrop East, Geldrop West, and Mierlo. For all the catchments, the network of conduits and nodes from the FH model is simplified into one sewer tank. The other elements that are included in the conceptual model are dependent on the characteristic components of that catchment in the FH model. Therefore, the different layouts of the 3 catchments are discussed below:
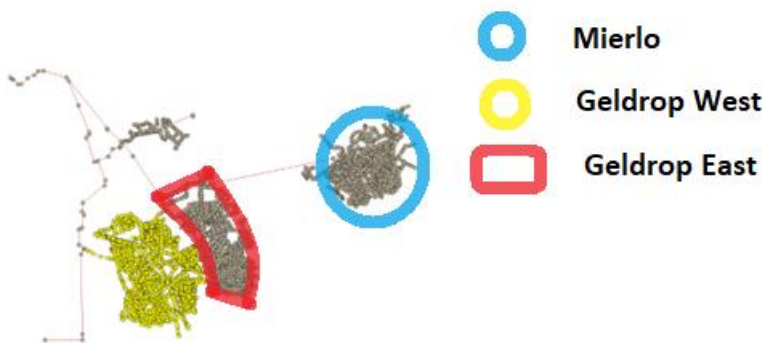

Figure 13: Division municipality Geldrop-Mierlo in 3 sewer catchments

The model structure followed previously developed structures used for RTC in the research of Van Daal-Rombouts et al. (2017), who used this layout and the corresponding principles to design a conceptual model. Here, this simplification is applied to the catchments Geldrop East, Geldrop West, and Mierlo. Figure 14 shows the schematic representation of Geldrop East & West. Geldrop East & West consists of a sewer tank that fills up by urban runoff, DWF, and water directed back from the storage tank. The outflow of the sewer tank is divided into discharge towards the WWTP via a transport line, discharge via a CSO, and flow to the settling tank. If the full capacity of the storage tank is reached, the water will discharge over a CSO to the river. If the storage tank does not fill up completely and the sewer has available capacity, the water will be redirected by a pump to the sewer tank.

The following components are deemed to be necessary to keep as it is in the FH model:

- Transport line RZ: Since Geldrop Mierlo is located at the most downstream end of RZ, the dynamics in RZ influence the dynamics in UDS Geldrop Mierlo. Therefore it is important that the dynamics in RZ are simulated as accurately as possible, to ensure that this influence of RZ is considered during the simulation process. Therefore, the part of transport pipeline RZ that covers Geldrop-Mierlo, is copied into the conceptual model.
- CSO Collse Molen: Because CSO Collse Molen is connected to the transport line (RZ), it can have a destructive ecological impact if it spills. Therefore, great emphasis is put on this CSO location to prevent it from overflowing. The weir characteristics and the connected conduits to this CSO location are copied from the FH model, to be able to exactly monitor its behavior and dynamics. By doing so, it was possible during the optimization process to put extra emphasis on preventing this CSO location from overflowing.
- Pumps with corresponding pump curves: the existing pumps and the corresponding pump curves are copied from the FH model into the conceptual model. Pumps are considered characteristic of the hydraulic behavior in the system.
- Settling tank with corresponding storage curves: the settling tanks cause additional in-sewer storage options that impact the hydraulic behavior in the system and might impact the occurrence of CSO events.

The sewer tank of Geldrop West is connected to the transport pipeline(RZ) via a vortex valve. This valve can be adjusted, and thereby control the flow that enters RZ from Geldrop West.

Geldrop East has the same layout as Geldrop West, except that the connection is not a vortex valve but a regular conduit. Besides that, Geldrop East has 2 storage tanks, that both have an outfall and a pump. The sewer tanks of Geldrop West and Geldrop East are connected via a regular conduit. Water can flow in both directions.
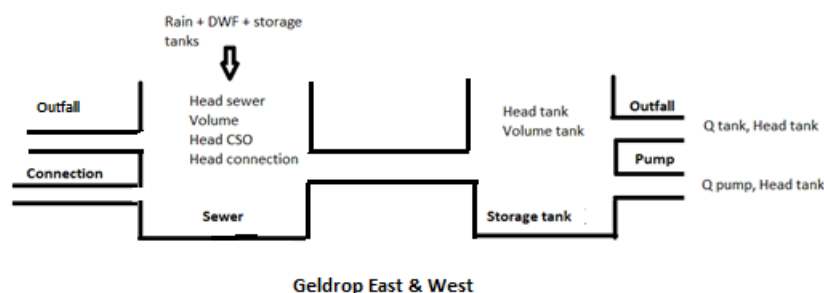
Figure 14: Schematic overview catchment Geldrop West & Geldrop East

Mierlo consists of a sewer tank that fills up by urban runoff and DWF. The outflow of the sewer is divided into an overflow that is pumped out of the sewer and a CSO location. The catchment Mierlo does not contain a settling tank, like in Geldrop East & West), therefore the layout of this catchment in the conceptual model is slightly different. The schematic representation of Mierlo is shown in Figure 15.

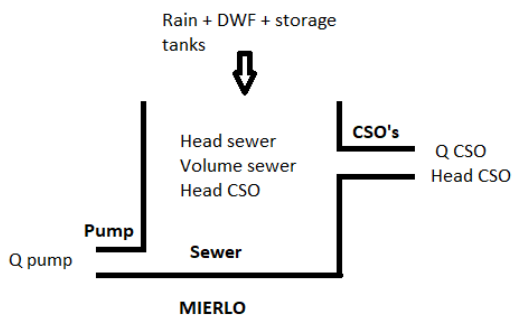*Figure 15: Schematic representation of the model Mierlo*

The schematic overview of the conceptual model in SWMM can be found in figure 16.
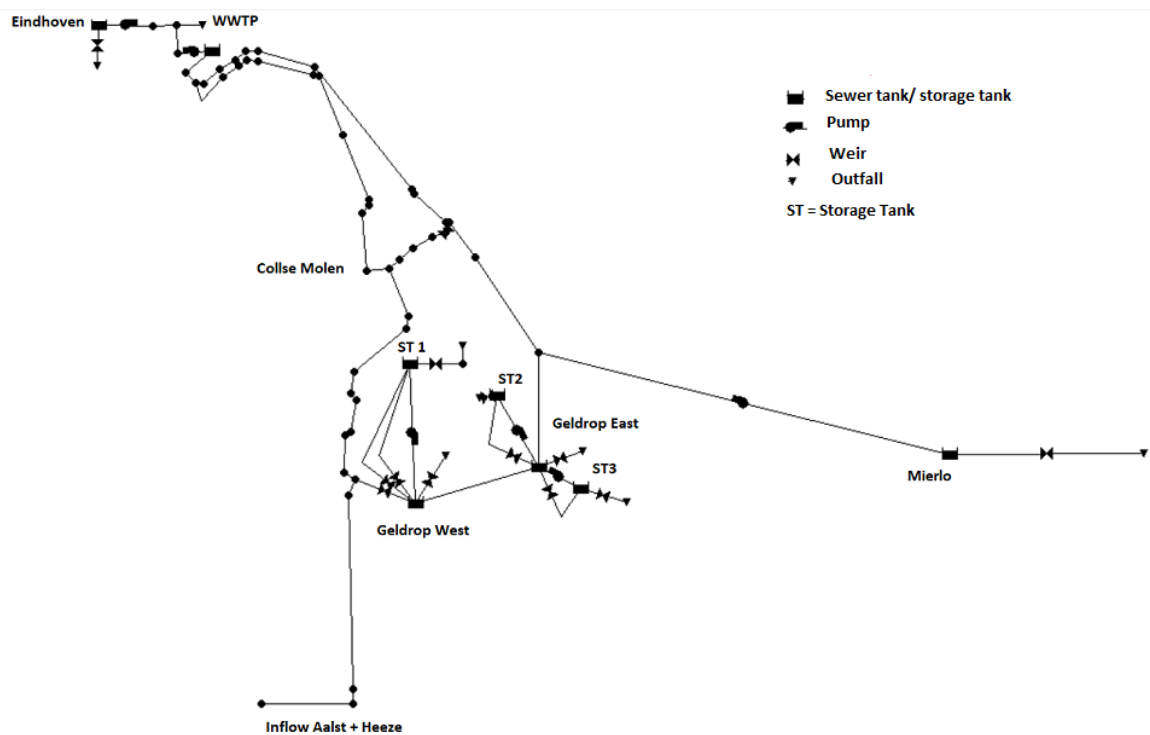

Figure 16: Schematic overview conceptual model in SWMM

Calibration/ validation conceptual model

The conceptual model is calibrated during event 2 (table 5) and validated during the events described in table 8.

Table 8: Selected rain events with key characteristics

Event [dd-mm-yyyy]	Rainfall depth [mm]	Max rain intensity [mm/hr]
Event 6: 12/13/2020– 12/15/2020	10.7	3.0
Event 7: 10/27/2020 - 10/30/2020	12.4	8.0

By calibrating the model during different events than used in the calibration of the FH model, it is ensured that the model is not overfitted for certain events. The characteristic of event 4 (table 5) is the high hourly rainfall intensity. The characteristic of event 6 is the long duration of the continuous inflow of lower rainfall events. Event 7 is characteristic of a single high rainfall peak. The different events induce a broad spectrum of system states, which will help calibrate the model.

3.2.3 Optimization process

During the optimization, the head of the node just upstream of the WWTP in the FH model is used to determine whether the optimization process can start. This threshold is set to a head of 12 m +NAP.

The actuators that are optimized in the system are:

- Pump target setting Mierlo
- Pump target setting Eindhoven to WWTP
- Vortex valve flow limit Geldrop West

To ease the optimization process, the boundaries for the actuator settings are represented by integer values between [-10, 10]. These integer values are translated to values between [-1, 1] in the case of the target settings of the pumps. Whereas these integer values are translated to [-0.16, 0.16] in the case of the vortex valve. The integer values indicate the change compared to the previous timestep. Meaning, that if a pump has a target setting of 0.1 at timestep [x] and the integer value is 3, the target setting at timestep [x+1] is 0.4. It is not possible that the target setting of the pumps exceeds 1, since this indicates a non-available pumping capacity. The maximum flow through the vortex valve is 0.25 m3/s, therefore the maximum flow through the valve in the optimization process cannot exceed this threshold. An overview of the population of the GA is presented in figure 17.
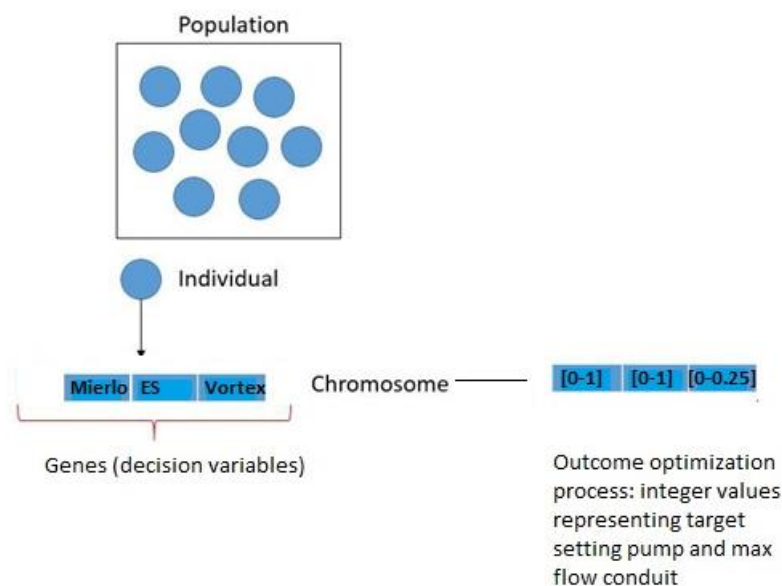
Figure 17: Explanation population GA

Rainfall events used during the optimization process

The MPC procedure is tested with 2 different events. The first event is event 4 (table 5). The second event is from 02/16/2020-02/17/2020. The rain event is characterized by a single peak of 10.1 mm depth with a maximum rainfall intensity of 31mm/hr. Both the selected events have in common that the total amount of rainfall per event is high, but the events complement each other because the maximum rainfall intensity for event 2 is larger than for event 1, whereas the duration of event 1 is longer. These differences result in a different outcome of the MPC procedure and indicate whether the MPC procedure anticipates correctly on the different events.

3.3 Ecological issues concerning wastewater system Eindhoven

The size of the wastewater system compared to the Dommel can be expressed by the ratio between the WWTP effluent and the river base flow. The ratio is approximately 1:1 during a dry day in a dry summer period. This means that downstream of the WWTP, the total amount of river water consists of equal parts of original river water and treated wastewater. During a large rain event in the dry period, this ratio can extend to 9:1, meaning that 90% of the river water consists of WWTP effluent and 10% consists of original river water. These ratios indicate that the influence of the WWTP on the Dommel is significant and that hereby the river is vulnerable to malfunctioning of the WWTP or sewer systems.

The high share of the effluent as explained above induces strict rules for the operation of the WWTP. The main problems that can be found due to WWTP effluent in the Dommel are dissolved oxygen depletion, ammonia peaks, and seasonal average nutrient concentration levels (Langeveld et al., 2017). WWTP effluent appeared to be the main source for toxic ammonia peaks in the Dommel. These ammonia peaks are caused by peak inflow to the WWTP. The surface water quality standards that apply for the river Dommel, are relatively strict due to the river's function of 'fish water for Cypriniformes'. However, the Dommel River does not yet meet the requirements of the European Union Water Framework Directive (WFD)(Directive 2000/60/EC of the European Parliament and of the Council establishing a framework for the Community action in the field of water policy).

Dissolved oxygen (DO) depletion is mainly caused by CSO events. A major problem in the municipality of Geldrop-Mierlo is the occurrence of CSO events that discharge on the Kleine Dommel. The Kleine Dommel is a river with a low flow. The low flow implies that CSO events might cause great oxygen dips. This might have a notable impact on the ecology of this water. Therefore, the European Water Framework Directive set regulations, to minimize the environmental impact on the Kleine Dommel.

The following locations along the river were considered during the DO analysis: S001, S084, S032, S061, S010, S099, and S012 (Figure 18). The Kleine Dommel is indicated in red.
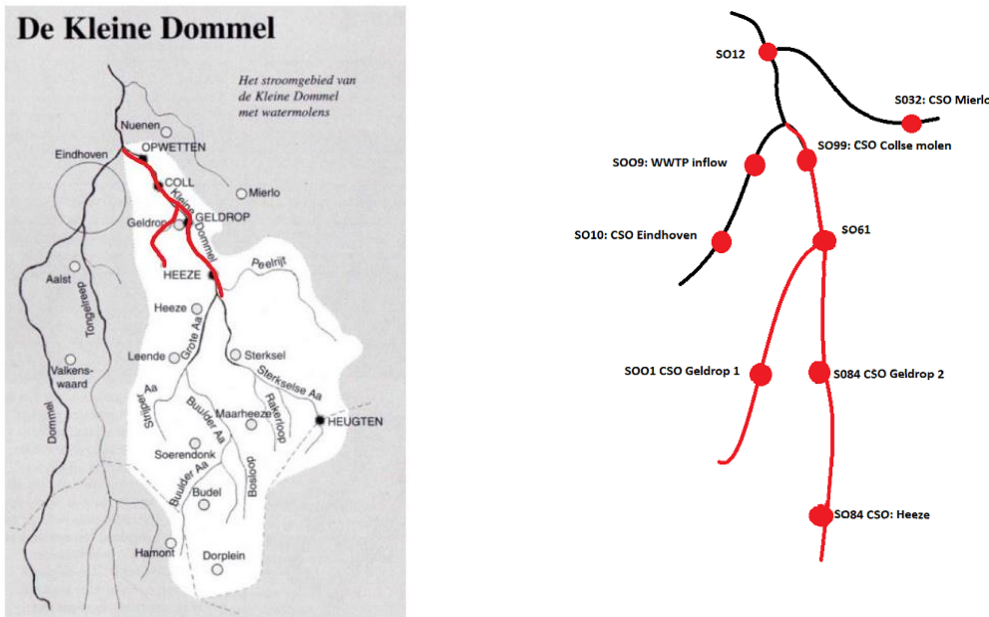

Figure 18: Overview locations data collection (watermolen-coll (collsemolen.nl))

The NH_4^+ concentration was only obtained at location S009 since this is the location where the Dommel receives the WWTP effluent.

3.4 RTC in the case study area

As is described in the introduction, there are multiple possibilities for a RTC to improve the wastewater system of Eindhoven. The complexity of this research can be found by balancing oxygen dips caused by CSO events in Geldrop-Mierlo (on the Kleine Dommel) and ES (on the Dommel) and reducing NH_4^+ peak concentration in the WWTP effluent. This study tries to balance these events by optimizing the available storage in Geldrop-Mierlo. The system boundaries are set by the upstream pumping station Aalst and the capacity of the WWTP.

This area could be suitable for the implementation of RTC because of multiple reasons. The total area of the UDS consists of approximately 600 km^2, meaning that severe storms are likely to pass over parts of the area only. This might create a possibility for RTC optimization to use the differences in in-sewer stored volume as a buffer to obtain the set objectives. Another areal benefit of this UDS could be that the arrival times of peak inflow of the sewer catchments are different. Therefore, there could be possibilities for RTC to optimize this inflow towards the WWTP.

Earlier research proved that the use of RTC by activating in-sewer storage volume to reduce and delay hydraulic peak loading of the WWTP during heavy rain events is an effective measure (Langeveld et al., 2013). In addition to the aforementioned RTC method is a new RTC concept introduced by van Daal-Rombouts et al. This method, the smart buffer, minimizes the peak load to the biology at the WWTP

by using the RTC method described above in combination with using only one of the three primary clarifies (PCs) during DWF and using the other two PCs only during storm events (van Daal-Rombouts et al., 2017).

The RTC potential of this case study is also assessed with the PASST tool. The scoring table that is used to assess this, and the explanation of the scoring table, can be found in Appendix 6. Table 9 shows the outcome of the pre-assessment of the RTC potential of this case study area based on the scoring table. The awarded scores for each answer are stated after the answer. Appendix 7 gives an additional explanation to this table.

Table 9: PASST table applied to case study

Catchment	Wastewater production	Sewer system		Operational system behavior	Receiving water	Wastewater treatment plant (WWTP)
A.1. Catchment area (Flow length in the main collector) *Large: > 5 km (2)*	B.1 Area with increased pollution of surface runoff *None (0)*	C.1. Number of existing control devices *Several (4)*	C.5. Number of discharge devices *None (0)*	D.1. Local flood areas *None (0)*	E.1. Local differences in hydraulic capacity *Strong (4)*	F.1. Admissible combined wastewater inflow
A.2. Differences between current and planned development of the area *Small (1)*	B.2. Variability in time and space of wastewater production *None(0)*	C.2. Slope of trunk sewers *Flat (4)*	C.6. Total storage volume *>5000 m3 (4)*	D.2. Number of non-uniformly used tanks *>1 (4)*	E.2. Local differences in load capacity *Medium (2)*	F.2. Sensitivity of WWTP to hydraulic or pollutant peaks *Very sensitive (2)*
		C.3. Capable loops in the sewer system *None (0)* C.4. Number of existing storage tanks *>4 (4)*	C.7. Specific storage volume *> 40 m3/ha (4)*	D.3. Non-uniform discharge behavior *Significant (4)*	E.3. Sensitivity of the receiving water body *Very sensitive (2)*	

The final score of this pre-assessment is 41, which indicates that further investigation in implementing RTC is recommended (>35 score) since RTC has the potential in improving the system performance.

4 Results

The methodology that is explained in Chapter 2, is used to obtain the results for the research questions and the corresponding sub-questions. In this chapter, the results, that are obtained during this study, will be presented.

This chapter consists of 5 sections. Chapter 4.1 presents the dynamics of the oxygen and ammonium concentrations during different rainfall events. These dynamics give insight into the characteristics of the rainfall event that causes an ammonium peak/ DO dip. This relation will be used during the optimization process (Chapter 4.5). Chapter 4.2 describes the calibration and validation results of the full hydrodynamic (FH) model against available measurement data. Chapter 4.3 presents and discusses the creation of the conceptual model. Chapter 4.4 discusses the calibration and validation results of the conceptual model against the FH model. Lastly, in Chapter 4.5 the optimization results are presented and discussed.

4.1 Dynamics oxygen and ammonium objectives

In this chapter, the dynamics of the ammonium and DO concentrations are explored using the simulator WEST. The ammonium and DO concentrations are simulated in the WEST simulator for 365 days: from 1 January 2019 – 31 December 2019. The trade-off will be explored by determining the effect of certain rainfall characteristics on the DO and ammonium concentration levels in respectively the CSO discharge and WWTP effluent.

Rainfall characteristics

During the year 2019, a total of 911 mm of precipitation fell in the case study area. Especially during the months March-July, the precipitation that fell in the UDS is higher than expected for that period (Figure 19). A total of 165 rainy days were recorded in the year 2019. This is above the mean total amount of rainy days, which is 137 days per year. An extreme rainfall event is defined by a rainfall intensity that is higher than 10 mm/ 12 hrs. In this case study, a total of 26 days exceeded this rainfall intensity, and are therefore defined as extreme events.

Overall, the rainfall events in 2019 show extremer characteristics than the average rainfall characteristics. However, this will not influence the outcome of this sub-question negatively, since a wider range of rainfall events will induce a wider range of system states and hereby the dynamics in the system will become more clear.
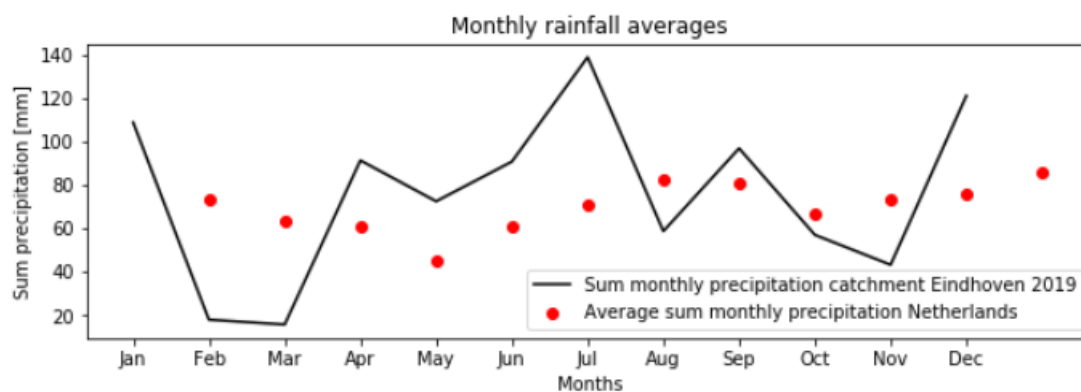

Figure 19: Monthly precipitation for Netherlands (average over years) & Eindhoven (year 2019)

Dissolved Oxygen Dips Occurrence

In this analysis, there is a distinction made between rainfall events in 2019 that cause a DO dip (DO concentration < 4 mg/L) or an ammonium peak (> 3 mg/L) and all the rainfall events that occurred in the year 2019. The ammonium and DO concentration levels are abstracted from the output of a simulation from the WEST simulation tool.

To get a better understanding of the dynamics of DO and ammonium concentration during WWF flows, individual events are analyzed on rainfall intensity, DO concentration, and ammonium concentration. Figure 20 shows an overview of a rainfall event that causes both a DO dip and an ammonium peak. The ammonium peak is caused by a rainfall intensity of 3 mm/hr. The total duration of the ammonium peak is 14 hours. The CSO event, and thereby the DO dip, takes place directly after the end of the rainfall event. This can be explained by the increasing filling degree of the sewer catchment (Figure 21). Figure 21 shows that the filling degree of catchment ES is above 1. This means that there is no available in sewer volume available and that CSO events will occur. The filling degree of RZ remains at a level of 0.9 to prevent the CSO location Collse Molen from spilling. This suggests RTC potential as a means of CSO reduction, as some additional storage could be activated to further minimize the impact of CSOs.
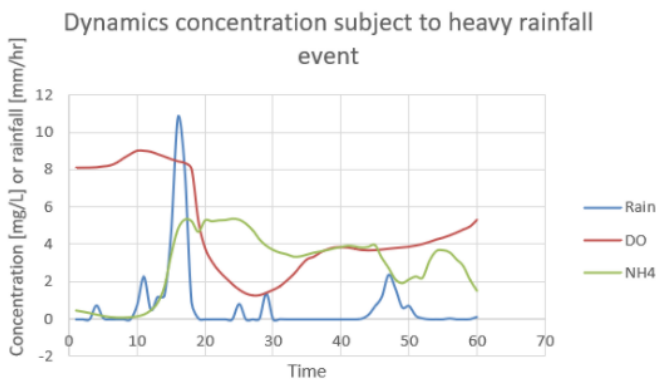

Figure 20: Ammonium and DO concentration in river during heavy rainfall event
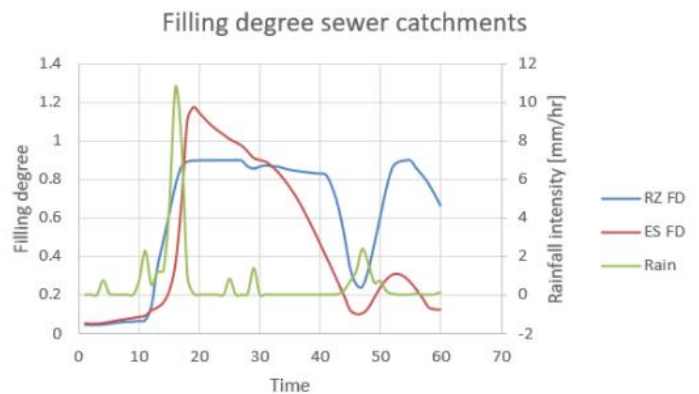
Figure 21: Ammonium and DO concentration in UDS during heavy rainfall event

The focus on a single event, as described above, can give a better insight into the system dynamics but it does not give a clear insight into the systems' behavior during rainfall events with different characteristics. Therefore, the occurrence of all DO dips and ammonium peaks over 1 year are analyzed, to ensure that the tradeoff is based on rainfall events with different characteristics.

2019 counts a total of 185 rain events, from which 60 rain events cause an oxygen dip somewhere in the UDS of Eindhoven. 75% of the rainfall events that cause an oxygen dip have a rainfall depth >7 mm. Whereas 25% of all the rainfall events in 2019 have a rainfall depth > 7 mm. This suggests that during rainfall events with a rainfall depth > 7 mm, the chance of the occurrence of a DO dip increases. Those findings are plotted in boxplots in figure 23. Boxplot 1 shows the results for all rain events in 2019, whereas boxplot 2 shows the results for the rain events that cause a DO dip.

Aside from the rainfall depth, the maximum intensity during a rainfall event is an important characteristic as well. 75% of the time, the maximum intensity of a rainfall event that causes a DO dip, is 2.5 mm/hour or higher. Whereas, 75% of all the rain events in 2019, have a maximum intensity of 2 mm/hr and lower (figure 22). These results show a clear difference between the maximum rainfall intensity for events that cause a DO dip (Boxplot 2) and for regular events (Boxplot 1).
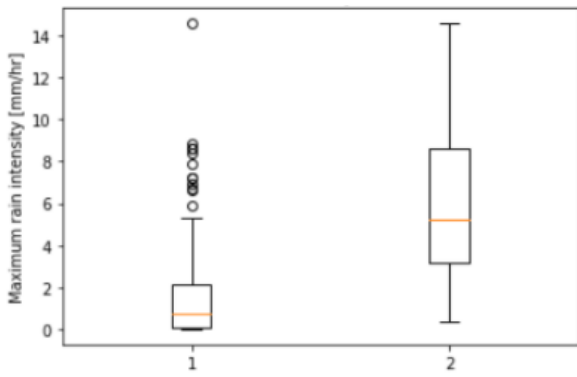
Figure 22: Boxplots maximum intensity rain events. Boxplot 1) for all rain events in 2019. Boxplot 2) for DO events
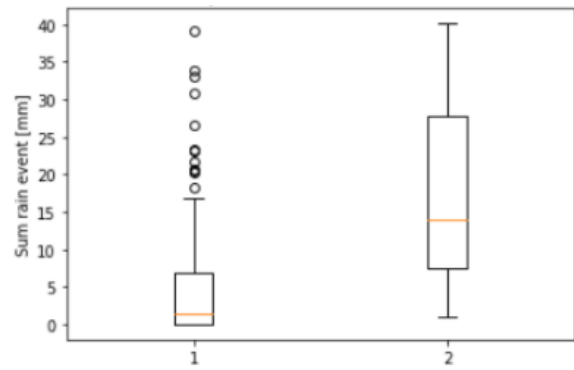

Figure 23: Boxplots total sum rainfall events. Boxplot 1) for all rain events in 2019. Boxplot 2) for DO events

To validate that the relationship between the rainfall characteristics and the occurrence of DO events is valid, the definition of an oxygen dip is changed to a concentration of 3 mg/L instead of 4 mg/L. The results show that the threshold for both the sum of a rainfall event and the intensity, shifts upwards (Figures 24 & 25). 75% of the DO dips with a concentration of 3 mg/L and lower, have a maximum rainfall intensity of 3.45 mm/hr and higher, and a total sum of rainfall of 11 mm and higher. For the threshold of 4 mg/L, both the maximum intensity and total sum of rainfall are lower compared to the results based on a threshold of 3 mg/L.

This result indicates that the relationship between the DO concentration and the rainfall characteristics is valid.
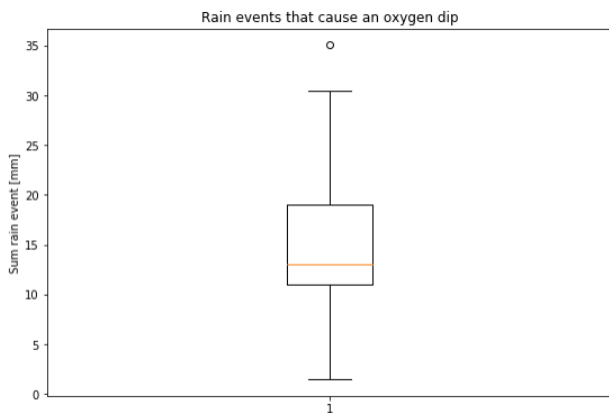

Figure 24: Boxplot total rainfall for events that cause oxygen dip
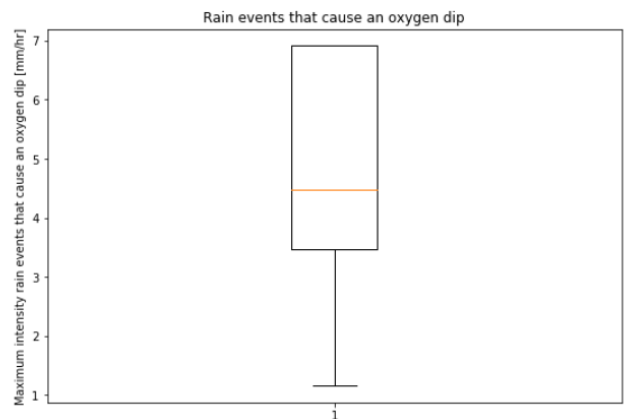
Figure 25: Boxplot maximum intensity rain events that cause oxygen dip

The above results give, besides the relation between rainfall characteristics and ammonium/ DO events, a rough indication of the tradeoff that can be implemented in the objective function. The decision tree in Figure 26 is computed, to support these findings and to give a more detailed trade-off. The decision tree gives insight into the trade-off between the DO and ammonium concentration, by categorizing predictions based on a dataset that includes information about the rainfall characteristics that caused a DO dip/ ammonium peak. The input data contained information regarding the duration, rainfall depth, and rainfall intensity of all the events in 2019. The decision tree is trained on 95% of the rainfall events of all these events. The remaining 5% of these events are used to validate the outcome of the decision tree, the tree is not trained on these events. 8 out of the 10 validation events show correct results, indicating that the decision tree is accurate enough to use to determine the trade-off

of the objectives. Figure 26 shows the outcome of the decision tree. It shows that only the maximum intensity and the rainfall depth (sum) are important for determining the trade-off since the duration of a rainfall event is not included in the decision tree. The rough indication that is made based on the boxplots in Figure 22 indicated that 75% of the rainfall events that cause a DO dip have a maximum intensity of 2.5 mm/hr and higher. As can be seen in Figure 26 the decision tree has multiple decision criteria, however, rainfall events that have a maximum intensity of 3.13 mm/hr and higher indicate that the objective function should aim to prevent DO dips. For the rainfall events with lower rainfall intensity, another distinction is made based on the rainfall depth. If the rainfall depth is higher than 4.8 mm, the objective function should aim to prevent DO dips.

So based on this decision tree, the trade-off between the two objectives can be based on either solely the maximum intensity (> 3.13 mm/hr is DO) or if the intensity is lower than 3.13 mm/hr, the rainfall depth should also be included in the analysis. If so, the thresholds of maximum intensity and the rainfall depth are respectively 3.07 mm/hr and 4.83 mm. For the case of using the DO objective, the rainfall intensity should be lower than 3.07 and the rainfall depth is >4.83 mm, for the ammonium objective this is vice-versa.
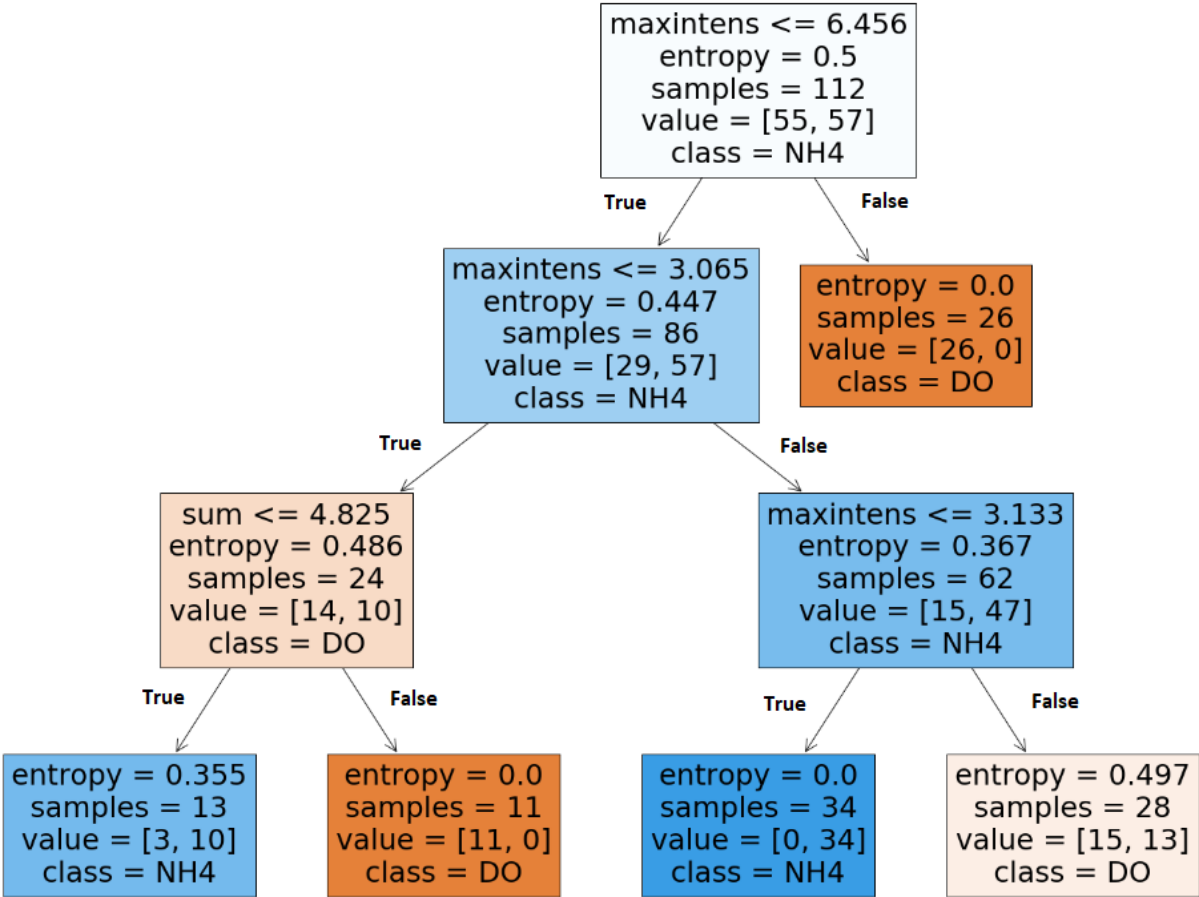

Figure 26: Decision tree trade-off DO and ammonium concentration

4.2 Calibration and validation results FH model

In this chapter, the calibration and validation results of the FH model are described. Events 1 and 4 are used during the calibration process, whereas events 2, 3, and 5 are used during the validation process.

An overview of the calibration & validation results (expressed as NSE values) are presented in table 10. The table contains the results for locations Dom008, Dom009, Dom0402 & Collse Molen (event 1, 2, 3) and the results for the locations GO1, GO2, and Mierlo (event 4 & 5) (Figure 12). The NSE values for the calibration events range from 0.62-0.91 (table 10). The overall best performance was for the head at location Dom009, whereas the lowest performance is found at location Mierlo. The NSE values for the validation events range from 0.2-0.92. The overall best performance was again for Dom009, whereas the lowest performance was for Dom0402. The lowest performance was found for the head in Mierlo and Dom0402. Dom0402 is located directly upstream of the WWTP and therefore gives a good indication of the accuracy of the WWTP pump settings in the FH model. The actual pump settings are dependent on the system states in the multiple sewer catchments that are connected to the WWTP. The pump settings in the FH model are described by a few rules, and do not include the system states of the multiple sewer catchments, since including the multiple sewer catchments in the model is out of the scope of this research. During the evaluation of the calibration and validation results, it is considered whether describing the pump settings of the WWTP with a few rules, is sufficient to capture the corresponding dynamics within the system.

Table 10: Overview calibration/ validation results

Rainfall event	Calibration/ validation	Rainfall depth [mm]	Max rainfall intensity [mm/hr]	NSE Dom008	NSE Dom009	NSE Dom0402	NSE Collse Molen
#1 02/20/2020-02/24/2020	Calibration	22.7	8.8	0.87	0.91	0.70	-
#2 06/15/2020-06/18/2020	Validation	47.9	43.4	0.65	0.90	-	0.92
#3 06/27/2020-07/01/2020	Validation	16.9	9.3	0.45	0.88	0.20	0.52
				NSE GO1	**NSE GO2**	**NSE Mierlo**	
#4 02/22/2020-02/23/2020	Calibration	18.6	13.5	0.73	0.89	0.62	
#5 02/09/2020-02/12/2020	Validation	23.5	20.5	0.75	0.88	0.50	

Below, the calibration and validation results of events 1 and 2 are discussed. In Appendix 8 the remaining calibration and validation events (events 3 -5) are discussed.

The calibration results of event 1 for locations Dom008 & Dom009 show that during the large peak (02/23/2020), the outflow from Dom008 to Dom009 is slightly lower than in the measurement data (Figure 27). This results in a lower peak in Dom009 and a higher peak in Dom008. The connection between Dom008 and Dom009 is simulated in the FH model as a vortex valve. Dom009 is located in RZ, and the head is predominantly determined by the inflow from the downstream pumping station (Aalst). The outflow from catchment GW (Dom008) to RZ (Dom009) is very small compared to the total flow in RZ. However, it appeared to be that the head at Collse Molen is very sensitive to the outflow from GW-RZ. Therefore, the vortex is tuned with the main aim to correctly simulate the head at location Dom009, since this head might influence the head, and thereby the overflow probability, at CSO location Collse Molen. It is found that the flow over the vortex is very sensitive to small adjustments. Considering this, the relatively low deviation during this peak is considered acceptable (Figure 28).

The calibration results for location Dom0402 give indirect insight into the accuracy of the operation of the WWTP in the FH model because Dom0402 is located directly upstream of the WWTP. The calibration result shows that during lower heads, the head of the FH model is too small. Whereas, during higher heads, the head is too large. The dynamics (emptying and filling of the system) occur at the same rate and time. Besides that, the influence of these higher peaks does not influence the head of the locations more upstream (Collse Molen & Dom009). Based on this, it can be concluded that the WWTP settings, which might differ a bit from the actual WWTP settings, have predominately an effect on the locations just upstream of the WWTP. Therefore, the system performance that is obtained with the current WWTP settings is considered sufficient.
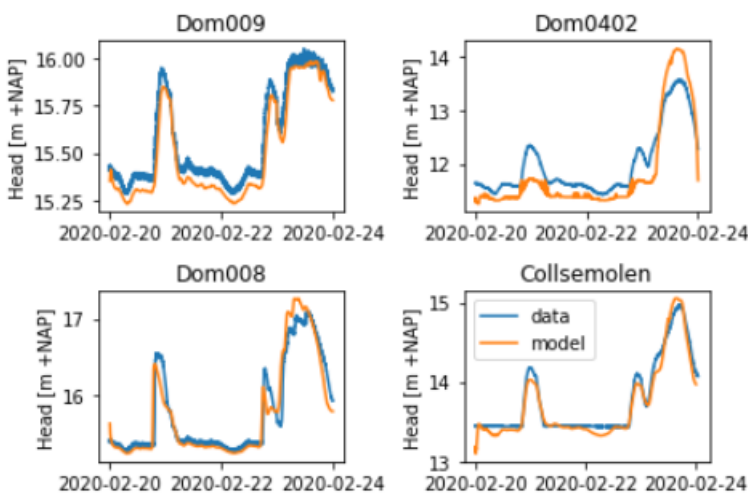
Figure 28: Calibration results event 1
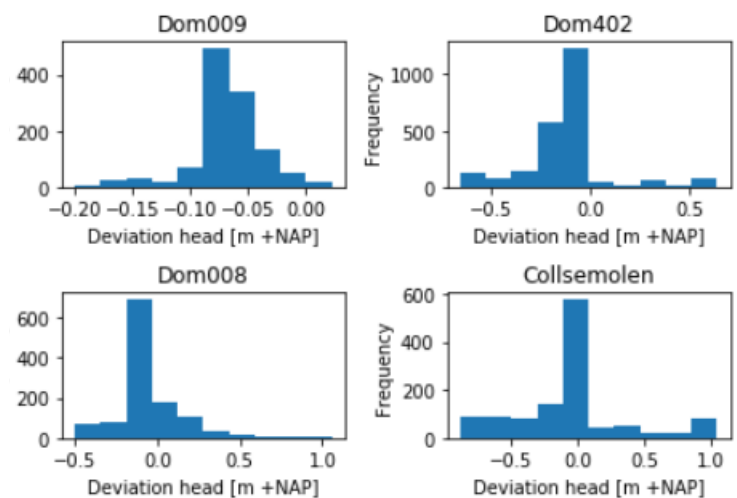
Figure 27: Deviation calibration results event 1

The validation results for Dom008 show an increased head for the first peak. This indicates that the total outflow from Dom008 to Dom009 is lower than in the measurement data, which results in a lower head at location Dom009. This is caused by a small deviation of the flow over the vortex (Figure 29). But, as explained in event 1, the flow over the vortex is very sensitive to small changes. Since the flow over the vortex does not impact the validation result of Collse Molen, the validation results are considered acceptable.

The measurement data of Dom0402 are missing, therefore this location is not considered in the calibration evaluation.

Figure 29: Validation results event 2

Figure 30: Deviation validation results event 2

4.3 Results creation conceptual model

The dynamics needed for the model structure selected for the internal-MPC model are derived from the FH model and explained in chapters 4.3.1-4.3.3. These relationships are thereafter applied to the conceptual model and the calibration and validation results of the model are discussed in chapter 4.4.

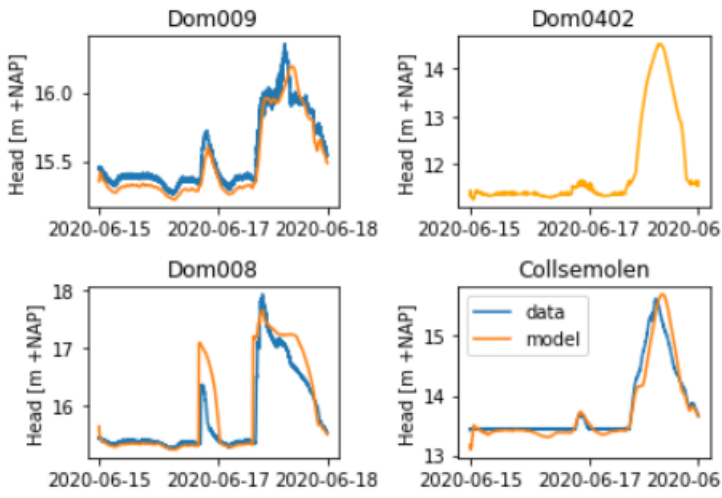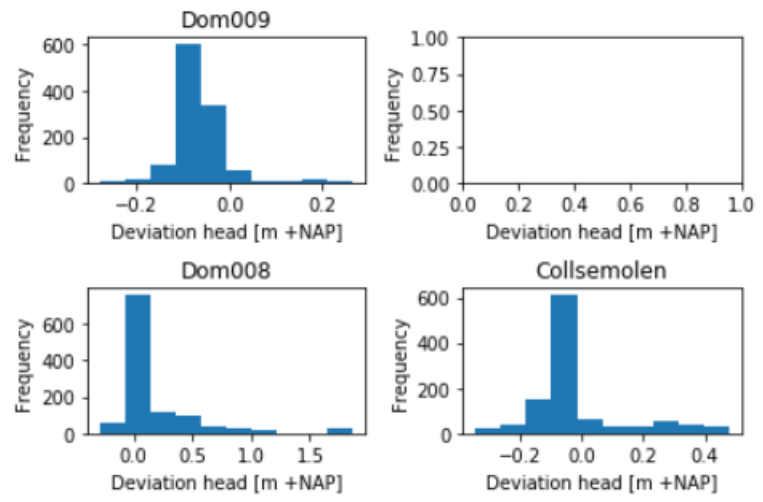### 4.3.1 Geldrop West

The storage curve of GW shows that during peak flows hysteresis occurs (Figure 31). Since the conceptual model will be based on a singular storage curve, the rising or the falling branch of the storage curve must be selected for the conceptual model. The choice for the rising or falling branch is made based on comparing the most significant system dynamics of the conceptual model and the FH model subject to both branches. The most significant system dynamics are compared in the analysis of the results: head at (1) CSO location Collse Molen, (2) outflow to RZ, and (3) total CSO discharge from catchment GW. For catchment Geldrop West, the falling branch is selected. Therefore it is expected that the head might be higher at a certain volume than simulated in the FH model. The implications of this choice will be further described in Chapter 4.4, but also affect the other relationships that will be discussed below.

The connection between RZ and GW is established via a vortex valve. Later on in this research, this connection will be replaced by a moveable weir to explore further RTC possibilities. The characteristics of this vortex valve in the FH model: shape, height, and discharge coefficient, are used in the conceptual model as well. Especially during the lower head, the relationship in the conceptual model differs from the FH model (Figure 31). This is a direct consequence of the used storage curve in the conceptual model. As can be seen in Figure 31, the storage curve for lower heads (< 16.5 m +NAP) increases faster because of the choice of the falling branch. This impacts the flow dynamics.

In the conceptual model, there is 1 CSO location per catchment that needs to simulate the different CSO flows from the FH model. The FH relation gives the clear insight that at a head of 17.6-17.7 m +NAP most of the CSO events occur (Figure 31). This information is used to set the height of the weir inlet in the conceptual model. The number of CSO locations in GW is high. The weirs of these CSOs have different settings. Therefore, at some CSO locations, a CSO event is initialized with a smaller amount of rain than at other CSO locations. These CSO events occur between 15.8-17.5 m +NAP. Since the frequency and magnitude of these events are little, these events are not considered in the conceptual model. The inlet offset for the weir is set to 17.5 m +NAP. The weir settings: height, length, and discharge coefficient are determined following a trial and error manner.
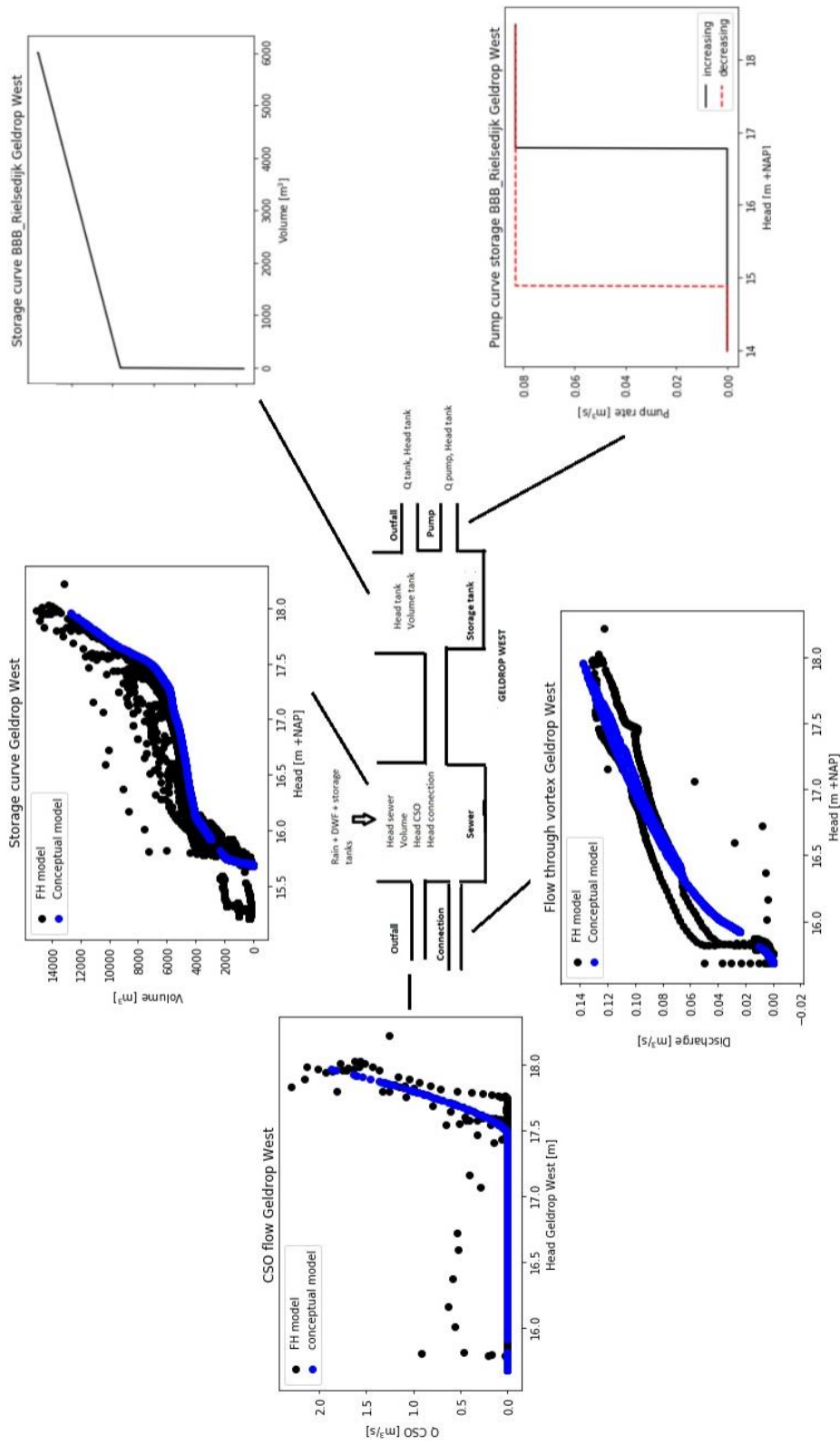
Figure 31: Dynamics FH model GW for in the conceptual model

4.3.2 Geldrop East

The catchment Geldrop East is connected to RZ and via 3 connection points connected to the catchment GW. The storage curve shows a hysteresis in the model, which requires a decision during the design of the conceptual model concerning the usage of the rising or falling branch of the storage curve (Figure 32). The choice for the rising or falling branch is made based on comparing the most significant system dynamics of the conceptual model and the FH model subject to both branches. This resulted in comparable outcomes. Since this study focuses on the correct simulation of the timing of CSO events, it is chosen to work with the falling branch as a storage curve since the head levels will be simulated correctly.

The CSO discharge curves from the FH model show a triangle shape between 16.5 and 17 m +NAP head. The majority of CSO events occur at 17 m+ NAP. However, between 16.5 and 17 m+ NAP remarkable more CSO events occur than at head levels lower than 16.5 m + NAP. Therefore, the CSO weir inlet height is set to 16.7 m +NAP. Hereby, the majority of events that occur between 16.5 and 17 m +NAP are captured, as well as the events that happen at 17 m +NAP. The impact of this design choice is that, for some events, the timing of the occurrence of a CSO event might be shifted. The weir parameters in the conceptual model are determined following a trial-and-error method. The following weir parameters are included: Discharge coefficient, height, and length of the weir.
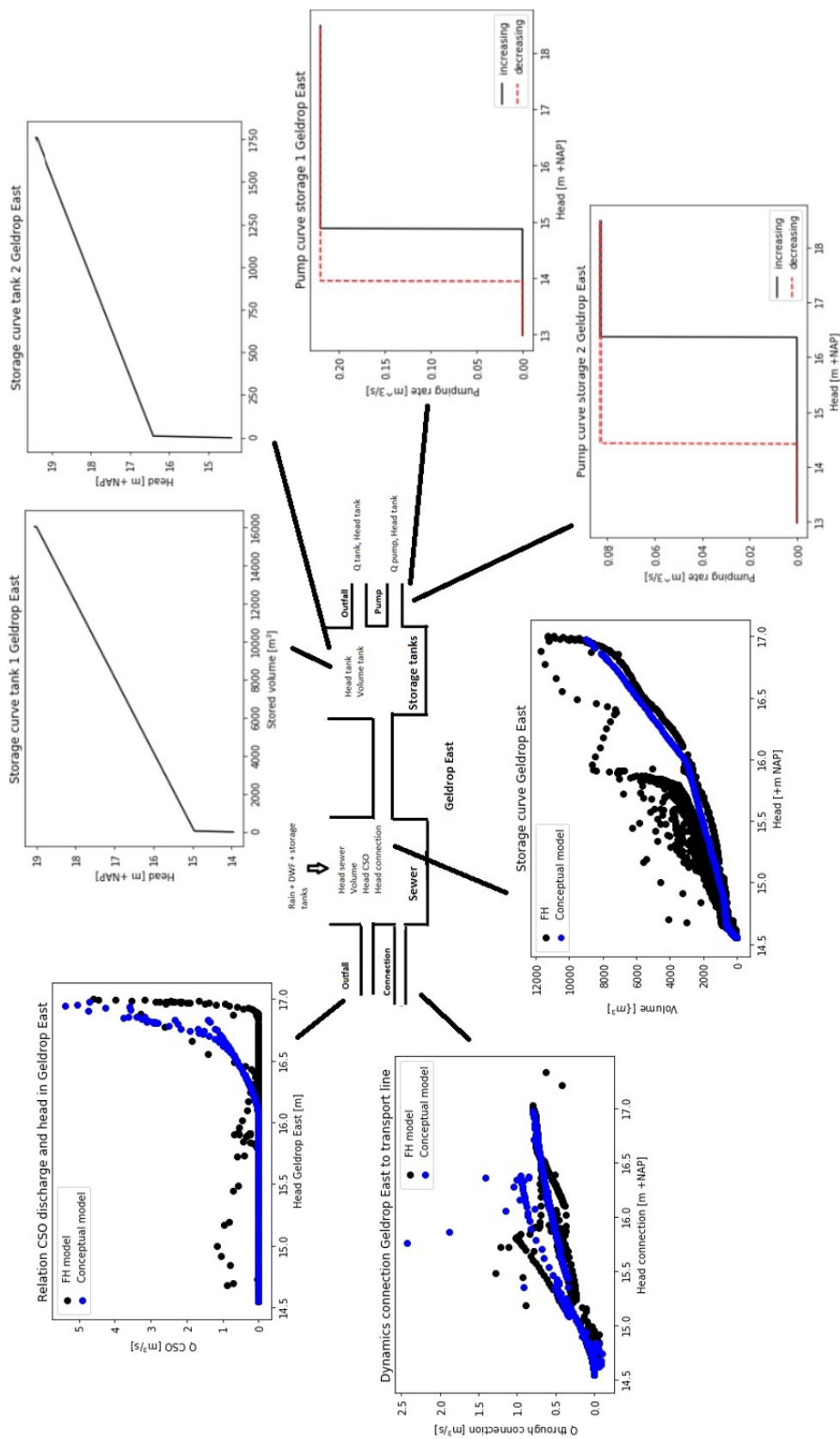
Figure 32: Dynamics FH model GE for in the conceptual model

4.3.3 Mierlo

Catchment Mierlo is different from the other two catchments because the outflow to RZ is pumped. This influences the head levels in the catchment. Figure 33 shows the storage curve. The vertical line at approximately 16 m+ NAP shows the DWF pattern in the catchment. The storage curve for Mierlo does not show a hysteresis curve since backwater flow from the transport line is not possible because the catchment is pumped. Therefore, the storage curve was straightforward to implement in the conceptual model.

Figure 33 shows the CSO discharge relation. This relation is very clear and shows that at a head of approximately 18.8 m +NAP CSO events occur. The inlet weir height in the conceptual model is set to this threshold.
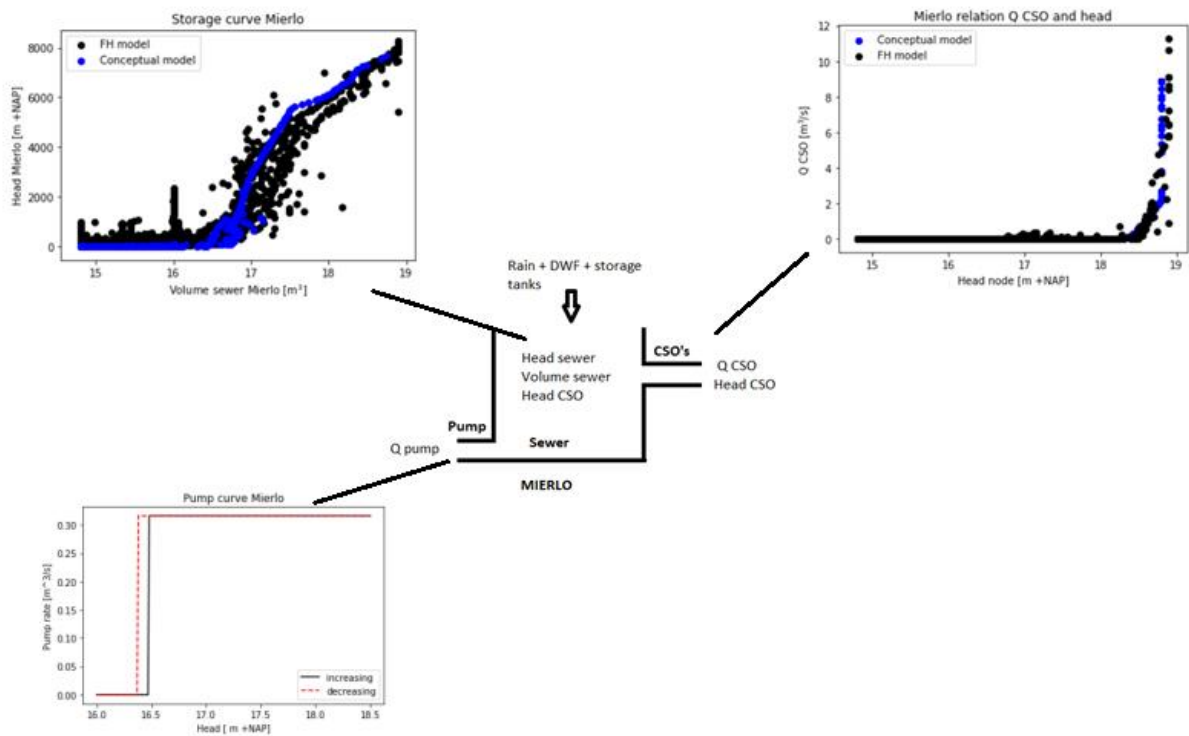
Figure 33: Dynamics FH model Mierlo for in the conceptual model

4.4 Calibration results conceptual model

In this paragraph, the calibration results of the most important characteristics (head & CSO discharge) of the catchments during event 6 will be discussed. The residual calibration results (outflow, volume, and head storage tanks) and the validation results of the other two events (event 4 & event 7) can be found in Appendix 9. The characteristics of the used events can be found in table 11.

Table 11: Rainfall events calibration/ validation conceptual model

| Event	Rainfall depth [mm]	Maximum rainfall intensity [mm/hr]	Calibration/ validation
Event 6: 06/15/2020- 06/18/2020	47.9	43.4	Calibration
Event 7: 10/27/2020 - 10/30/2020	12.4	8.0	Validation
Event 4: 02/22/2020 - 02/23/2020	18.6	13.5	Validation

The evaluation of the calibration of the conceptual model is based on the following dynamics: Head, volume, outflow with connection, CSO discharge, head storage tank, and pump capacity, since these are the main characteristics of the conceptual model. The performance of the calibration and validation is expressed using the NSE coefficient (Table 12). For event 6, both the falling and rising branches of the storage curve obtained from the FH model are considered to substantiate the choice concerning the falling/ rising branch. Catchment Mierlo does not show hysteresis, therefore there is only 1 branch included. The calibration results (event 6), show good NSE values (NSE > 0.7). The NSE value for the CSO events in the validation results is relatively low (NSE < 0.7). However, the calibration of the conceptual model primarily focuses on the correct determination of CSO volumes, and secondly the correct determination of the timing of CSO events. Considering this, the evaluation based on the NSE value should be supported by a visual analysis of the results of the calibration/ validation events. A description of the outcome of the calibration event is provided below, whereas the outcome of the validation is provided in appendix 9.

Table 12: Overview outcome calibration/ validation results conceptual model

Parameter/ Event	Event 6 falling branch	Event 6 rising branch	Event 7	Event 4
GW head	0.91	0.89	0.92	0.85
GW volume	0.89	0.86	0.30	0.97
GW outflow	0.86	0.79	0.50	0.87
GW CSO	0.81	0.8	-1.00	0.10
BBB Rielsedijk	0.84	0.83	1.00	
GE head	0.85	0.90	0.83	0.75
GE volume	0.91	0.77	0.87	0.96
GE outflow	0.76	0.80	0.81	0.92
GE CSO	0.85	0.85	-1.00	0.35
BBB 100564F	0.85	0.83	-0.03	
BBB 302	0.99	0.99		
Mierlo head	0.77		0.80	0.78
Mierlo volume	0.95		0.97	0.92
Mierlo pump	0.70		0.80	0.83
Mierlo CSO	0.86		-0.40	-1.00

Geldrop West

Based on the storage curve of catchment Geldrop West it can be expected, due to the hysteresis, that during certain events the head might show levels that are too high. Figure 34a shows that this consequence mainly impacted the calibration result for lower head levels. Because of that, the outflow to RZ is also higher than expected during the first peak, since this is forced by the head in GW. The higher outflow impacts the system state in such a way that during the second peak, the total stored volume is lower because of the increased outflow.

The head is calibrated sufficiently to simulate the system states in the FH model, therefore the timing of the CSO events is correct as well. The absolute discharged CSO volume is correctly simulated during the first peak. But during the second peak, the volume shows different results than in the FH model (higher during the beginning of the peak and lower in the second part of the peak). This is a consequence of the compromised weir inlet height, which can not simulate all the CSO locations in catchment GW.
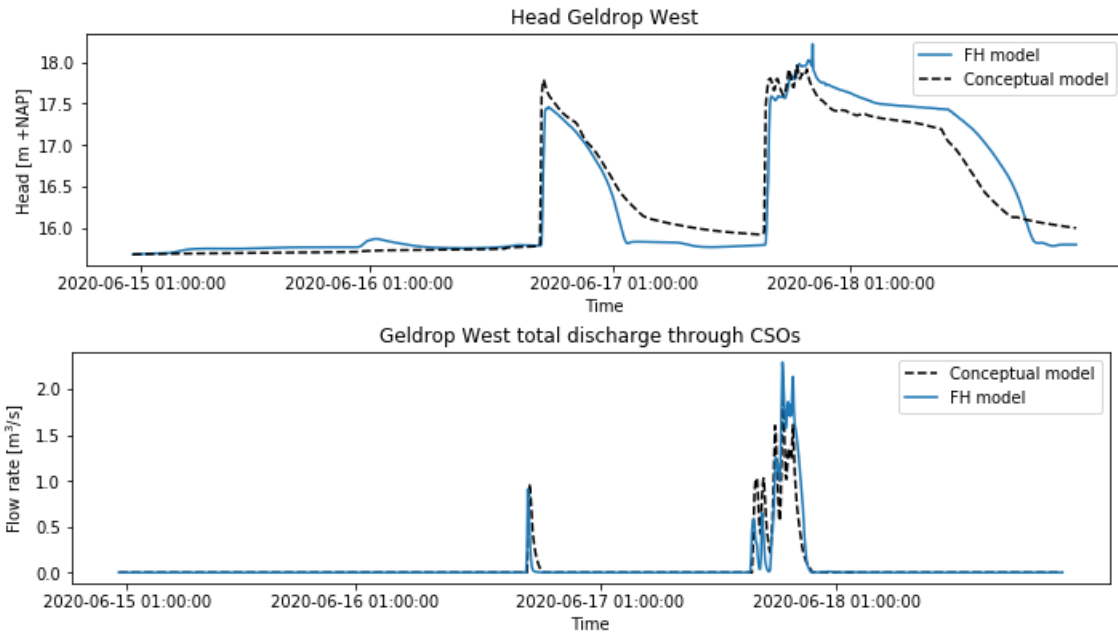
Figure 34: Geldrop West a) Total CSO discharge b) Head GW

Geldrop East

The falling branch of the storage curve from the FH model is used in the storage curve in the conceptual model. The consequence is, that the head in GE could be higher than in the FH model during certain events. Figure 35a shows the head for this event. It shows that the head for smaller events is too high, whereas the head for the higher event is accurate. The head around 06-17 15:00 is lower than in the FH model, because of the direct consequence of the design choice of the CSO weir inlet height. The weir inlet height is set to 16.7 m +NAP. As explained in Chapter 4.3.2., by choosing this weir inlet height, the CSO events that occur between 16.5-17 m +NAP are simulated as well. However, the majority of the CSO events occur at 17 m+ NAP. By including a wider range of CSO events, the consequence is that some CSO events will have a higher discharge than in the FH model. This event shows that the total CSO discharge is too high. This is the consequence of hysteresis. This results in a lower peak in head and volume.
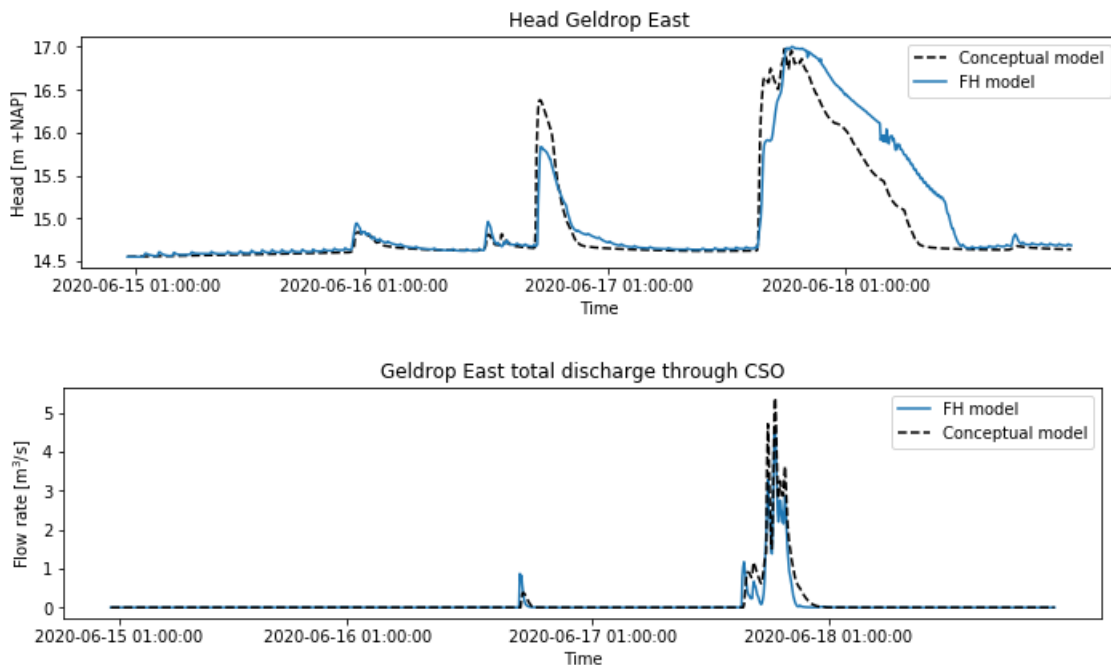
Figure 35: Geldrop East a) head b) CSO discharge

Mierlo

Catchment Mierlo is, compared to the other two catchments, different because the system state is dependent on the pump rate of pump Mierlo. Figure 36 gives insight into the calibration results for catchment Mierlo. Since the pump rates are fixed by the existing pump controls, the calibration process mainly focused on the CSO weir settings. The occurrence of flooded nodes in Mierlo was, compared to the other catchments, relatively high. Therefore, during the calibration process emphasis is put on the calibration of the CSO discharge and the flooded volume.

The total spilled CSO volume is higher than in the FH model, which causes a faster decline in total stored volume in the catchment. This CSO setting is selected since this setting can capture the peaks in CSO volume the best.

Figure 36: Mierlo a) Head b) CSO

To conclude, the conceptual model is considered sufficiently calibrated to fulfill the purpose of this study. The calibrated conceptual model is suitable to use as an internal MPC model during the optimization process. The next chapter will expand on the optimization problem.

4.5 MPC results

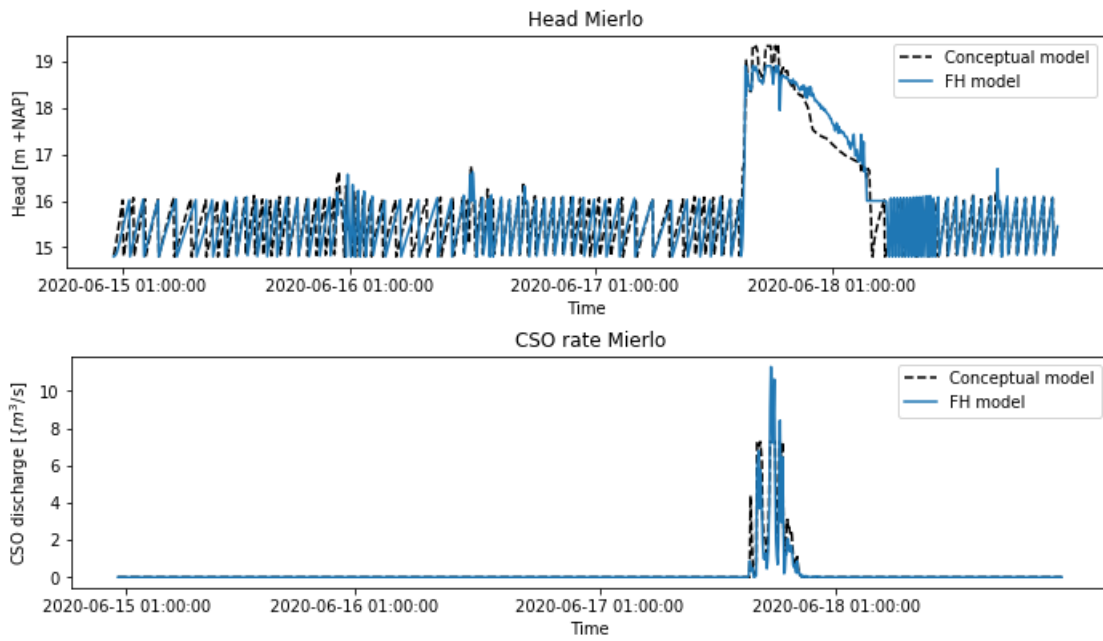Following the calibration of both the FH model and the conceptual model, the MPC procedure could be tested. The aim of the MPC procedure depends on the rainfall forecast, either to reduce DO dips or NH4+ peaks and hereby reduce the ecological impact of the UDS on the receiving waters. This chapter sets out the results of the MPC procedure during multiple events.

The MPC procedure is tested for multiple events. An overview of the characteristics of the rainfall events and the main findings are presented in table 13. The objective during both events is to prevent a decrease in DO concentration since the forecasted rainfall intensity is> 3.133 mm/hr and the rainfall depth is> 4.8mm. The performance of the system with the implemented MPC procedure is compared to the performance of the system without the MPC procedure. The change in CSO volume is in most cases 0 (table 13). This indicates that the MPC procedure did not improve the system performance considering the ecological impact on the receiving river water. For event 8, the spilled CSO volume in Mierlo even increased. The cause of this increase in CSO volume, and the reason that there is no change in the other catchments, are discussed per catchment in this chapter. Aside from the CSO volume presented in table 13, there is also CSO discharge in areas that are connected to the system via a pump. The MPC procedure cannot impact the head, and thereby the CSO discharge in these areas, since the head is determined by the pump. Therefore, these CSO discharges are not considered in this study.

Table 13: Overview rainfall characteristics MPC model

| Event	Rainfall depth [mm]	Maximum rainfall intensity [mm/hr]	Objective	CSO volume change GW [m^3]	CSO volume change GE [m^3]	CSO volume change Mierlo [m^3]
Event 8: 02/16/2020-02/17/2020	10.1	31.0	DO	0.0	0.0	+1416.0
Event 4: 02/22/2020 - 02/23/2020	18.6	13.5	DO	0.0	0.0	0.0

Geldrop West

Figure 50 a shows that the total outflow over the vortex increased significantly during the optimization of event 4. This increase in outflow caused a decreased head in the adjacent pipeline in the catchment GW (figure 37 d). However, figure 37c shows that this increased outflow does not impact the total spilled CSO volume. Therefore, the objective of this optimization problem is not obtained via the MPC procedure. This can be explained for two different reasons.

The first reason that the optimization didn't have the desired outcome is because the storage tank Rielsedijk is not utilized (figure 37e). Storage tank Rielsedijk is located just upstream of the vortex and is hereby sensitive to head changes caused by the vortex. The head in the catchment decreased below the invert level of the storage tank Rielsedijk. Therefore, this storage tank is not utilized after the implementation of the MPC procedure. The total in sewer stored volume decreased after the implementation of the MPC procedure, but because the full capacity of the storage tank Rielsedijk is not used as before, the influence on the head in the system is small.

The second reason that the MPC procedure did not show the desired results, can be explained by the hydraulic characteristics of the catchments' layout. The slope of catchment GW is relatively steep,

which decreases the possible impact of an applied control strategy. Besides that, the conceptual model is a simplified model based on 5 relationships obtained from the FH model. Therefore, the complex in-sewer dynamics are not captured in the conceptual model. An implication of this is that the simplification of the system impacts the optimization process in such a way that the optimization outcome does not apply to the FH model. For example, the spilled CSO volume in the conceptual model would be impacted by the changed actuator settings, whereas in the FH model this change in actuator settings does not impact the total stored volume due to a combination of the hydraulic constraints and the simplification of the model.

Figure 37b shows that the increased outflow of GW does not impact the head in RZ significantly. This leaves sufficient opportunity for Eindhoven to optimize.
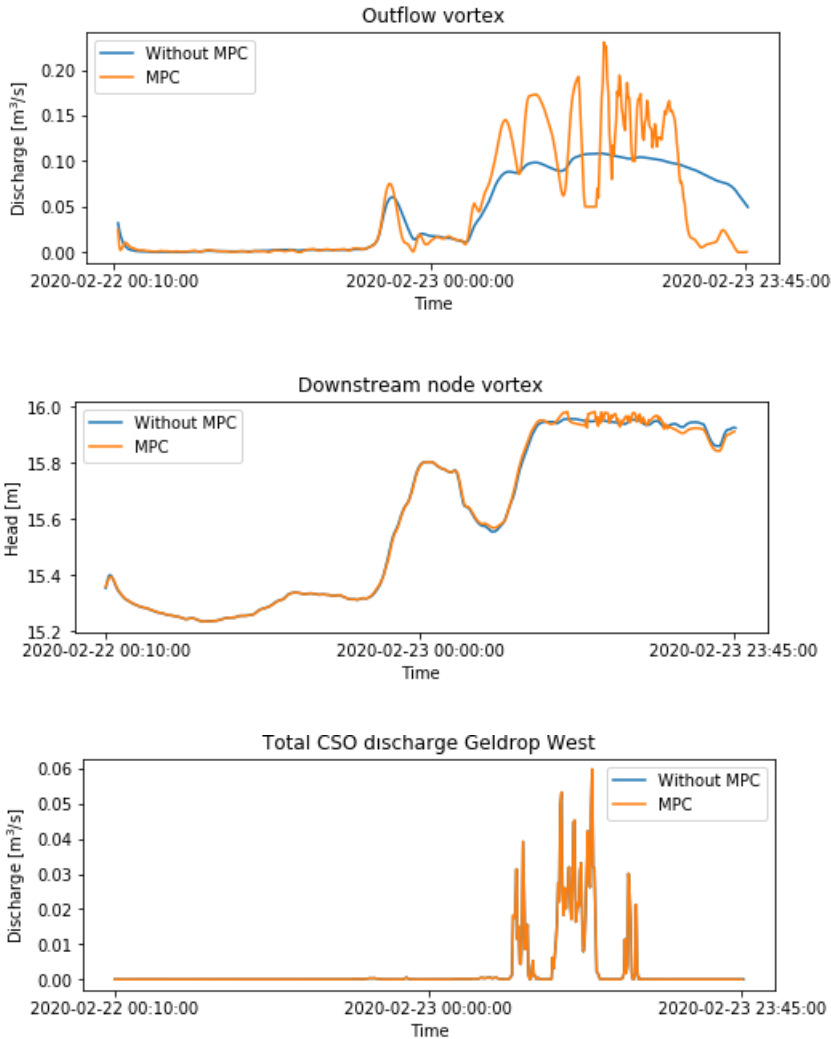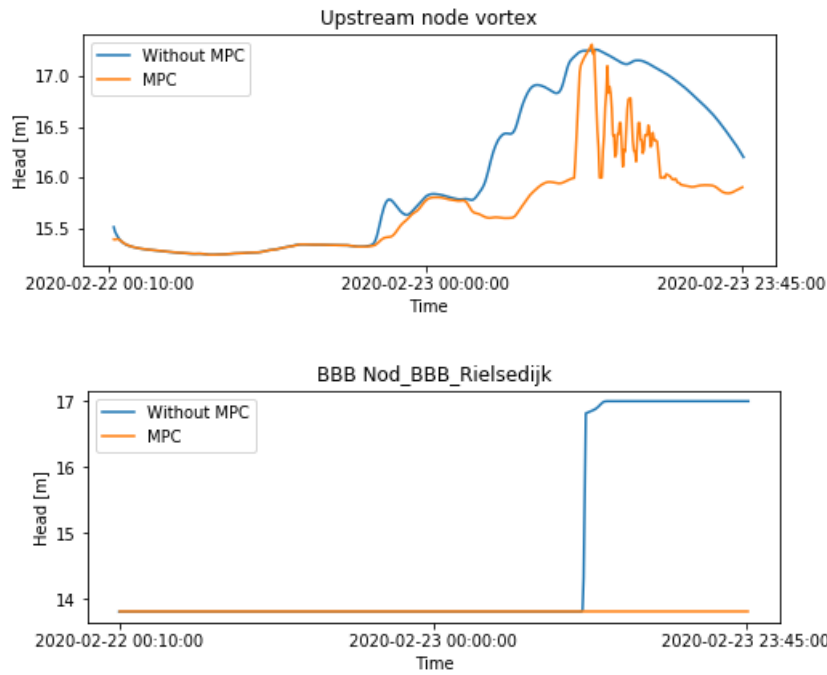
Figure 37:Geldrop West event 4 a) Outflow b)Head downstream vortex c) Total CSO d) Head upstream vortex e) Head BBB_Rielsedijk

Although the increased outflow from GW-RZ does not impact the spilled CSO volume, the head in the system decreased. Figure 38 presents all nodes that experience an influence of the MPC procedure, disregarding the scale of the influence. The influence of the MPC procedure on the total spilled CSO volume is described below for a selection of CSO locations. These CSO locations are selected because these CSO locations are located in the vicinity of nodes with a head impacted by the MPC procedure.
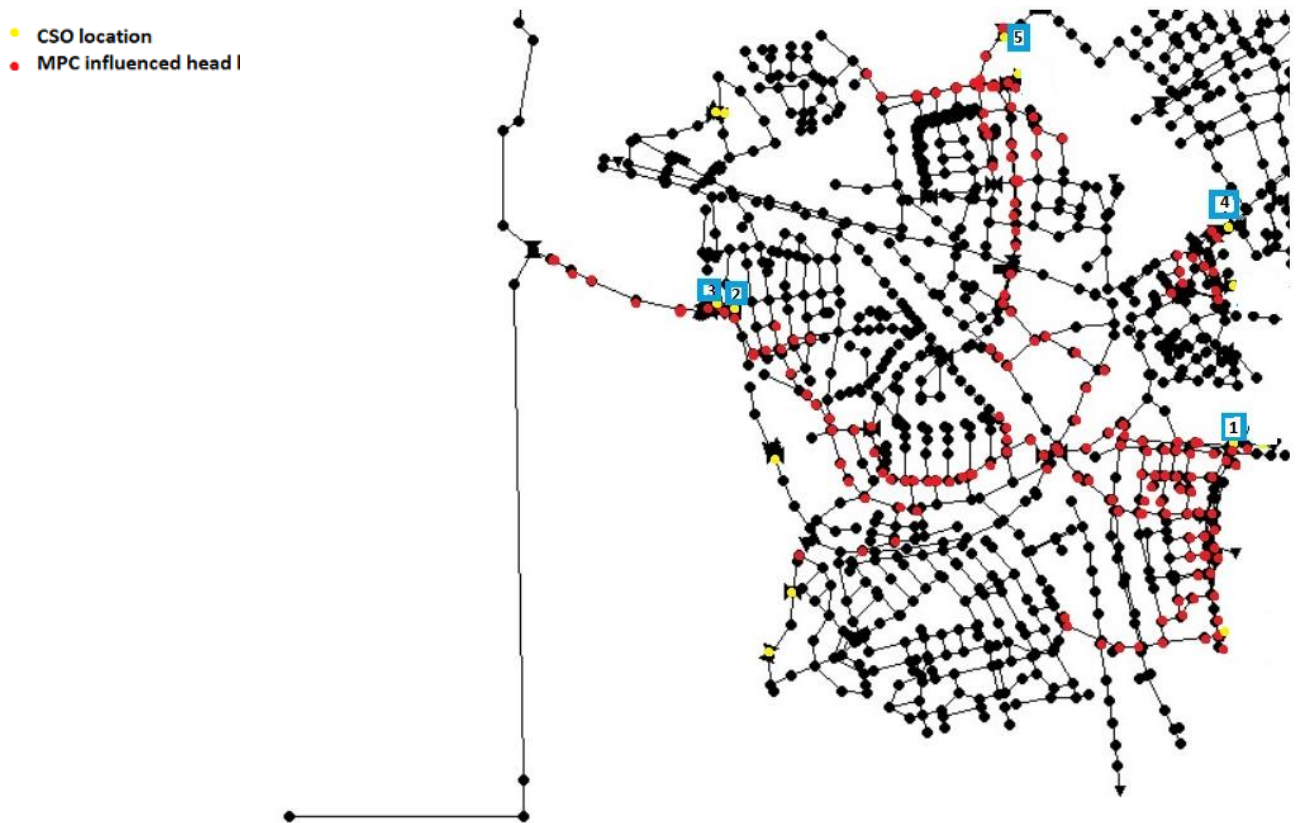
Figure 38: Overview Geldrop West: influence MPC procedure on node head

1) The head at CSO location 1 differs from the head before the implementation of the MPC procedure. However, the difference is very small (Figure 39) and therefore this does not impact the total spilled CSO volume.
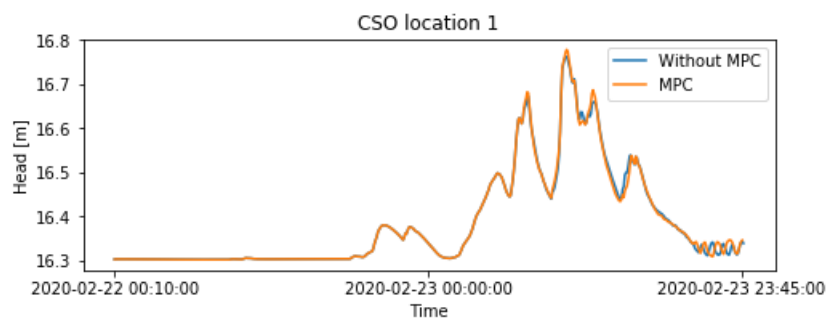
Figure 39: Head node connected to CSO location 1

2) Figure 40 shows the exact location of CSO locations 2 and 3. As can be seen, CSO location 2 is not directly connected to the conduits connected to the vortex, but location 2 is connected to the northern area of the system. As can be seen in figure 38, this area is not affected by the increased outflow through the vortex. Therefore, this CSO location is also not affected by the MPC procedure.

3) CSO location 3 is connected to the storage unit Rielsedijk (Figure 40). As explained above, after the increased outflow over the vortex, the head decreased below the invert level of the storage tank Rielsedijk. Therefore, this tank is not utilized anymore and the total CSO overflow remained 0. For this event, the CSO overflow from storage tank Rielsedijk was already 0 before the implementation of the MPC procedure. Therefore, the decrease of inflow towards Rielsedijk does not affect the total spilled CSO volume in the system.
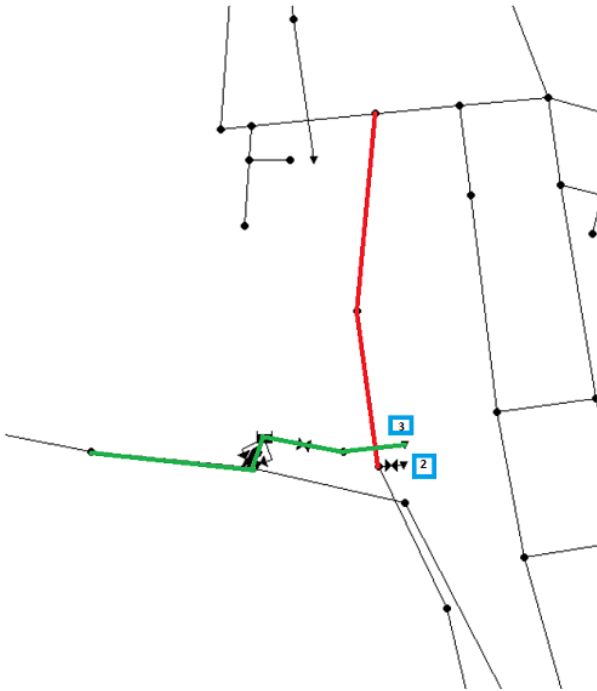
Figure 40: Close-up CSO location 2 & 3 overview

4) The head from the node connected to CSO location 4 is affected by the MPC procedure. However, initially, there was no CSO event. Therefore, the total spilled CSO volume remained 0. The differences in the head for the nodes in the surrounding of location 4 are caused by the increased outflow towards catchment Geldrop East (Figure 41).

Figure 41: Head node connected to CSO location 4

5) The head from the node connected to CSO location 5 is affected by the MPC procedure. However, initially, there was no CSO event. Therefore, the total spilled CSO volume remained 0.

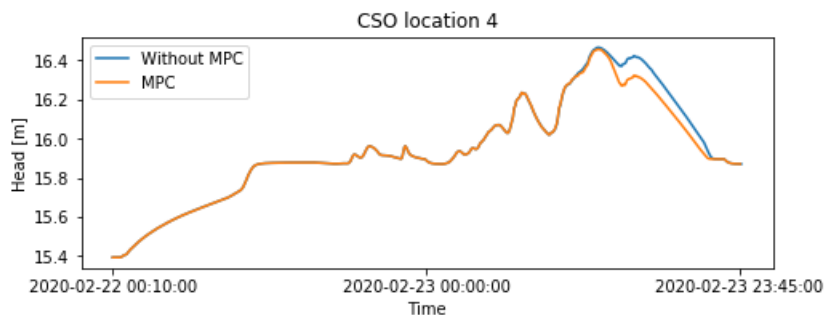The results showed that the available storage volume of BBB Rielsedijk is not utilized during the optimization since the head decreases below the invert level of the storage tank. To determine whether the full utilization of Rielsedijk would impact the performance of the MPC procedure, the invert level of the storage tank Rielsedijk is decreased to 0.4 m depth. This invert level correlates with a depth just above the depth during DWF. Meaning that the storage tank will be utilized during WWF, and hereby also after the implementation of the MPC procedure.

Figure 43 shows the results after the implementation of the MPC procedure and the decreased invert level of storage tank Rielsedijk. By comparing figure 43e with figure 37a, it is remarkable that the outflow in figure 43e is lower than in figure 37a. The increased inflow to storage tank Rielsedijk results in a decreased head in pipeline 1 (figure 42). The direct connection of pipeline 1 and the vortex causes a decrease in outflow from GW to RZ.
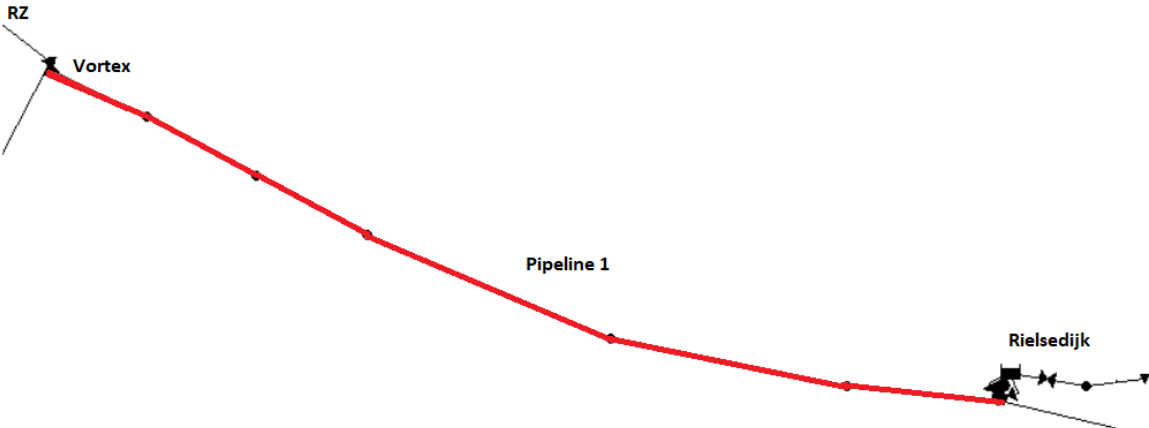
Figure 42: Layout Rielsedijk - Vortex

The total CSO discharge did not decrease after the implementation of the MPC procedure and the lowering of the invert level of storage tank Rielsedijk. The head in the nodes indicated in figure 38, decreased further than without lowering the invert level of storage tank Rielsedijk. However, the decrease in outflow compensated for the expected positive impact of lowering the invert level of storage tank Rielsedijk. The combination of this impact and the hydraulic characteristics of the catchment led to no impact on the total CSO discharge of catchment GW after the implementation of the MPC procedure.
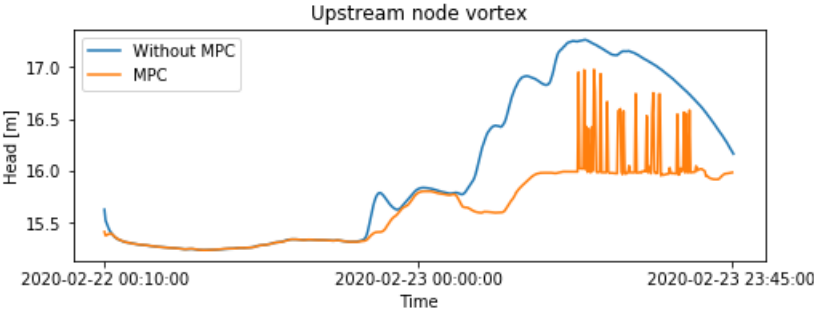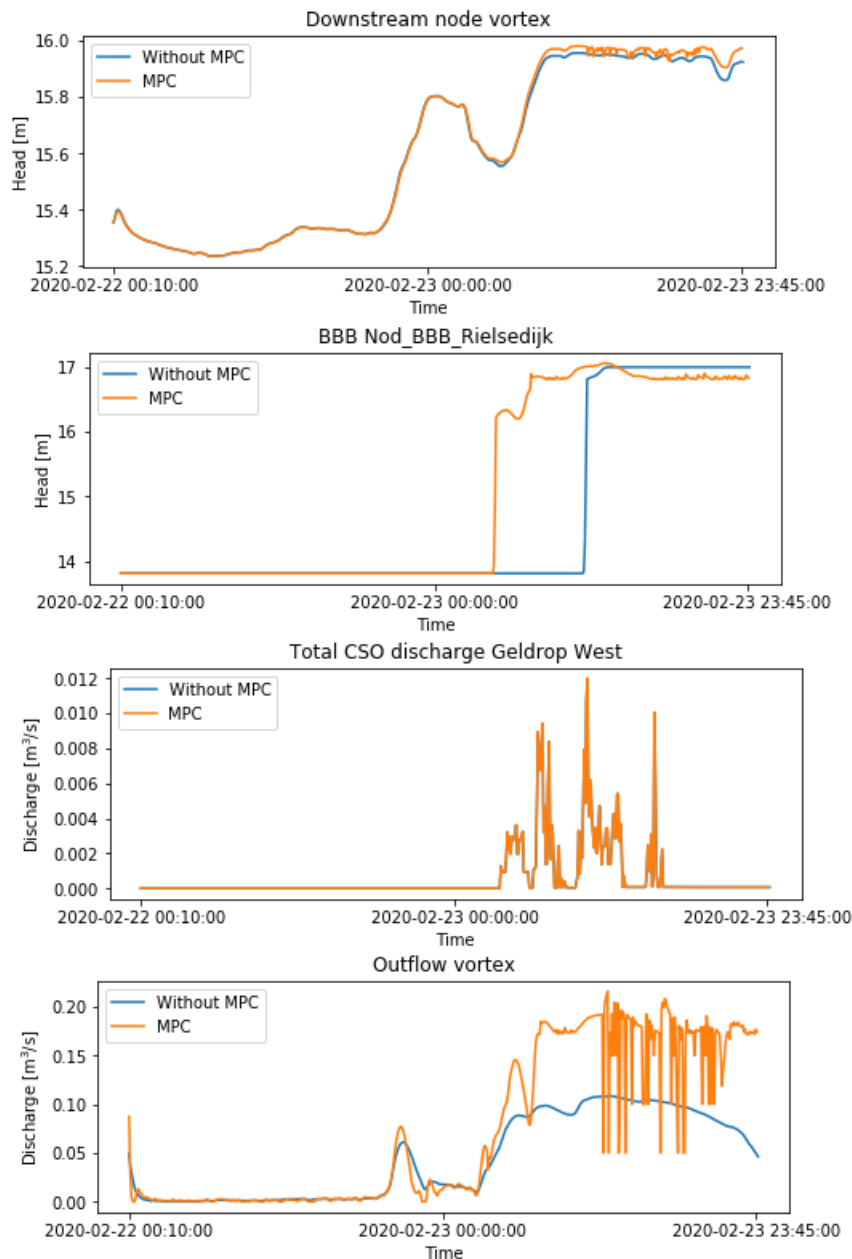
Figure 43:MPC result Geldrop West decreased invert storage tank (Event 4) a) Head upstream vortex b) Head downstream vortex c) Head Rielsedijk d) Total CSO e) Outflow GW-RZ

The MPC results for event 8 show a similar outcome to the results obtained with event 4. Figure 44a shows that the optimization resulted in a peak outflow through the vortex during this peak rainfall. The influence of this peak outflow on the head at the node downstream of the vortex is negligible (figure 44c). The head in the node upstream of the vortex decreases significantly as the outflow through the vortex increases (figure 44d). Because of the decrease in head, the head level became lower than the invert level of storage unit Rielsedijk. Therefore, Rielsedijk does not fill up (figure 44b). As for the first MPC optimization event, the total CSO volume does not decrease after the implementation of the MPC procedure.
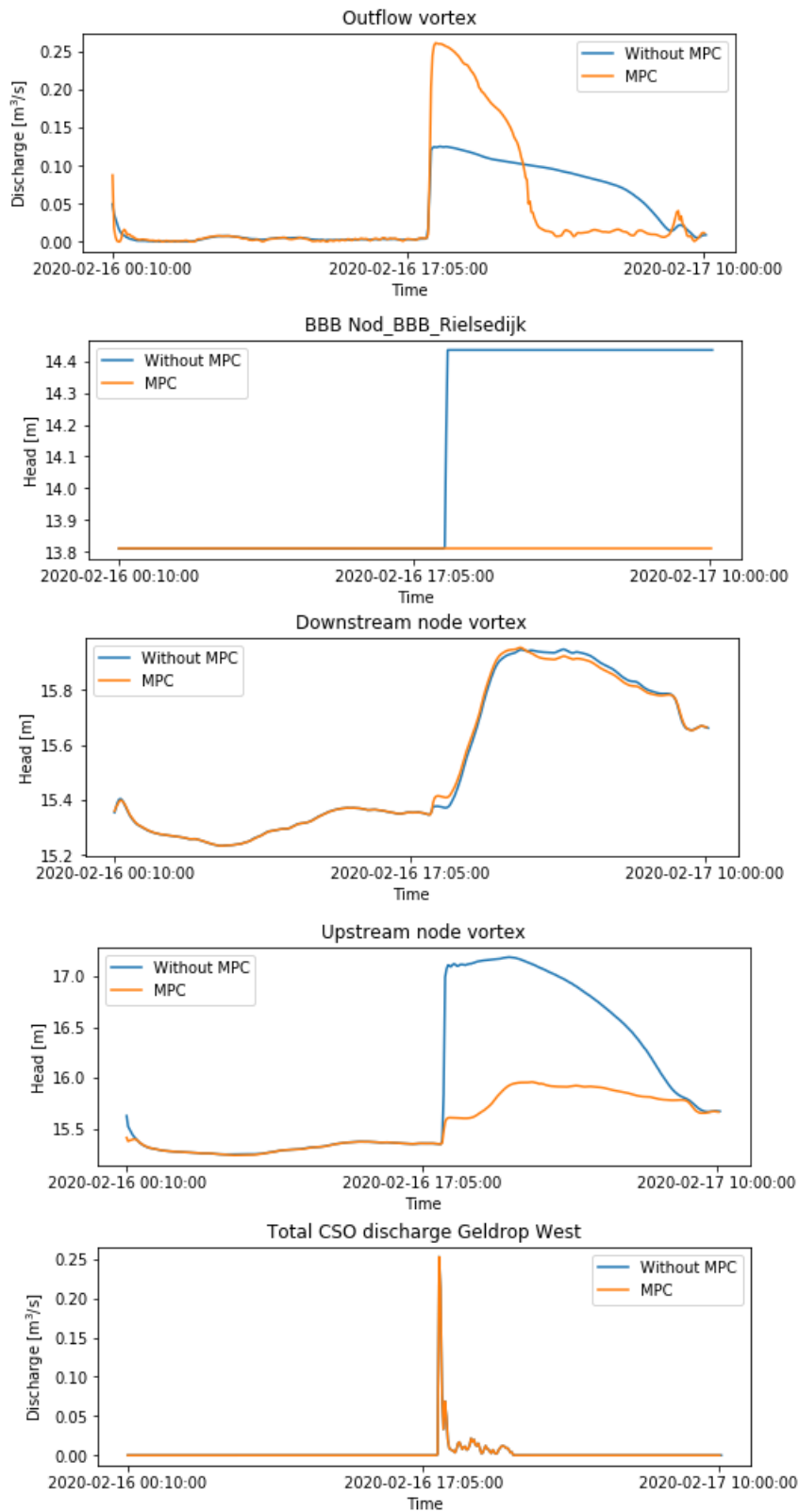
Figure 44: MPC result GW event 8: a) Outflow GW-RZ b) Head Rielsedijk c) Head downstream vortex d) Head upstream vortex e) Total CSO discharge

Catchment Geldrop East does not have a direct actuator and is hereby dependent on the actuators of the catchment Mierlo and Geldrop West. Catchment GW and GE are connected at three different connection points, so if the head in GW decreases because of a changing actuator setting, it allows GE to discharge more via these connection points.

However, the outflow via the connection towards RZ is significantly higher and has thereby a bigger impact on the dynamics within the catchment. The outflow towards RZ is dependent on the pumping capacity of Mierlo. If the pumping capacity of the pump in Mierlo decreases, the outflow of GE towards RZ can increase.

Figure 45 shows the results of the optimization. Figure 45a shows the outflow of GE towards RZ. The MPC procedure resulted in a high peak of 0.6 m3/s. This peak occurred because the pump in Mierlo shut off, and hereby the head in the connection point of GE decreased. This initiated a higher outflow of GE towards RZ. However, this didn't influence the total amount of CSO volume in GE (figure 45b).
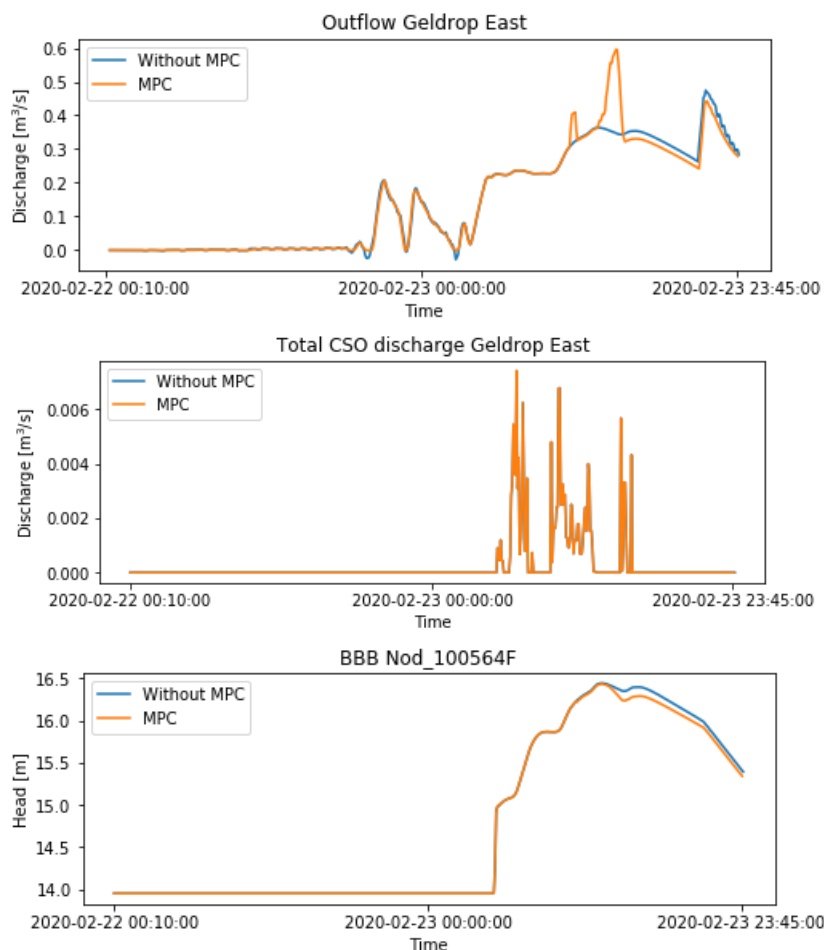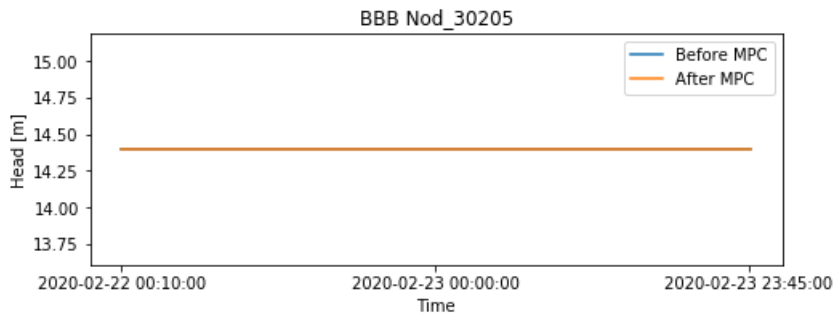
Figure 45: MPC results GE event 4: a) Outflow GE-RZ b) CSO discharge c) Head storage tank100564F d) Head storage tank 30205

The objective of this optimization problem is not obtained via the MPC procedure. This can be explained for two different reasons. The first reason that the optimization didn't have the desired outcome might be caused because the storage curve of GE shows hysteresis. As explained in chapter 2.3.2, hysteresis cannot be included in the storage curve of the conceptual model. Therefore, either the falling or rising branch of the storage curve is chosen to work with. The consequence of this is that some of the CSO events will be modeled slightly differently in the conceptual model than in the FH model. This behavior impacts the MPC optimization outcome. Since the predicted CSO volume is slightly different than in the FH model, this influences the outcome of the objective function and hereby the outcome of the optimization process. This can also be found in this case. The wrong outcome of the conceptual model influenced the objective function and indicated that an increase in the outflow of GE would lower the total CSO volume. However, in the FH model, an increased outflow did not reduce the total CSO volume.

The second reason that the MPC procedure did not improve the system performance, can be explained by the set-up of the conceptual model. The conceptual model is calibrated based on 4 different relationships, in which the dynamics within the catchment in the FH model are simplified. The simplification impacts the accuracy of the optimization outcome. In the case of catchment GE, the impact of the outflow of catchment GE towards RZ is different for the conceptual model than for the FH model. The impact of the optimization outcome is influenced by this difference. Therefore, the increased outflow from GE-RZ in the FH model does not decrease the total amount of spilled CSO volume.

The optimization outcome for the catchment Mierlo shows the impact of both explanations (figure 49). The optimization resulted in a decrease in the pump rate of pump Mierlo, hereby the outflow from GE-RZ increased. The decreased pump rate resulted in more CSO events in Mierlo. This outcome was acceptable during the optimization process since the overall outcome of the objective function improved: the total CSO discharge in GE reduced significantly and hereby compensated for the increased CSO discharge in Mierlo. These optimization results were implemented in the FH model, but the different dynamics in the FH model caused that the total CSO discharge increased. The total CSO discharge in Mierlo increased because of the decreased pump rate, but the CSO discharge in GE did not decrease because of the higher outflow. Hereby, the net spilled CSO volume is higher than before the MPC procedure was implemented (figure 45b & 49b). The exact nodes that are impacted by the MPC procedure are shown in figure 46.
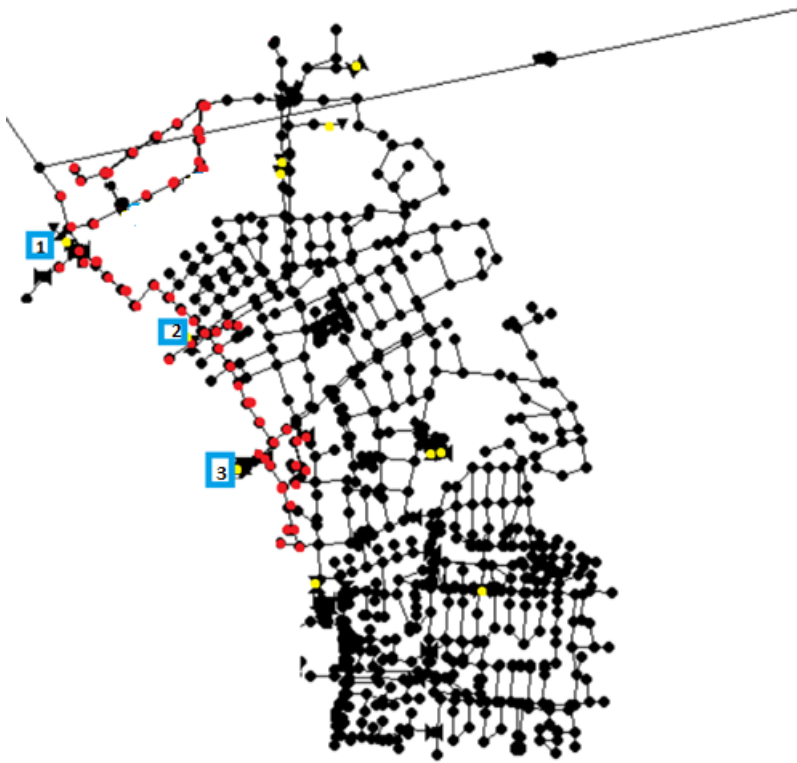
Figure 46: Overview Geldrop East: influence MPC procedure on node head

The MPC procedure mostly impacted the nodes that are located nearby the connection point to RZ or the nodes that are located nearby one of three connection points from Geldrop West (Figure 47).

After the MPC procedure was implemented, the flow from GW-GE increased. It can be concluded that the effect of the increased outflow from GE-RZ on the head of the nodes at the connection points is more significant than the impact of the increased outflow of the vortex on the head of the nodes at the connection points. However, the impact of the increased outflow is small and therefore not considered to influence the optimization problem significantly.
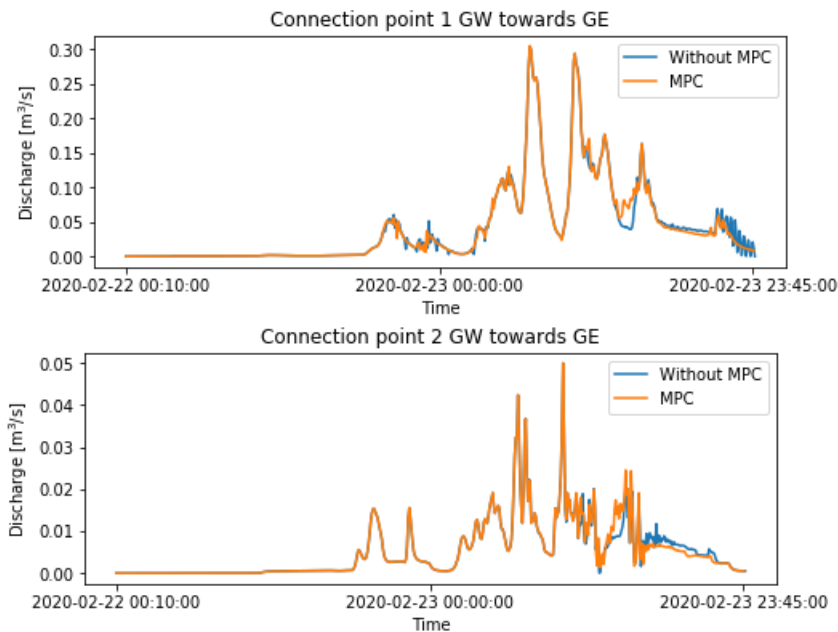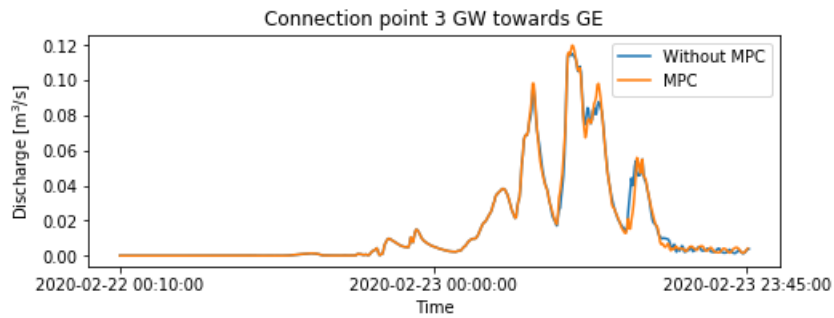
Figure 47: Connection points GW-GE

The selection of CSO locations that will be discussed can be found in figure 46. These CSO locations are selected because these CSO locations are located in the vicinity of nodes with a head impacted by the MPC procedure. In the remaining CSO locations, the head is not influenced by the MPC procedure.

1) The node that is connected to CSO location 1 is a storage tank. The inflow towards this storage tank, and thereby the head, is reduced because of the MPC procedure. However, initially, there was no CSO event. Therefore, the total spilled CSO volume remained 0.

2) The head from the node connected to CSO location 2 is affected by the MPC procedure. However, initially, there was no CSO event. Therefore, the total spilled CSO volume remained 0.

3) The head from the node connected to CSO location 3 is affected by the MPC procedure. However, initially, there was no CSO event. Therefore, the total spilled CSO volume remained 0.

These results for event 8 show that the pumping rate of Mierlo is crucial for the effect of the system performance in GE (Figure 48). The indirect influence of the MPC procedure on Geldrop East is caused by changes in the pumping rate of Mierlo. Since there are no changes in the pumping rate, Geldrop East cannot discharge more towards RZ. Therefore, the MPC procedure does not impact the system's performance. The MPC potential of GE is limited because of the dependency on Mierlo.
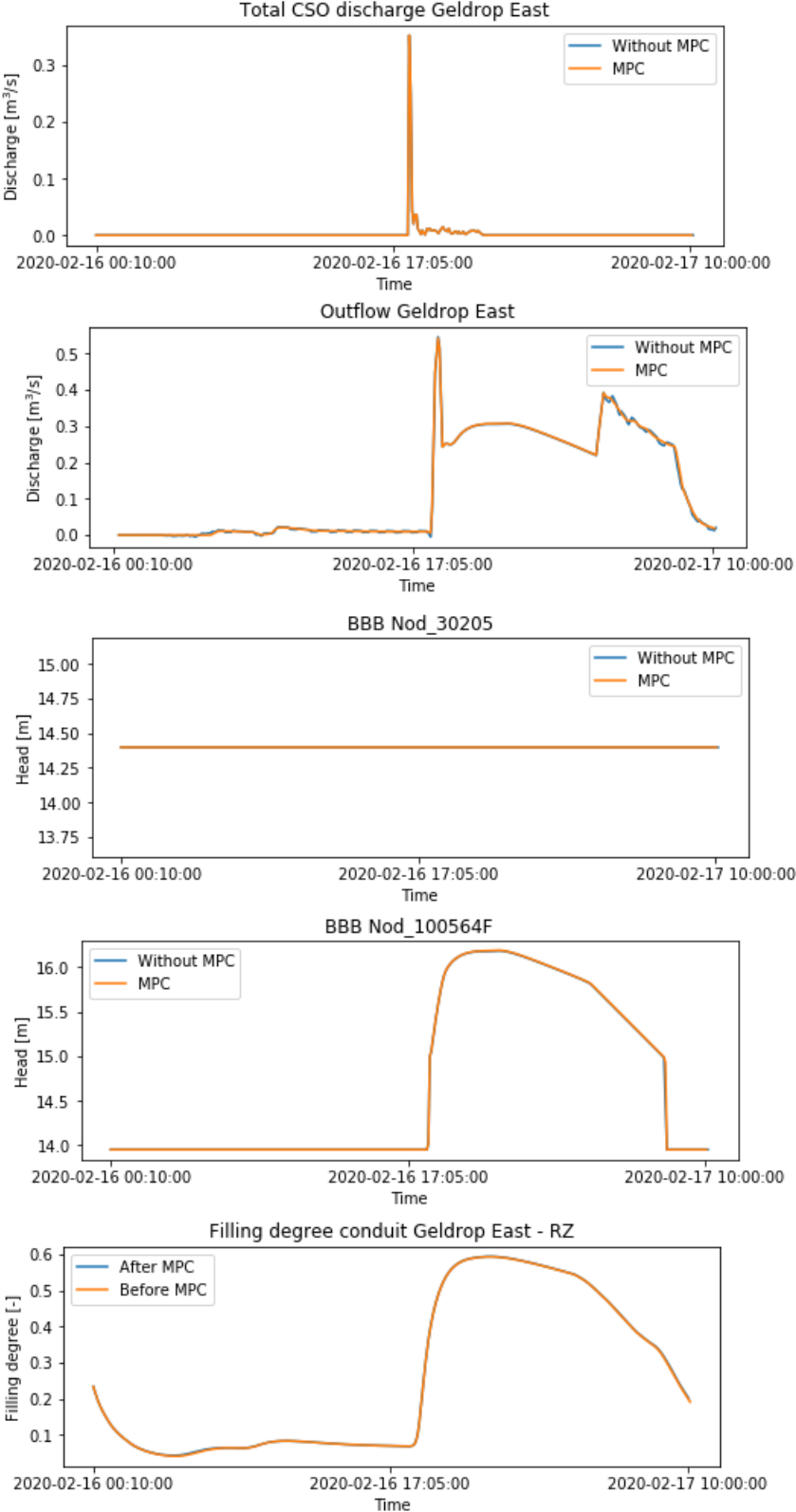
Figure 48: GE event 8 a)CSO discharge b)Outflow GE-RZ c)Storage unit 30205 d) Storage unit 100564F e)Filling degree GE-RZ

The total spilled CSO volume of the catchment Mierlo is extremely sensitive to small changes in the pump rate since 2 CSO locations are located just upstream of the pump. A small change in the pumping rate influences the head just upstream of the pump and hereby the CSO discharge at these two locations.

As can be seen in figure 49a, the pump rate during the model run without MPC is maximum, whereas CSO events already occur. A small change to the pump rate, would therefore already induce an increase in the total spilled CSO volume (figure 49b). This would not be a problem if this is compensated by the reduction of total spilled CSO volume in GE. Unfortunately, this is not the case because of the points explained in the section *Geldrop East.* The maximum pump rate in the model without MPC, combined with the fact that during the maximum pump rate CSO events already occur, indicates that pump Mierlo is not very suitable as an actuator.
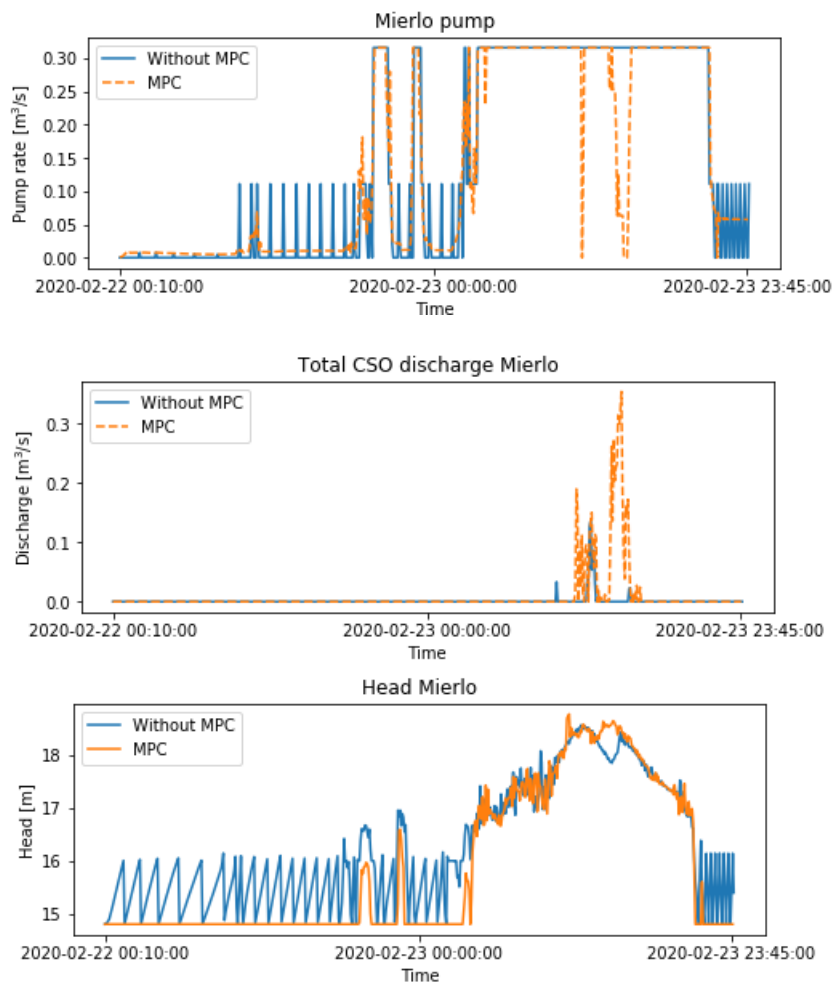
Figure 49: Mierlo event 4 a) Pump rate b) CSO discharge c) Head

For event 8, the maximum pump rate remains maximum after the implementation of the MPC procedure. The only possibility for the MPC procedure to acquire improvement is to lower the pump capacity of Mierlo and hereby increase the outflow of Geldrop East with the effect that the total CSO discharge in Geldrop East decreases. However, for this event, this is not the case and therefore the optimization result is to maintain the maximum pumping capacity during WWF (Figure 50)
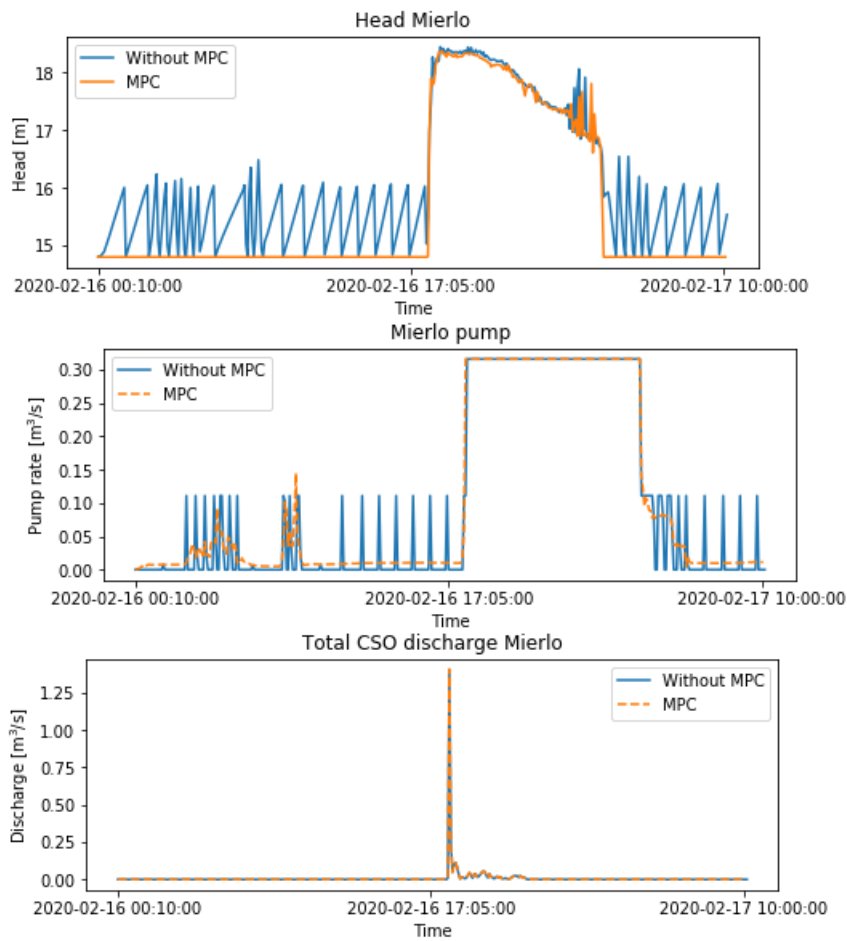
Figure 50: Mierlo event 8 a) Head b) Pump rate c) CSO discharge

5. Discussion

According to Mollerup et al. (2016), it might not be necessary for a small sewer system (the case study in that research is 320 ha) with few actuators, and hereby limited complexity, to implement an optimization-based control system since regulatory control (single input, single output feedback loops) might be as effective. The RTC potential is dependent on the size of the case study, but also the control range and control possibilities. The case study used in this research is small, hence 3190 ha, and hereby larger than the system used in the research from Mollerup et al. The small size of the catchment could indicate that the RTC strategy is not outperforming regulatory control. However, after the pre-assessment using the PASST tool, this case study area showed RTC potential mainly because of the multiple control and storage possibilities, different hydraulic characteristics of receiving water, and the mildly sloping transport line RZ. However, the results showed that after the implementation of the RTC strategy the performance of the system remained the same or even deteriorated. In this chapter, the possible causes for this, and the results, will be discussed and further explained. As stated in Dirckx et al. (2007) the PASST tool can solely be used as an indicator for RTC potential and is thereby not a guarantee for success.

Setting up models

During the decision on which models (FH/conceptual) will be used in the MPC procedure, consideration must be made concerning the simulation time and the complexity of the model. By using 2 FH models, used as a system model and as an internal MPC model, the accuracy of the optimization results will be close to the actual system dynamics, and would therefore be the most suitable option. However, the simulation time is too large and therefore implementation of the optimization outcome in real-time is not possible. Since this research aims to make a control strategy that can be implemented in real life, it is decided that the use of 2 FH models is prevented. The opposite of using 2 FH models, is using 2 conceptual models in the MPC procedure. The simulation time would improve significantly, but the downside is that the uncertainty of the conceptual model affects the optimization results. Therefore these results might not apply to the actual system. The compromise of having both a short simulation time and a relatively complex system is by using both the FH model and the conceptual model during the MPC procedure, like in this research. However, even by using the two different models, the impact of the accuracy of the conceptual model should be considered. The design choices during setting up the conceptual model, influence the accuracy of the conceptual model. In this research, the conceptual model is simulated in 3 different catchments (GW, GE, Mierlo). But since it appeared that the conceptual model does not capture the dynamics within the catchments, it can be discussed whether this design choice led to the most accurate conceptual model. One way to improve the accuracy of the conceptual model is to include more sub-catchments. By incorporating more difficulty, e.g. creating more catchments in the conceptual model to be able to simulate the characteristics within the system better, the accuracy and hereby quality of the conceptual model would improve. But by including more sub-catchments, e.g. 6 subcatchments instead of 3, also more sensors are needed to acquire information about the real-time system state. By including a larger amount of sensors, the chance of errors/ the impact of the uncertainty of these sensors becomes larger and impacts the optimization outcome. Therefore, also in this design choice, a trade-off should be made between the accuracy of the conceptual model and the implementation of the conceptual model in real-time. During this research, it was expected that by capturing the most important FH dynamics within these 3 sub-catchments, the conceptual model would be accurate enough to simulate the dynamics of the FH model.

Calibration

Calibration aims to adjust a set of parameters so that the model agreement is maximized concerning the set of measurement data. In this research, calibration was not the main focus. However, the model still needed to be calibrated to ensure valid optimization results. The calibration process is executed

in a trial-and-error manner. This manner can improve the model agreement concerning the set of measurement data, but it does not ensure the optimal model agreement. To improve the accuracy of the research, the calibration process can be optimized using calibration algorithms, such as the DREAM algorithm explained in Vrugt et al. (2009).

A limitation in the calibration process of the FH model was the availability of measurement data. The available measurement data was data from measurement points that are located close to each other. This might affect the calibration outcome for the locations that are not closely located nearby the measurement points, negatively. Therefore, for proper calibration, more measurement data points are needed.

The conceptual model is calibrated using the same method as in van Daal-Rombouts et al. (2016). The rainfall characteristics for the 3 events used during calibration/ validation of the conceptual model are different. The model is calibrated on an event with a lower maximum rainfall intensity compared to the two validation events. This can result in validation results that show different filling/ emptying characteristics than in the FH model. This effect is visible in the validation results of GE, where the system fills up (up to 3000 m^3) slower than in the FH model, whereas the calibration results are accurate during these volumes. The implication of this on the optimization process is limited since the higher volumes are accurately simulated and these are important for the simulation of CSO events.

Results control

As explained in Chapter 4.5, unfortunately, the control strategy applied to this case study did not obtain the desired set objectives. Multiple reasons could cause this result: the system is not suitable for RTC, the conceptual model is not able to capture the dynamics of the FH model, and the conceptual model is not accurate enough to use during the optimization process. Below, these possible causes will be discussed and explained further.

The hydraulic constraints of the case study area restricted the effect of the RTC strategy. For GW, the system is designed based on the fixed outlet via the vortex to RZ. In this study, the vortex is considered as an actuator, meaning that the outlet via the vortex became adjustable. The system of GW is designed on the fixed vortex. The design implications of this are that the system is relatively steep with large hydraulic resistance. The impact of an increased discharge on a steep system does not reach as far as the impact of an increased discharge on a flat system. For the catchment Mierlo and GE, it was expected that the actuator pump Mierlo would be sufficient to improve the system performance. However, the location of the actuator appeared to be important since a CSO location in Mierlo was directly located upstream of the pump and thereby the system performance was very sensitive to small changes in the pump rate. In the PASST assessment, the number of actuators is considered. However, in the case of GE and Mierlo, it would have been useful to indicate the possible impact of each actuator, to hereby prevent the expectation that one actuator might be able to impact an area that is too large to affect completely, such as in the case for GE. The results suggest that this case study area is not suitable for the implementation of a RTC strategy due to the hydraulic constraints explained above. However, it is recommended to study the impact of executing (small) system changes to enhance the effect of a RTC strategy. This could include changes in the slope of the pipelines, different use of storage units, and the placement of more actuators (within the system).

Another reason that might have impacted the MPC procedure, is the ability of a conceptual model to capture the dynamics of the FH model. In this research, the hysteresis dynamics in the FH model are not included in the conceptual model because it could only include a singular storage curve. Choosing 1 branch (falling/ rising) impacts the filling of the system, and hereby the dependent events (e.g. CSO discharge, outflow dynamics). However, the singular storage curve impacted the calibration outcome by either affecting the curves of the head or the stored volume in the system. This implies that either

the timing or the CSO discharge was impacted by this. It can be concluded that the impact of not considering hysteresis in the conceptual model is considered acceptable.

The rate of change of the actuator setting is determined during the optimization process, and hereby dependent on the accuracy of the conceptual model. The conceptual model is built and calibrated on the main characteristics of the FH model (CSO discharge, outflow dynamics, storage curve). These characteristics capture the FH model dynamics in a few relationships. These relationships contain information about the system state within the whole catchment. The calibration and validation results showed that the conceptual model in this research is accurately capturing the most important dynamics in the FH model. However, during the optimization process, it appeared that the accuracy of the conceptual model was lacking because it did not capture the dynamics within the sewer catchments, which appeared to be of importance for the optimization process. Therefore, it can be concluded that even though the calibration results seem accurate, it is not a guarantee on being accurate enough to use during the MPC optimization.

6. Conclusion

The main purpose of this thesis was to develop a control strategy that decreases the negative ecological impact of the UDS of Eindhoven, caused by ammonium peak loading and DO dips. The main area of interest is whether the contradictive nature of the objectives could eventually decrease the overall negative ecological impact of the UDS on the receiving river. A calibrated model of the case study area Geldrop-Mierlo is used to test the control strategy. Both, a simplified conceptual model and a full hydrodynamic (FH) model are used during the optimization process. The performance of this control strategy is tested for 3 different events, that have different rainfall characteristics. The performance is measured by the total amount of spilled CSO volume and the ammonium peak inflow towards the WWTP.

The main research question that was developed for this study is:

Is a dynamic RTC strategy capable of reducing the ecological impact caused by a combined sewer system?

The research question is answered by the following sub-questions:

Can the trade-offs between ammonium loading and dissolved oxygen (DO) concentration be linked to rainfall characteristics?

The rainfall characteristics are described in maximum rainfall intensity, duration of the rainfall event, and rainfall depth. The decision tree that gives insight into the trade-off, indicates that the duration of the rainfall event does not impact the trade-off and is therefore not included in the decision tree. The chance of the occurrence of a DO dip increases as the maximum rainfall intensity is higher than 3.1 mm/hr or that the maximum rainfall intensity is lower than 3.0 mm/hr but the total rainfall depth is > 4.8 mm.

The trade-off between the ammonium loading and dissolved oxygen concentration can be linked to the rainfall characteristics: rainfall intensity and rainfall depth. This threshold can be implemented in the objective to function to indicate which objective should be applied at that time.

Is it possible to capture the performance of a sewer system in both a full hydraulic model and a simplified (conceptual) model?

The answer to this question is dependent on the application of the model. In this research, the FH model is considered a detailed model that simulates the system performance of the actual sewer system accurately. The performance is measured by the most important characteristics of the sewer system at certain points in the system: head, discharge, and volume. The performance is considered accurate, if the dynamics of the parameters described above, show the same dynamics as in the measurement data. This can be quantified by the NSE value. The accuracy of the system is dependent on the available measurement data.

As described in the discussion, the accuracy of the conceptual model is influenced by the rate of simplification, hysteresis, and hydraulic constraints. The performance of the model in this research is dependent on a few relationships abstracted from the FH model. Logically, the accuracy of the conceptual model is decreased compared to the FH model, since the few relationships do not capture all the complex relationships from the FH model. However, is the conceptual model accurate enough to be used as a model to simulate the performance of a sewer system?

To answer this question, it is important to consider the desired outcome and purpose of the conceptual model. In this research, the conceptual model was used during the optimization process. For the catchment GW, the accuracy of the conceptual model is considered sufficient since the application of the model in the optimization process results in logical changes in the actuator setting. For catchment GE and Mierlo, it appeared that the dynamics within the system in the conceptual model were not described accurately enough, which impacted the optimization process. Since the design and calibration of the conceptual model catchments are the same for the 3 different catchments, it can be stated that local characteristics cause that for the catchment GW the conceptual model is accurate whereas for catchment GE and Mierlo it isn't. A possible reason for this is that pump Mierlo is the only actuator for both GE and Mierlo. This reduces the RTC potential and increases the sensitivity of the accuracy of the optimization outcome. Based on this, it can be concluded that the accuracy of the conceptual model should be dependent on the purpose of the model and the characteristics of the case study area.

What is the environmental impact of a RTC strategy that dynamically optimizes the system for both dissolved oxygen and ammonium concentrations?

The conclusion for this specific case study is that the MPC procedure does not reduce the environmental impact caused by the UDS. Therefore, the effective operation of the forecast dependent objective function remains uncertain. To conclude whether the MPC procedure is effective, it is recommended to apply the MPC procedure to a case study from which it is already proven to be suitable for RTC strategies.

All the 3 catchments are subject to hydraulic constraints that caused that the control strategy could not reduce the environmental impact of the UDS. Examples of hydraulic constraints in this area are (1) CSOs that are located in a pumped area, (2) CSOs that are located far from the main transport line, (3) invert level of storage tanks, (4) availability of actuators, (5) slope of the system. Firstly, CSOs that are located in an area that is connected to the transport line via a pump, do not experience the influence of a decrease in head at the downstream area (caused by the MPC procedure). Therefore, these CSO locations are not sensitive to the MPC procedure, which reduces the possibility of reducing the environmental impact of the UDS on the receiving waters. Secondly, the influence of the MPC procedure is mainly found in the main transport line in the catchment. CSOs that are located at a far distance from this transport line, do not experience the effect of the MPC procedure. Thirdly, the MPC procedure caused the head to decrease below the invert levels of the storage tanks. This caused that the available storage of the tanks was not used. This is not a desirable effect of the MPC procedure, since this increases the pressure on the system. Concerning the availability of actuators, it is important to ensure a sufficient amount of actuators in the system. In the case study in this research, the MPC performance in 1 catchment was dependent on an actuator of another catchment. This reduces the control possibilities for both catchments. Finally, the slope of the system determines the control possibilities, since the slope determines the experienced effect of changing the actuator settings.

For catchment GE and Mierlo, aside from the impact of the hydraulic constraints, the conceptual model accuracy also reduces the possibility of the MPC procedure to have a positive environmental impact.

Since the hydraulic constraints of this case study restrict the control strategy from working, the decreased negative ecological impact cannot be measured. But because the overall principle of the control strategy is working (actuators follow logical settings), it is expected that for case study areas without (/ limited) hydraulic constraints, this control strategy would decrease the overall negative ecological impact of the UDS.

7. Future research

Link MPC-WEST

Since the RTC strategy has a volume-based objective, it would be interesting to use the simulation results as an input for the WEST simulator. In this case, the water quality parameters of the Kleine Dommel and the Dommel can be measured and compared to the water quality parameters of the rivers before the implementation of the control strategy. By doing so, the ecological impact can be measured not only indirectly, via de volumes as in this research, but also directly.

Creation conceptual model

It is recommended to perform research to the models used in the MPC. In this research, a combination of the FH model and the conceptual model are used. The FH model resembles the system state of the real system the best, whereas the conceptual model has a fast computation time which is needed in RTC. The use of two FH models in the MPC procedure would result in the best optimization results, but the computation time would be too long for the strategy to be effective in a real system. However, the simplification of the conceptual model impacted the optimization results for the case of Mierlo and GE negatively. Therefore, it is recommended to explore the possibilities of improving the computation time of the conceptual model without compromising the quality of the model.

Calibration conceptual model

The calibration in this research is evaluated based on the system performance during multiple rainfall events. However, it would be interesting to switch the focus during the calibration process from the system performance subject to different rainfall events to the impact of actuator settings on the system functioning. By doing so, the impact of the actuator settings might be simulated more accurately in the models.

Impact of expanding control possibilities

It is recommended to extend the optimization strategy by including more actuators, and hereby check whether the this would improve the optimization outcome. This case study area does not have more available actuators, but hypothetical actuators can be added to the system. For this research, it is expected that by placing an actuator at the most downstream point of catchment GE would significantly impact the optimization outcome.

Another option to expand the control possibilities is to include more catchments. It is out of het scope of this research to include all of the catchments of UDS Eindhoven. However, it is recommended to explore the possibilities of RTC while considering more catchments. By considering more catchments, there are more optimization possibilities for RTC because of the larger amount of in-sewer volume that might be available. The head in RZ indicates that there are control possibilities for including multiple catchments, since the filling degree of RZ < 1.

Changing external factors

It is recommended to test the RTC strategy with multiple case study areas that contain different hydraulic constraints and characteristics. By considering an area that is suitable for the application of a RTC strategy, the effectiveness of this RTC strategy can be proved by a decreased ecological impact. It is also recommended to test the RTC strategy subject to more rainfall events. By doing the above, it can be tested whether the RTC strategy is effective under the influence of a wide range of external influences.

References

Abdel-Aal, M., Shepherd, W., Ostojin, S., Mounce, S., Shucksmith, J., Schellart, A., . . . Tait, S. (2020). *Developing and testing a Fuzzy Logic algorithm to alleviate the risk of flooding by controlling a flow control device in a laboratory setting.* Sheffield: CENTAUR project.

Abimbola Owolabi, T., Reza, M. S., & Zayed, T. (2022). Investigating the impact of sewer overflow on the environment: A comprehensive literature review paper. *Journal of Environmental Management*.

Amerlinck, Y. (2015). *Model refinements in view of wastewater treatment plant optimization: improving the balance in sub-model detail.* Gent: PhD thesis, Ghent University.

Bachmann, A., Wetzel, J., & Dittmer, U. (2016). *Assessing the Potential of Pollution Based RTC in a Combined Sewer System Based on Highly Resolved Online Quality Data.* Rotterdam, The Netherlands: Proceedings of the 8th International Conference on Sewer Processes and Networks.

Baek, H., Ryu, J., Oh, J., & Kim, O. (2015). Optimal design of multi-storage network for combined sewer overflowmanagement using a diversity-guided, cyclic networking particle swarm optimizer- A cast study in the Gunja subcatchment area, Korea. *Expert Systems with Applications 42*, 6966-6975.

Behrendt, M. (2020). *CC BY-SA 3.0.* Retrieved from Creative Commons: https://creativecommons.org/licenses/by-sa/3.0

Benedetti, L. N. (2011). Modelling for integrated sewer-WWTP operation with ATS in Copenhagen. *In proceedings of the 12th Nordic Wastewater Conference.* Helsinki.

Bertrand-Krajewski, J. L., Bardin, J.-P., Mourad, M., & Beranger, Y. (2003). Accouting for sensor calibration, concentration heterogeneity measurement and sampling uncertainties in monitoring urban drainage systems. *Water Science and Technology*, 95-102.

Bertrand-Krajewski, J. L., Chebbo, G., & Saget, A. (1998). Distribution of pollutant mass vs. volume in stormwater discharges and the first flush phenomenon. *Water Research*, 2341–2356.

Borsányi, P., Benedetti, L., & Dirckx, G. (2008). Modelling real-time control options on virtual sewer systems. *Journal of Environmental Engineering and Science*, 395-410.

Castelltort, F., Bladé, E., Balasch, J., & Ribé, M. (2020). The backwater effect as a tool to assess formative long-term flood regimes. *Elsevier*, 29-43.

Cen, L., & Xi, Y. (2007). October Particle swarm optimization for optimal flow control in combined sewer networks - a case study. *IEEE*, 261–266.

Deletic, A., Dott, C. B., McCarthy, D. T., Kleidorfer, M., Freni, G., Mannina, G., . . . Bertrand-Krajewski, J. L. (2012). Assessing uncertainties in urban drainage models. *Physics and Chemistry of the Earth, Parts A/B/C*, 3-10.

Dirckx, G., Thoeye, C., De Gueldre, G., & Van de Steene, B. (2007). PASST een RTC strategie in Vlaanderen? *Rioleringswetenschap 7.25*, 38-52.

(2000). *Directive of the European Parliament and of the Council Establishing a Framework for Community Action in the Field of Water Policy (2000/ 60 / EC).*

Du, J., C. L., Xhang, Q., Yang, Y., & Xu, W. (2019). Different Flooding Behaviors Due to Varied Urbanization Levels within River Basin: A Case Study from the Xiang River Basin, China. *International Journal of Disaster Risk Science*, 89-102.

Engelhard, C., De Toffol, S., & Rauch, W. (2008). Suitability of CSO performance indicators for complimance with ambient water quality targets. *Urban Water Journal*, 41-47.

Erbe, V., & Schütze, M. (2005). An integrated modelling concept for immission-based management of sewer system, wastewater treatment plant and river. *Water Science &Technology*, 95-103.

Eulogi, M., Ostojin, S., Skipworth, P., & Shucksmith, J. (2020). *Hydraulic optimisation of multiple flow control locations for the design of local real time control systems.* Urban Water.

Fiorelli, D., Schütze, G., Klepiszewski, K., Regneri, M., & Seiffert, S. (2013). Optimised real time operation of a sewer network using a multi-goal objective function. *Urban Water*, 342–353.

Frehmann, T., Nafo, I., Niemann, A., & Geiger, W. (2002). Storm water management in an urban catchment: Effects of source control and real-time managmenet of sewer systems on reiceing water quality. *Water Science Technology*, 19-26.

Fuchs, L., & Beeneken, T. (2005). Development and Implementation of a Real-Time Control Strategy for the Sewer System of the City of Vienna. *Water Science and Technology*, 187-194.

Garcia, L., Barreiro-Gomez, J., Escobar, E., Téllez, D., Quijano, N., & Ocampo-Martinez, C. (2015). Modeling and real-time control of urban drainage systems: A review. *Advances in Water Resources*, 120-132.

Gastkemper, H. (2013). *Riolering in beeld.* Stichting RIONED.

Gelormino, M. S., & Ricker, N. L. (1994). Model-predictive control of a combined sewer system. *International Journal of Control*.

Gernaey K., J. S. (2004). Benchmarking combined biological phosphorus and nitrogen removal wastewater treatment processes. *Control Engineering Practice*, 357-373.

Giraldo, J. M., Leirens, S., Díaz-Granados, M. A., & Rodríguez, J. P. (2010). Non-linear optimization for improving the operation of sewer. *International Congress on Environmental Modelling and Software*, 1-8.

Goldberg, D., & Holland, J. (1988). Genetic Algorithms and Machine Learning. *Machine Learning*, 95-99.

Hassanat, A., Almohammadi, K., Alkafaween, E., Abunawas, E., Hammouri, A., & Prasath, V. (2019). Choosing Mutation and Crossover Ratios for Genetic Algorithms—A Review with a New Dynamic Approach. *Information*, 1-36.

Heineman, M. (2004). NetSTORM- A Computer Program for Rainfall-Runoff Simulation and Precipitation Analysis. *World Water and Environmental Resources Congress .*

Heusch, S. (2011). *Modellprädiktive Abflusssteuerung mit hydrodynamischen Kanalnetzmodellen.* Darmstadt, Germany: Technische Universität Darmstadt.

Kanso, A., Chebbo, G., & Tassin, B. (2005). Stormwater quality modelling in combined sewer: calibration and ucenrtainty analysis. *Water Science Technology*, 63-71.

Kassem, A., & Hassan, A. (2012). Performance improvements of a permanent magnet synchronous machine via functional model predictive control. *Journal of Control Science and Engineering*.

Kroll, S. (2019). Design of Real-Time Control Strategies for Combined Sewer Networks.

Kroll, S., Weemaes, M., Van Impe, J., & Willems, P. (2018). A Methodology for the Design of RTC Strategies for Combined Sewer Networks. *Water*.

Langeveld, J., Benedetti, L., Klein, J., Nopens, I., Amerlinch, Y., Nieuwenhuijzen, A. v., . . . Weijers, S. (2013). Impact-Based Integrated Real-Time Control for Improvement of the Dommel River WAter Quality. *Urban Water Journal*, 312-329.

Langeveld, J., Van Daal, P., Schilperoort, R., Nopens, I., Flameling, T., & Weijers, S. (2017). *Empirical Sewer Water Quality Model for Generating Influent Data for WWTP Modelling.* Nijmegen, The Netherlands: Water.

Loucks, D., & van Beek, E. (2017). *Urban Water Systems.* Water Resource Systems Planning and Management.

Löwe, R., Vezzaro, L., Steen Mikkelsen, P., Grum, M., & Madsen, H. (2016). Probabilistic runoff volume forecasting in risk-based optmization for RTC of urban drainage systems. *Envinronmental Modelling & Software*, 143-158.

Lund, N., Falk, A., Borup, M., Madsen, H., & Mikkelsen, P. (2018). Model predictive control of urban drianage systems: A review and perspective towards smart real-time water management. *Critical Reviews in Environmental Science and Technology*, 279-339.

Maciejowski, J. (2002). *Predictive Control with Constraints;.* London, UK: Pearson Education Limited.

McDonnell, B. E., Ratliff, K. M., Tryby, M. E., Wu, J. J., & Mullapudi, A. (2020). PySWMM: The Python Interface to Stormwater Management Model (SWMM). *Journal of Open Source Software*, 2292.

Meng, F., Fu, G., & Butler, D. (2020). Regulatory implications of integrated real-time control technology under environmental uncertainty. *Environmental Science & Technology*, 1314–1325.

Mollerup, A. L., Thornberg, D., Mikkelsen, P. S., Johansen, N. B., & Sin, G. (2013). 16 Years of Experience with Rule Based Control of Copenhagen's. *11th Int. IWA Conf. on Instrumentation, Control and Automation* , 4.

Mollerup, A., Mikkelsen, P., Thornberg, D., & Sin, G. (2016). Controlling Sewer Systems- a Critical Review Based on Systems in Three EU Cities. *Urban Water Journal*, 1-8.

Moreno-Rodenas, A. M., Tscheikner-Gratl, F., Langeveld, J. G., & Clemens, F. (2019). Uncertainty Analysis in a Large-Scale Water Quality Integrated Catchment Modelling Study. *Water Research*, 46–60.

Mounce, S., Shepherd, W., Ostoijn, S., Abdel-Aal, M., Schellart, A. N., Shucksmith, J., & Tait, S. (2020). Optimisation of a fuzzy logic-based local real-time control system for mitigation of sewer flooding using genetic algortihms. *Journal of Hydroinformatics*.

Mulder, K. (2019). Future options for sewage and drainage systems three scenarios for transitions and continuity. *Sustainability*, 1383.

Nash, J., & Sutcliffe, J. (1970). River flow forecasting through conceptual models part I — A discussion of principles. *Journal of Hydrology*, 282-290.

Neugebauer, K., Schilling, W., & Weiss, J. (1991). A network algortihm for the optimum operation of urban drainage systems. *Water Science Technology*, 209-216.

Ngamalieu-Nengoue, U., Iglesias-Rey, P., & Saldarriaga, J. (2019). Urban Drainage Network Rehabilitation Considering Storm Tank Installation and Pipe Substitution. *Water*, 1-22.

Ocampo-Martinez, C., Ingimundarson, A., Puig, V., & Quevedo, J. (2008). Objective prioritization using lexicographic minimizers for MPC of sewer networks. *IEEE Transactions on Control Systems Technology*.

Ocampo-Martinez, C., Puig, V., Cembrano, G., & Quevedo, J. (2013). Application of MPC Strategies to the Mangement of Complex Networks of the Urban Water Cycle. *IEEE Control Systems Magazine*.

Ochoa-Rodriguez, O., Wang, L., Willems, P., & Onof, C. (2019). A Review of Radar- Rain Gauge Data Merging Methods and Their Potential for Urban Hydrological Applications. *Water Resources Research*, 6356-6391.

Olantunbosun Sojobi, A., & Zayed, T. (2022). Impact of sewer overflow on public health: A comprehensive scientometric analysis and systematic review. *Environmental Research*.

Overeem, A., Holleman, I., & Buishand, A. (2009). Derivation of a 10-year Radar-based Climatology of Rainfall. *Journal of Applied Meteorology and Climatology*, 1448–1463.

Pleau, M., Colas, H., Lavallee, P., Pelletier, G., & Bonin, R. (2005). Global Optimal Real-Time Control of the Quebec Urban Drainage System. *Environmental Modelling & Software*, 401–413.

Quijano, J., Zhu, Z., Morales, V., Landry, B., & Garcia, M. (2017). Three-dimensional model to capture the fate and transport of combined sewer overflow discharges: A case study in the Chicago Area Waterway System. *Sci. Total Environ.*, 362-373.

Rauch, W., & Harremoës, P. (1996). Minimising acute river pollution from urban drainage systems by means of integrated real time control. *First International Conference on New/Emerging Concepts for Rivers, S.* Chicago, IL.

Rauch, W., & Harremoës, P. (1999). Genetic algorithms in real time control applied to minimize transient pollution from urban wastewater. *Water Research*, 1265–1277.

Rawlings, R., Mayne, D., & Diehl, M. (2017). Model Predictive Control: Theory, Computation, and Design. Santa Barbara, California: Nob Hill Publishing.

Rossman, L. (2015). *Storm Water Manamgent Model User's Manual Version 5.1 .* Cincinnati: U.S. Environmental Protection Agency.

Sadler, J. M., Goodall, J. L., Behl, M., Morsy, M. M., Culver, T. B., & Bowes, B. D. (2019). Leveraging open source software and parallel computing for model predictive control of urban drainage systems using EPA-SWMM5. *Environmental Modelling & Software*.

Schütze, M., Butler, D., & Beck, M. B. (2002). Modelling, Simulation and Control of Urban Wastewater Systems. *Springer*.

Schütze, M., Campisano, A., Colas, H., Schilling, W., & Vanrolleghem, P. (2014). Real Time Control of Urban Wastewater Systems- Where Do We Stand Today? *Journal of Hydrology*, 335-348.

Schütze, M., Colas, H., Campisano, A., & Vanrolleghem, P. (2003). Real-Time Control of Urban Water Systems. *International Conference on Pumps, Electromechanical Devices and Systems Applied to Urban Water Management*.

Schütze, M., Erbe, V., Haas, U., Scheer, M., & Weyand, M. (2004). PASST-A planning aid for sewer system real time control. *proceedings of the 6th International Conference on Urban Drainage Modelling, UDM*, (p. 286). 2004.

Schütze, M., Erbe, V., Haas, U., Scheer, M., & Weyand, M. (2008). Sewer System Real-Time Control Supported by the M180 Guideline Document. *Urban Water Journal*, 69-78.

Schütze, M., Lange, M., Pabst, M., & Haas, U. (2017). Astlingen- a benchmark for real time control (RTC). *Water Science & Technology*.

Sojobi, A., & Tarek, Z. (2022). Impact of sewer overflow on public health: A comprehensive scientometric analysis and systematic review. *Environmental Research*.

Solgi, R. (2020). *genticalgorithm*. Retrieved from https://pypi.org/project/geneticalgortihm

Soriano, L., & Rubió, J. (2019). Impacts of Combined Sewer Overflows on surface water bodies. The case study of the Ebro River in Zaragoza City. *J. Clean. Prod.*, 1-5.

Stikkers, A. (n.d.). *BSc eindproject.*

Sun, C., Romero, L., Joseph-Duran, B., Meseguer, J., Muñoz, E., Guasch, R., . . . Cembrano, G. (2020). Integrated pollution-based real-time control of sanitation systems. *Journal of Environmental Management*, 110798.

Troutman, S., Love, N., & Kerkez, B. (2020). *Balancing water quality and flows in combined sewer systems using real-time control.* Environmental Science Water Reseach & Technology.

Umbarkar, A., & Sheth, P. (2015). Crossover Operators in Genetic Algorithms: A Review. *ICTACT Journal on soft computing*, 1-10.

United Nations. (2017). *UN World Development Report, Wastewater: The Untapped Resource.* UNEP.

van Daal, P. & Van Mill, G. (2020). *Pilot debietmeting vrijvervalleiding kern Geldrop - resultaten en evaluatie.*

van Daal-Rombouts, P. (2017). *Performance evaluation of real time control in urban wastewater systems.* doi:10.4233/uuid:b1d5d733-b271-474f-ad32-b5fdde257161

van Daal-Rombouts, P., Sun, S., Langeveld, J., Bertrand-Krajewski, J., & Clemens, F. (2016). Design and performance evaluation of a simplified dynamic model for combined sewer overflows in pumped sewer systems. *Journal of Hydrology*, 609-624.

van der Werf, J. A., Kapelan, Z., & Langeveld, J. (2021). 1 Quantifying the true potential of Real Time Control in urban drainage systems. *Urban Water Journal*, 873–884.

van der Werf, J. A, Kapelan, Z., & Langeveld, J. (2022). Towards the long term implementation of real time control of combined sewer systems:. *Water Science & Technology*.

van Riel, W. (2017). *Gemeentelijk Rioleringsplan 2018-2022 Geldrop-Mierlo.* SWECO.

Verzarro, L., & Grum, M. (2012). *A generalized Dynamic Overflow Risk Assessment (DORA) for urban drainage RTC.* bELGRADE.

Verzarro, L., Christensen, M., Thirsing, C., Grum, M., & Mikkelsen, P. (2014). Water quality-based real time control of integrated urban drainage systems: a preliminary study from Copenhagen, Denmark. *Procedia Engineering*, 1707-1716.

Vrugt, J., Braak, t. C., Gupta, H., & Robinson, B. (2009). Equifinality of formal (DREAM) and informal (GLUE) Bayesian approaches in hydrologic modeling? *Stochastic Environmental Research and Risk Assessment*, 1011-1026.

Wang, J. (2014). Combined sewer overflows (CSOs) impact on water quality and environmental ecosystem in the Harlemn river. *J. Environ. Prot. (Irvine,. Calif)*, 1373.

Waterschap de Dommel. (n.d.). *Overzichtskaarten Waterschap De Dommel.* Boxtel.

Weyand, M. (2002). Real-time control in combined sewer systems in Germany – some case studies. *Urban Water*, 347–354.

Willems, P. (2006). Random number generator or sewer water quality model? *Water Science Technology*, 387-394.

Willems, P., Arnbjerg-Nielsen, K., Ollson, J., & Nguyen, T. (2012). Climate change impact assessment on urban rainfall extremes and urban drainage: Methods and shortcomings. *Atmos. Res*, 106-118.

Wolfs, V., Villazon, F., M., & Willems, P. (2013). Development of a Semi-Automated Model Identification and Calibration Tool for Conceptual Modelling of Sewer Systems. *Water Science and Technology*, 167-175.

Wolfs, V., Villazon, M. F., & Willems, P. (2013). Development of a semi-automated model identification and calibration tool for conceptual modelling of sewer systems. *Water Science & Technology*, 167-174.

Yang, X.-S. (2014). Chapter 5- Genetic Algorithms. In X. Yang, *Nature-Inspired Optimization Algorithms* (pp. 77-87). Elsevier.

Appendix

Appendix 1 – WWTP Eindhoven in WEST, *Layout*
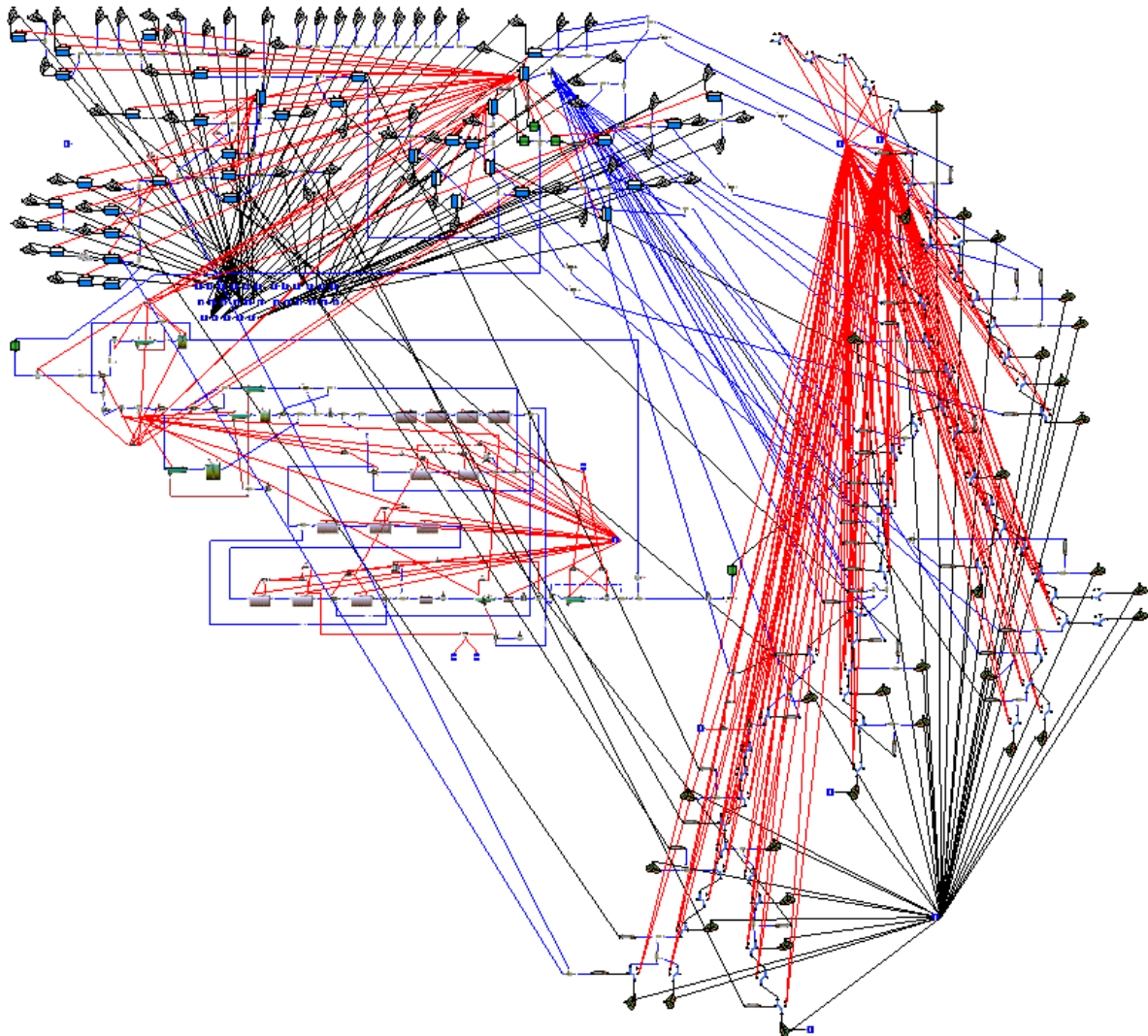
Appendix 2 – Explanation genetic algorithm

Selection

The optimization problem will be solved by finding the optimal settings for the selected actuators in the system.

The GA process starts by creating an '*initial population'.* The initial population consists of multiple individuals. Each individual stands for a solution to the problem that needs to be solved. An individual is characterized by a chromosome, that consists of multiple 'genes'.
The genes are joined into a string to form a chromosome, which forms eventually the solution. Once each individual in the population has been generated, the rest of the GA process can start. The size of the population at the start of the GA is user-defined. A low population can cause that the solution quickly converges, which makes it hard to find the global optimum (Hassanat et al., 2019). On the other hand, a high population increases the computational load. To ease the optimization process, the boundaries for the actuator settings are represented by integer values.
Each individual is evaluated based on the objective function and ranked based on the fitness for the objective function. The fitness score indicates the ability of an individual to compete with other

individuals. The individuals with the best fitness function are selected. The user-defined, elite ratio, determines what percentage of the individuals with the best fitness are selected to become the next generation and produce offspring. If the elite ratio is too big, the chance of being trapped in local optima is big. Therefore, the elite ratio should be small.

Reproduction

After the selection process of the most promising individuals, the reproduction process can start. The offspring are produced by the parents based on the user-defined, crossover-type, and crossover probability (Yang, 2014).

In this research, the uniform crossover method is used (figure 51) to reproduce new individuals with a selection of the elite individuals. The uniform crossover method is chosen because each chromosome within an individual represents a string of actuators. During crossover, it is important that the order of this string does not mix. E.g. otherwise one individual can consist of multiple genes that represent a pump. The crossover probability indicates how the genes of the parents will be exchanged.
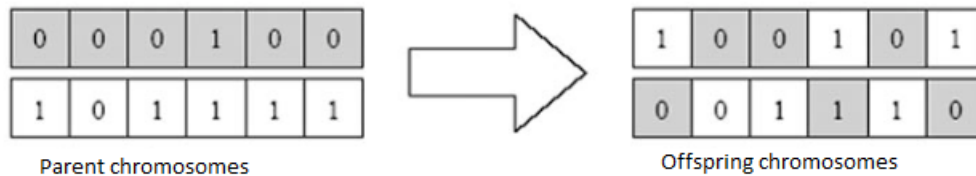

Figure 51: Uniform crossover

Hereafter, the mutation generator introduces random values to the genes of the new offspring created in the uniform crossover process. During the mutation process, a gene within an individual receives a randomly generated value. Mutation ensures that the local optima within the optimization process can be escaped and it enables the algorithm to explore more diversity. The mutation is dependent on the user-defined mutation probability. The mutation probability indicates the probability of each gene to mutate (Yang, 2014). The new population, consisting of new individuals, undergoes the same evaluation and reproduction process as their parents up till the point that the user-defined termination criteria are met. The termination criteria are either set by the maximum number of iterations or by the maximum number of iterations without improvement.

The choice of the algorithm parameters (population size, crossover probability, mutation probability, parents portion, elite ratio, number of iterations, and iterations without stopping criteria) is based on trial-and-error. The algorithm parameters are chosen in such a way that the GA has sufficient possibilities to find an optimum in the least possible simulation time.

Appendix 3 - Correction factor measurement data FH model

The water level at Geldrop_1 is measured using a Flow Tronic Ultrasone level measurement, with a resolution of <1 mm and an accuracy of 0.3% of the measuring range. The water height measurement in meter water column above the sensor. The measuring range is 4 meter water column with an accuracy of 0.1%. The velocity at Geldrop_2 is measured using a Flow Tronic Ultrasone Doppler measurement (Beluga). Measuring range is -2 - +6 m/s with a resolution of 0.001 m/s. According to the

specifications is the accuracy 1% of the measuring range, resulting in an discharge accuracy of approximately 5% (Van Daal & Van Mill, 2020).

The water level data for Geldrop_1 is corrected by:

$$H_1[m\ water\ column] = H_{1\ logged} - 2.863$$

The water level data for Geldrop_2 is corrected by:

$$H_2\ [m + NAP] = H_2[m\ water\ column] + 17.847 - 3.208$$

The velocity measurement for Geldrop_2 is used to calculate the discharge at Geldrop_2:

$$Discharge_2 = 1.324 * A * v$$

In which 1.324 is a correction factor, A is the wetted perimeter and v is velocity

$$A = -0.7701\ H_2{}^3 + 1.398\ H_2{}^2 + 0.3829 * H_2$$

Appendix 4 – Adjustment input data conversion InfoWorks to SWMM

	Name	Type	Region		Length		Geom1	Geom2
-	10725	combined	area 1	1	41.0	RECT	1250	750
-	A*HLCMRZ1132	foul		1	199.7	RECT	2650	2100
-	A*HLCMRZ1133	foul		1	151.6	RECT	2650	2100
-	A*HLCMRZ1134	foul		1	41.7	RECT	2650	2100
-	A*HLCMRZ1135	foul		1	18.0	RECT	2650	2100
-	A*HLGDRW1317	foul		1	552.8	RECT	2000	1800
-	A*HLRZ00130213021302		foul	1	116.3	RECT	2000	1800
-	A*HLRZ00110111011101		foul	1	118.6	RECT	2650	2100
-	A*HLRZ00110411041104		foul	1	483.0	RECT	2650	2100
-	A*HLCMRZ1131		foul	1	261.2	RECT	2650	2100
-	A*HLRZ00110411041104		foul	1	82.7	RECT	2000	1800
-	A*HLRZ00121912191219		foul	1	580.9	RECT	2000	1800
-	A*HLRZ00122112211221		foul	1	105.8	RECT	2000	1800
-	A*HLRZ00124812481248		foul	1	54.1	RECT	2000	1800
-	A*HLRZ00124912491249		foul	1	653.9	RECT	2000	1800
-	A*HLRZ00128312831283		foul	1	592.9	RECT	2000	1800
-	A*HLGDRW1290		foul	1	96.3	RECT	2000	1800
-	A*HLRZ00130313031303		foul	1	127.5	RECT	2000	1800
-	A*HLRZ00130613061306		foul	1	169.8	RECT	2250	1800
-	A*HLRZ00130713071307		foul	1	203.6	RECT	2250	1800
-	A*HLRZ00130813081308		foul	1	74.7	RECT	2250	1800
-	A*HLRZ00130913091309		foul	1	142.5	RECT	2250	1800
-	A*HLRZ00131013101310		foul	1	60.8	RECT	2250	1800
-	Ontvangkelder	foul		1	29.6	RECT	2250	1800
-	A*HLRZ00959959959		foul	1	1822.2	RECT	1900	1500
-	A*HLRZ00957957957		foul	1	863.0	RECT	1900	1500
-	A*HLRZ00891891891		foul	1	136.4	RECT	1900	1500
-	A*HLRZ00970970970		foul	1	145.2	RECT	1900	1500
-	A*HLRZ00972972972		foul	1	140.7	RECT	1900	1500
-	A*HLRZ00974974974		foul	1	352.3	RECT	2650	2100
-	A*HLRZ00976976976		foul	1	66.5	RECT	2650	2100
-	A*HLRZ00978978978		foul	1	300.8	RECT	2650	2100

-	A*HLRZ00980980980	foul		1	84.8	RECT	2650	2100	
-	A*HLRZ00982982982	foul		1	199.8	RECT	2650	2100	
-	A*HLRZ00109910991099		foul	1	633.3	RECT	2650	2100	
-	BBB1	combined	BBB1	1	18.0	RECT	4000	2250	
-	BBB4	combined	BBB4	1	28.0	RECT	3000	2000	
-	BBB7	combined	BBB7	1	25.0	RECT	3000	2000	
-	BBB7	combined	BBB7	1	25.0	RECT	3000	2000	
-	BEK1	combined	uitloop BBB1	1	100.0	RECT	2740	1240	
-	BEK4	combined	uitloop BBB4	1	78.0	RECT	9100	2200	
-	BEK7	combined	uitloop BBB7	1	83.0	RECT	8200	2400	
-									

Appendix 5: Adjustment input data SWMM

```
Con_100101.1    RECT_OPEN  0.500000     1.500000 0.000000  0.000000
Con_100244.1    RECT_OPEN  0.500000     1.000000 0.000000  0.000000
Con_100361.1    RECT_OPEN  0.500000     3.400000 0.000000  0.000000
Con_100564.1    RECT_OPEN  0.500000     13.500000 0.000000  0.000000
Con_100564F.2   RECT_OPEN  0.500000     13.500000 0.000000  0.000000
Con_10071-01.1  RECT_OPEN  0.500000     0.800000 0.000000  0.000000
Con_100782-10.1 RECT_OPEN  0.500000     2.000000 0.000000  0.000000
Con_10143-01.2  RECT_OPEN  0.500000     2.000000 0.000000  0.000000
Con_10420.1     RECT_OPEN  0.5000000    12.300000 0.000000  0.000000
Con_10420.3     RECT_OPEN  0.5000000    12.300000 0.000000  0.000000
Con_1117.2      RECT_OPEN  0.500000     3.000000 0.000000  0.000000
Con_1121.2      RECT_OPEN  0.500000     1.500000 0.000000  0.000000
Con_1204.2      RECT_OPEN  0.500000     0.900000 0.000000  0.000000
Con_1330.2      RECT_OPEN  0.500000     1.000000 0.000000  0.000000
Con_1543.2      RECT_OPEN  0.500000     3.000000 0.000000  0.000000
Con_159.2       RECT_OPEN  0.500000     4.000000 0.000000  0.000000
Con_160098-01.1 RECT_OPEN  0.500000     0.800000 0.000000  0.000000
Con_160173-10.1 RECT_OPEN  0.500000     4.000000 0.000000  0.000000
Con_160173-10.2 RECT_OPEN  0.500000     3.200000 0.000000  0.000000
Con_160235F     RECT_OPEN  0.500000     1.500000 0.000000  0.000000
Con_160246.2    RECT_OPEN  0.500000     1.000000 0.000000  0.000000
Con_160247.1    RECT_OPEN  0.500000     1.000000 0.000000  0.000000
Con_160272.2    RECT_OPEN  0.500000     0.800000 0.000000  0.000000
Con_160321.2    RECT_OPEN  0.500000     1.000000 0.000000  0.000000
Con_160322.1    RECT_OPEN  0.500000     3.000000 0.000000  0.000000
Con_160415.1    RECT_OPEN  0.500000     0.800000 0.000000  0.000000
Con_160420.1    RECT_OPEN  0.500000     0.800000 0.000000  0.000000
Con_161012.1    RECT_OPEN  0.500000     0.800000 0.000000  0.000000
Con_163010.2    RECT_OPEN  0.500000     0.800000 0.000000  0.000000
Con_163013.2    RECT_OPEN  0.500000     1.000000 0.000000  0.000000
Con_163027U.2   RECT_OPEN  0.500000     2.000000 0.000000  0.000000
Con_1686.2      RECT_OPEN  0.500000     3.000000 0.000000  0.000000
Con_1902.2      RECT_OPEN  0.500000     1.000000 0.000000  0.000000
Con_190220.1    RECT_OPEN  0.500000     0.800000 0.000000  0.000000
Con_1921.2      RECT_OPEN  0.500000     2.000000 0.000000  0.000000
Con_20071-02.2  RECT_OPEN  0.500000     1.800000 0.000000  0.000000
Con_20089F.1    RECT_OPEN  0.500000     4.250000 0.000000  0.000000
Con_2123.2      RECT_OPEN  0.500000     1.000000 0.000000  0.000000
Con_2145.2      RECT_OPEN  0.500000     1.000000 0.000000  0.000000
```

```
Con_25.2        RECT_OPEN  0.500000    4.000000 0.000000  0.000000
Con_30001-04.1 RECT_OPEN  0.500000     0.800000 0.000000  0.000000
Con_30079-03.1 RECT_OPEN  0.500000     0.750000 0.000000  0.000000
Con_302.2       RECT_OPEN  0.500000    4.000000 0.000000  0.000000
Con_30205.1    RECT_OPEN  0.500000    23.550000 0.000000  0.000000
Con_30209.1    RECT_OPEN  0.500000    23.550000 0.000000  0.000000
Con_40182.2    RECT_OPEN  0.500000    1.200000 0.000000  0.000000
Con_452.2       RECT_OPEN  0.500000    3.000000 0.000000  0.000000
Con_50028-07.1 RECT_OPEN  0.500000    4.500000 0.000000  0.000000
Con_559.3       RECT_OPEN  0.500000    2.000000 0.000000  0.000000
Con_60071-06.1 RECT_OPEN  0.500000     5.000000 0.000000  0.000000
Con_70004.1    RECT_OPEN  0.500000    2.600000 0.000000  0.000000
Con_70101-07.1 RECT_OPEN  0.500000    1.000000 0.000000  0.000000
Con_70231-07.1 RECT_OPEN  0.500000    1.000000 0.000000  0.000000
Con_70273.3    RECT_OPEN  0.500000    4.200000 0.000000  0.000000
Con_754.2       RECT_OPEN  0.500000    2.000000 0.000000  0.000000
Con_80225.2    RECT_OPEN  0.500000    2.360000 0.000000  0.000000
Con_80226.2    RECT_OPEN  0.500000    7.800000 0.000000  0.000000
Con_80604.1    RECT_OPEN  0.500000    4.500000 0.000000  0.000000
Con_80900.2    RECT_OPEN  0.500000    2.000000 0.000000  0.000000
Con_90102.2    RECT_OPEN  0.500000    1.800000 0.000000  0.000000
Con_939.2       RECT_OPEN  0.500000    4.000000 0.000000  0.000000
Con_A*HLCMRZ1135.1 RECT_OPEN  0.500000     9.000000 0.000000  0.000000
Con_BBB_Rielsedijk.2 RECT_OPEN  0.500000    24.600000 0.000000  0.000000
Con_BBB1.3     RECT_OPEN  0.500000    4.000000 0.000000  0.000000
Con_BBB2-C.1   RECT_OPEN  0.500000     8.000000 0.000000  0.000000
Con_BBB4.3     RECT_OPEN  0.500000    3.000000 0.000000  0.000000
Con_BBB7-1.2   RECT_OPEN  0.500000     6.250000 0.000000  0.000000
Con_BEK7.1     RECT_OPEN  0.500000    3.000000 0.000000  0.000000
Con_N*1-D2.33y.3 RECT_OPEN  0.500000     1.600000 0.000000  0.000000
Con_N*OVED01.2 RECT_OPEN  0.500000     2.000000 0.000000  0.000000
```

Appendix 6 – Scoring table for assessment of RTC potential of sewer systems

	Criterion	Evaluation		
A.	**Catchment**	Scores (value in brackets)		
A.1	Catchment area (Flow length in the main collector)	Long > 5 km (2)	Medium (1)	Short < 1 km (0)
A.2	Differences between current and planned development of the area	Large (2)	Small (1)	None (0)
B.	**Wastewater production**			
B.1	Areas with increased pollution of surface runoff	Several (2)	1–2 (1)	None (0)
B.2	Variability in time and space of wastewater production (e.g. producers of heavily polluted wastewater, connections from separate systems)	High (2)	Medium (1)	None (0)
C.	**Sewer system**			
C.1	Number of existing control devices (e.g. pumps, slides, weirs)	Several (4)	1–2 (2)	None (0)
C.2	Slope of trunk sewers	Flat < 0,2% (4)	Medium (2)	Steep > 0,5% (0)
C.3	Capable loops in the sewer system	Several (4)	1–2 (2)	None (0)
C.4	Number of existing storage tanks (tanks and storage pipes ≥ 50 m^3)	>4 (4)	1–4 (2)	0 (0)
C.5	Number of discharge devices	>6 (4)	2–6 (2)	<2 (0)
C.6	Total storage volume (tanks and storage pipes)	>5000 m^3 (4)	2000–5000 m^3 (2)	<2000 m^3 (0)
C.7	Specific storage volume (= total storage volume related to impervious area)	>40 m^3/ha (4)	20–40 m^3/ha (2)	<20 m^3/ha (0)
C.8	Number of collectors to the WWTP	>2 (3)	2 (1)	1 (0)
D.	**Operational system behaviour**			
D.1	Local flood areas	Several (2)	1–2 (1)	None (0)
D.2	Number of non-uniformly used tanks	>1 (4)	1 (2)	None (0)
D.3	Non-uniform discharge behaviour	Significant (4)	Medium (2)	Insignificant (0)
E.	**Receiving water**			
E.1	Local differences in hydraulic capacity	Strong (4)	Medium (2)	None (0)
E.2	Local differences of load capacity (e.g. swimming, fish farming, protected areas)	Significant (4)	Medium (2)	Insignificant (0)
E.3	Sensitivity of the receiving water body	Very sensitive (2)		Less sensitive (0)
F.	**Wastewater treatment plant (WWTP)**			
F.1	Admissible combined wastewater inflow (*)	>1,0 $f_{S,QM} \cdot Q_{S,aM}$ + $Q_{F,aM}$ (3)	>$f_{S,QM} \cdot Q_{S,aM}$ + $Q_{F,aM}$ (1)	<$f_{S,QM} \cdot Q_{S,aM}$ + $Q_{F,aM}$ (0)
F.2	Sensitivity of WWTP to hydraulic or pollutant peaks	Very sensitive (2)		Less sensitive (0)

(*) The values of the combined wastewater inflow and the appropriate factor $f_{S,QM}$ are related to the ATV-DVWK guidelines A 198 (ATV-DVWK 2003).
Scores: 0–24: probably not suitable for RTC.
25–35: probably suitable for RTC.
>35: very suitable for RTC.

A.1 Catchment extent (Flow length in the main collector) In large catchments, rainfall is usually non-uniformly distributed. Therefore, the system is often non-uniformly utilized, in particular when there are long flow times in the sewer system. Storage volume available in some parts of the catchment can possibly be used for a reduction of the pollution load in other parts. Alternatively, available sewer capacity can be used for an increased flow of the heavily polluted wastewater towards the WWTP.

A.2 Differences between current and planned development of the area Sewer systems are designed for a specific load and specific boundary conditions (area size/wastewater flow). In case of non-completed development of urban areas, the flows are lower than planned. Storage volumes are possibly not used optimally. With the help of RTC it is possible to react flexibly to the different degrees of development of the area.

B.1 Areas with increased pollution of surface runoff Some catchment areas have specific parts with particularly polluted rainwater. It may be beneficial to direct this heavily polluted water to the WWTP with high priority, or to store it and not to discharge this heavily polluted water, but the water from less polluted areas. With the help of RTC it is possible to influence the throttle flow out of the tanks in an appropriate way.

B.2 Variability in time and space of wastewater production (e.g. producers of heavily polluted wastewater, connections from separate systems) Inflows from separate sewer systems or single

source inflows of heavily polluted wastewater can cause significantly higher pollutant concentrations in specific areas of the sewer system. With the help of RTC, the throttle outflows can be set dynamically so as to prevent discharges from the areas with highly polluted wastewaters.

C.1 Number of existing control devices (e.g. pumps, slides, weirs) RTC control actions take place at pumps, slides, weirs etc. If such control devices are already available in the system, RTC can be realized easily by only a few additions with regard to measurement or control devices.

C.2 Slope of trunk sewers In trunk sewers with large profile dimensions and small slopes additional storage volume can be activated by cascades. Flow chart of RTC planning procedure.

C.3 Capable loops in the sewer system Loops in the sewer system provide the possibility to distribute the flow through different branches of the network. Therefore a more flexible management of flows is possible.

C.4 Number of existing storage tanks (tanks and storage pipes 50 m³) Fixed throttle outflows of the storage tanks can result in uneven utilization of tanks. With an increasing number of storage tanks the potential of equalizing the utilization of the tanks with the help of RTC increases.

C.5 Number of discharge devices If there are several discharge devices in the sewer system, it is possible to react to different conditions in a more flexible way. The advantages of RTC can be better utilized than in a system with a small number of discharge devices.

C.6 Total storage volume (tanks and storage pipes) The ability to activate large storage volume is characterized by a good cost-benefit ratio because part of the costs of RTC are fixed costs and do not relate to the size of the tank.

C.7 Specific storage volume (¼ total storage volume related to impervious area) If there is only little specific storage tank volume, the storage tanks are full even during small rain events. In this case, RTC cannot help significantly to reduce the discharge volume.

C.8 Number of collectors to the WWTP If there are several collectors leading to the WWTP, it can be expected that in case of rainfall the collectors are not used in a uniform way. With the help of RTC, less utilized sewers can be used in a better way.

D.1 Local flood areas In case of heavy rainfall there are often locally limited areas which are flooded whilst other areas have enough flow capacity available. If there are no structural bottlenecks, such flooding indicates that available resources are being insufficiently used. This situation can be improved by RTC.

D.2 Number of non-uniformly used tanks An uneven utilization of storage tanks is an indication that the available volumes are not used in an optimum way. If this is the case for only one tank, then already local RTC can result in a better utilization of the available storage volume. If several tanks are used in an unbalanced way, global RTC, enabling dynamic operation of throttle outflows depending on the current state of the network, can improve the situation.

D.3 Non-uniform discharge behavior Non-uniform discharge behavior indicates non-optimum use of the storage capacities. The stronger the differences concerning discharge behavior are, the more improvement can be expected with regard to a better utilization of the storage capacity, (for example by operation of throttle outflows depending on the current state of the network).

E.1 Local differences in hydraulic capacity If there are differences in the hydraulic capacity of the receiving water bodies, RTC can be used for discharging hydraulic peaks into those receiving water bodies which have higher hydraulic capacity (e.g. with the help of adjustable weirs).

E.2 Local differences of load capacity (e.g. swimming, fish farming, protected areas) By better operation of the throttle outflows at existing storage tanks, discharges can be influenced in such a way that priority is given to discharges into receiving waters with higher capacity.

E.3 Sensitivity of the receiving water body Where there are sensitive receiving waters, it is necessary to either avoid discharges or to reduce discharge volume significantly. RTC is useful in this case because the system becomes more flexible and the existing storage volume can be better utilized.

F.1 Admissible combined wastewater inflow In some cases the WWTP is able to treat more than the maximum permissible inflow to the WWTP according to A198 (ATV-DVWK 2003), even during longer periods and without impairing the treatment efficiency. The A198 guideline document defines the maximum permissible inflow to the WWTP as $f_{S,QM} * Q_{S,aM} + Q_{F,aM'}$, where $Q_{S,aM}$ is the dry weather flow to the WWTP, $Q_{F,aM}$ the inflow from extraneous sources (e.g. infiltration/inflow), and $f_{S,QM}$ a case-specific factor for estimating the maximum dry weather flow to the plant. The result can be a reduction of discharges from the sewer system. RTC enables an increased inflow to the WWTP depending on its current treatment capacity (integrated RTC).

F.2 Sensitivity of WWTP to hydraulic or pollutant peaks If the WWTP is sensitive to hydraulic or load peaks, RTC can assist in increasing slowly into the WWTP during rain. This results in a better utilization of storage volume in the sewer system. Integrated RTC of sewer system and WWTP can possibly reconcile the contradicting requirements of the subsystems (sewer system and WWTP) and lead to optimum operation of the entire system (Schütze et al., 2008).

Appendix 7 – Explanation results PASST scoring table

A1: The flow length of RZ in the sewer catchment is approximately 9900 meter

A2: The expectation is that there will be an increase of 75 houses per year in the case study area. In the cities/ villages the houses need to be connected to the free-decay/ gravity systems. Whereas in the outer areas, the houses need to be connected to a pressurized system. The (new) home-owners need to deliver their water separately. All the developments and adjustments in the aboveground facilities, have to consider the municipalities' risk on flooding. For the construction of new houses, the principle of the water authority from De Dommel is followed: 'Hydrologisch Neutraal Ontwikkelen', meaning 'Hydrologic Neutral Development'. Practically, this means that developments must be in the same order of magnitude as the baseline situation.
From 2018-2022 the municipality is replacing the current sewer pipelines with new pipelines. Based on this information, the difference between the current and planned development of the area is small.

B1: Both Geldrop and Mierlo have an area with a high concentration of industrial activity. However, it is expected that these areas do not cause an increased pollution of surface runoff.

B2: There are no connections of separate systems that cause a variability in time/ space of wastewater production in the case study area

C1: The number of control devices are: pump Mierlo, vortex valve Geldrop West, pump Eindhoven, pump WWTP

C2: The slope of RZ varies, since it consists of multiple connected pipelines. But the overall slope of pipeline RZ is < 0.2% and hereby it is considered as flat.

C3: The sewer system is partly looped, but the loops are expected to not have an impact on the RTC performance. Therefore these loops are not considered.

C4: There are 5 storage units in the case study area.

C5: There are no additional discharge devices in the case study area

C6: The sum of the storage units and the volume of transportline RZ is above 5000 m^3

C7: The collectors to the WWTP are: Eindhoven, Nuenen-Son and Geldrop-Mierlo

D1: There are no appointed local flood areas. However, the norm is that the entire area contains an additional 60 mm above-ground storage in public space. This area is not considered in this assessment.

D2: The tanks are located across the entire case-study area, meaning that the usage of the tanks are non-uniform in time. This could be an opportunity to improve the system performance using RTC.

D3: The case study area contains of areas that are characterized by non-uniform discharge behavior. For example, the discharge from catchment Geldrop East towards the transportline is dependent on the pump discharge of Mierlo – transportline. Operation of the pump Mierlo could indirectly improve the discharge behavior of Geldrop East.

E1: For the case of Mierlo, outlets are connected to the following waters:
- Luchense Wetering
- Overakkerse Loop
- Ditch/ trench
- Goorloop

- Beemschelsche loop. This water is connected to Goorloop, which discharges to the Eindhovensche Kanaal
- Beemsitsche loop. This water is connected to Goorloop, which discharges to the Eindhovensche Kanaal

For the case of Geldrop, outlets are connected to the following waters:
- De Kleine Dommel
- Beekloop

The WWTP discharges on the Dommel. As can be seen above, the variety of receiving water bodies have a different hydraulic capacity. De Kleine Dommel and the Dommel are the most important rivers in this study. The hydraulic capacity of the Dommel is considerably higher than the capacity of the Kleine Dommel.

E2: For this question, again the Dommel and the Kleine Dommel are the most significant water bodies. The water quality of both rivers are affected by different impacts caused by the UDS. The CSO location Collse Molen is located at the transport line RZ. If this CSO location spills, the DO concentration in the receiving water body (the Kleine Dommel) drops and the ecological impact is severe. Because of the low discharge of the Kleine Dommel, the impact of a CSO event can be significant. Therefore, a CSO event should be prevented at all times. Ammonium peak concentration in the WWTP effluent mainly impacts the Dommel. The different natures of the ecological impact (ammonium peak/ DO dip) cause local differences in load capacity.

E3: The Kleine Dommel is considered as a sensitive receiving water body.

F1: -

F2: The WWTP is sensitive for hydraulic or load peaks, causing possible ammonium peak concentrations in the WWTP effluent.

Appendix 8 – Additional validation results FH model

Event   **3**

Event 3 is characterized by a single rainfall event with a lower rainfall intensity than experienced during event 2. This gives insight into the calibration accuracy of the system state during lower head levels. Dom008 shows an additional peak in the model due to erroneous input rainfall data. The input rainfall data for a sub-catchment is created by taking the weighted share of multiple pixels that are connected to that sub-catchment. In this case, the pixel data is not accurate for the whole area covered by the pixel. This was proved by comparison of rainfall input data of adjacent nodes. The input data for the catchment differs from the actual rainfall. The conversion of pixel data to rain data for catchments can result, due to areal rainfall differences within a pixel, in erroneous input data for the model. The frequency of these errors will reduce if the pixel becomes smaller. The accuracy of the rainfall input data is hereby dependent on the available pixel data.

During the calibration process, multiple test simulations had the outcome that head loss at location Dom0402 does not impact the calibration result of the locations at Dom009 and more upstream. However, as this validation result shows, the head at Collse Molen is significantly lower than the head in the measurement data. The calibration & validation result of event 1 &2 showed that during more critical events (head levels of 16+m NAP), the head at location Collse Molen is simulated well. Therefore, this validation result is considered as accurate enough for the purpose of this research.
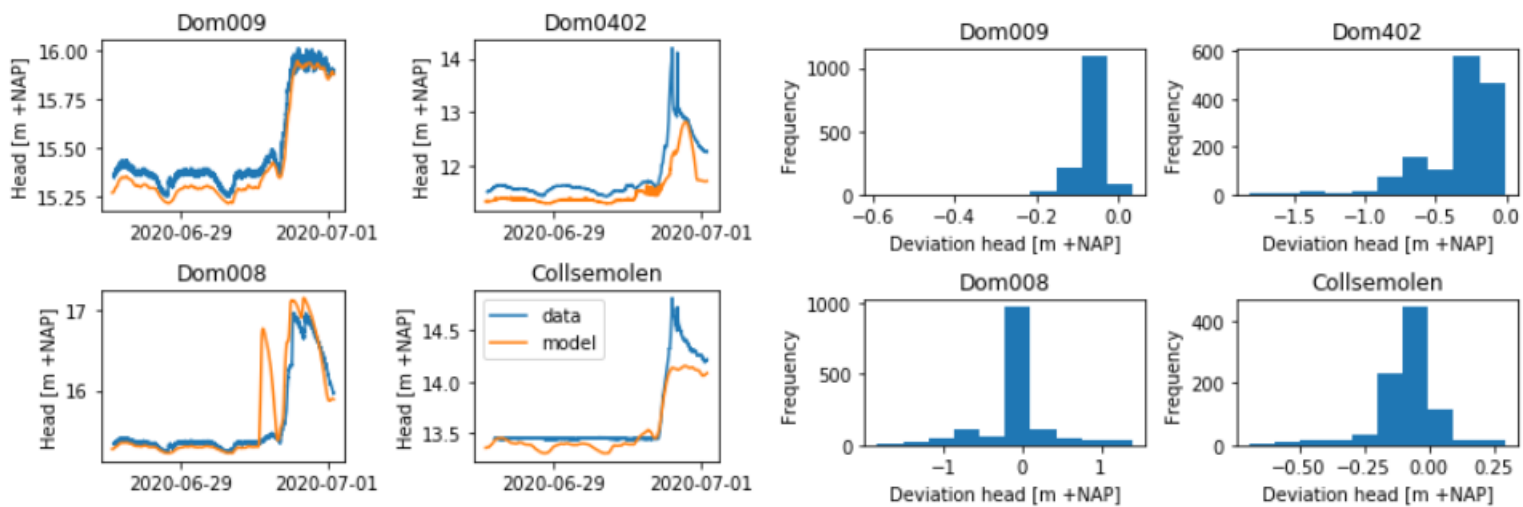
Event 4

Measurement location GO2 is located directly upstream of the connection of Geldrop East and the transport line. The first two smaller peaks are calibrated correctly, whereas the higher peaks show a slight distortion from the measurement data (Figure 35 & 36). The model shows a total of 3 peaks, similar to the measurement data, but the magnitude of the peaks is slightly off. The deviation is not significant, supported by the NSE value. GO1 follows the same pattern as GO2.

The calibration results for Mierlo show the same pattern as the measured head data, but the head in the model fluctuates more. These small fluctuations are caused by the turning on- and off of the pump that is discharging on the transport line. Since these fluctuations are caused by the pump, the impact of these fluctuations do not affect the system state within catchment Mierlo.
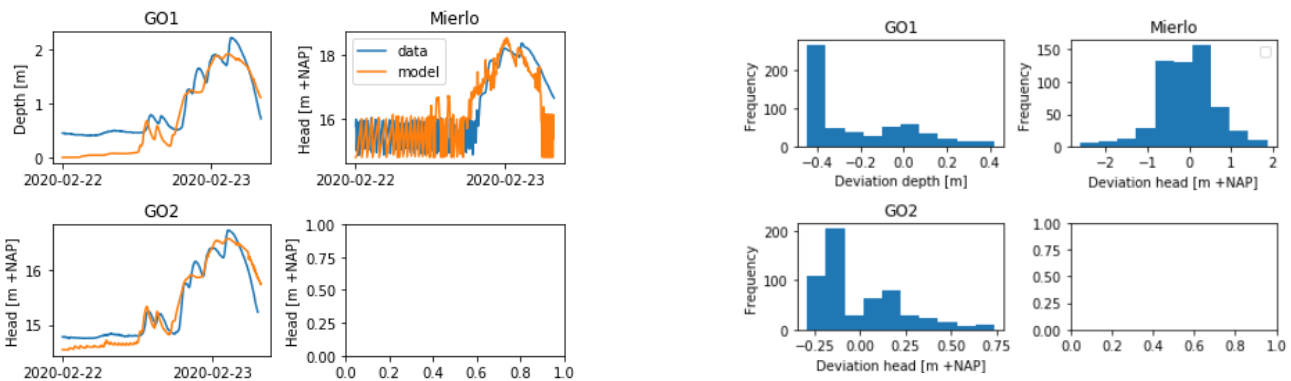
Event 5

The validation results of location GO1 and GO2 follow the WWF pattern correctly (Figure 37 & 38). The graph of GO2 shows that during the second peak, the head is fluctuating. This is caused by the connection to the transport line. This does not impact the overall system state. The third peak is in GO2, as well as in Mierlo, slightly too high. A possible cause for this is that the roughness coefficient of the downstream transportline is slightly too high. But since the validation results for the bigger peaks follow the measurement data, it is chosen to not change the roughness coefficient of this transportline.
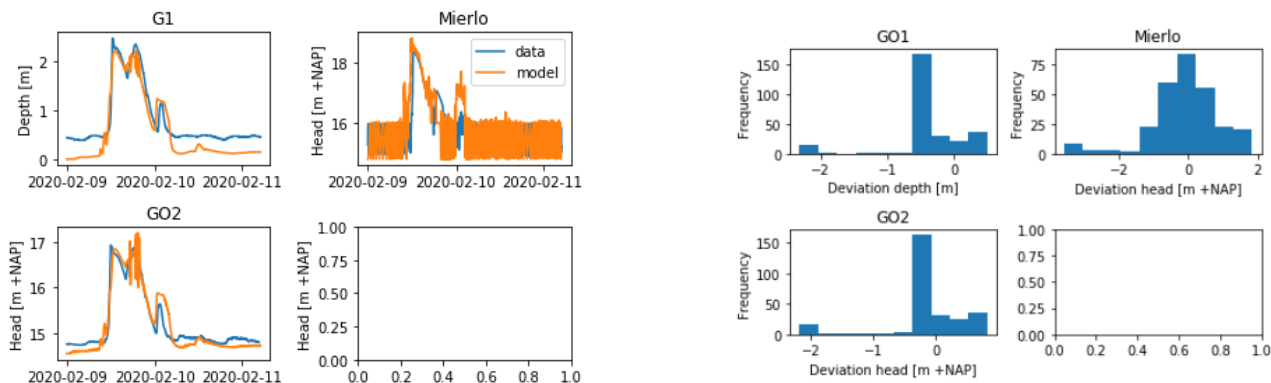
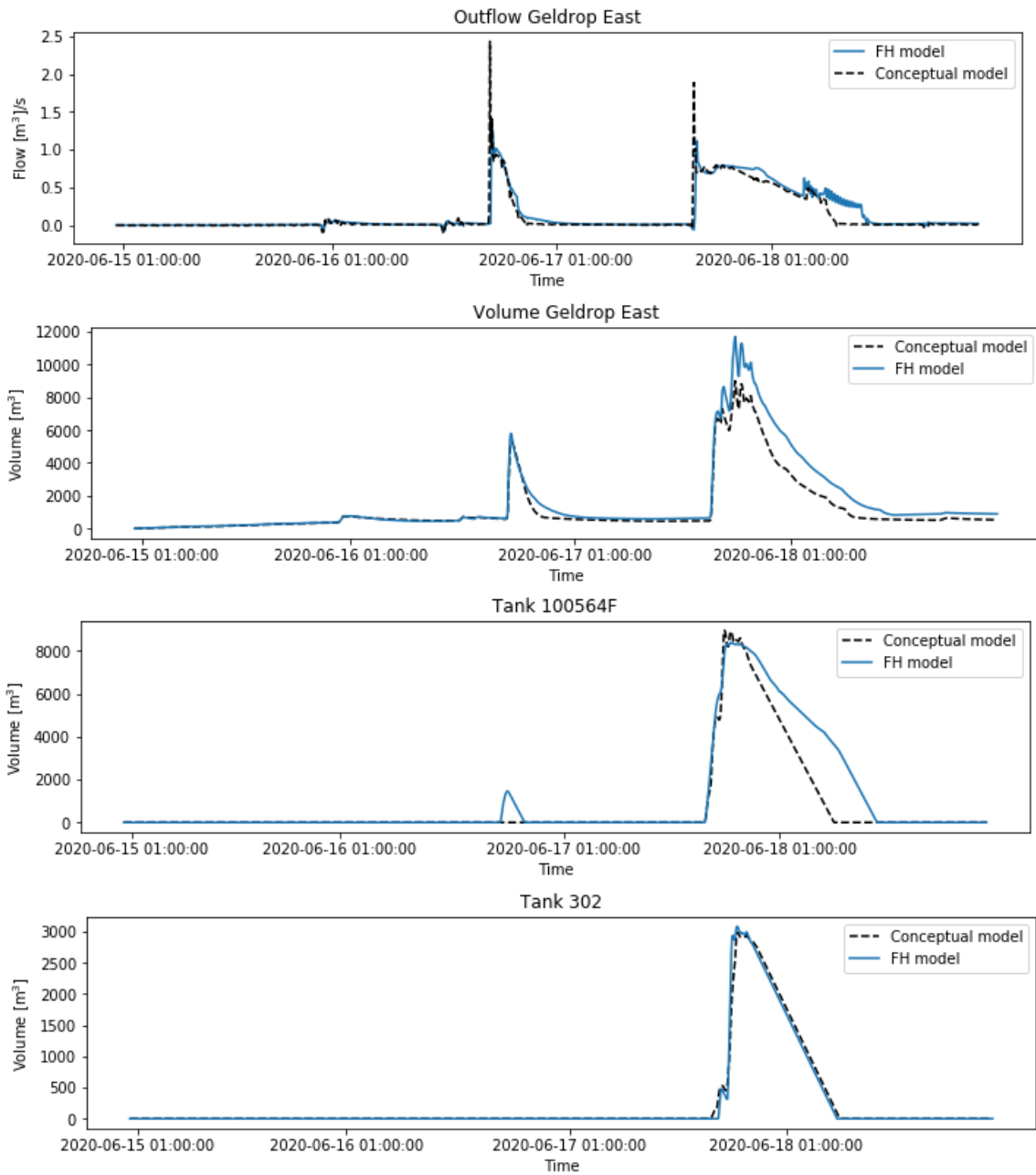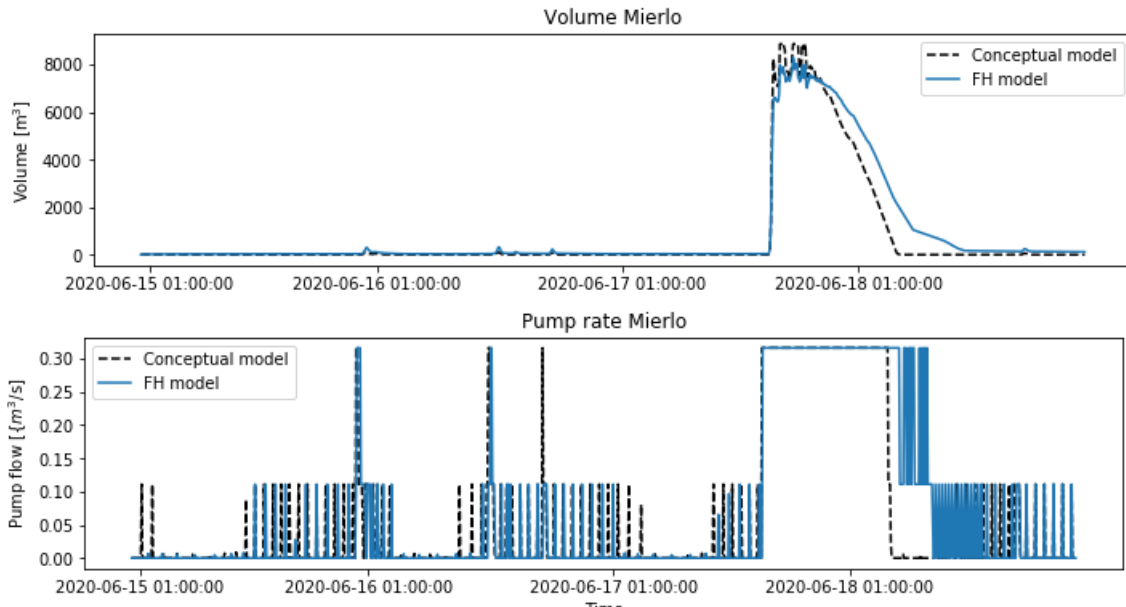# Appendix 9 – Additional validation results conceptual model

Event **6**

Geldrop West
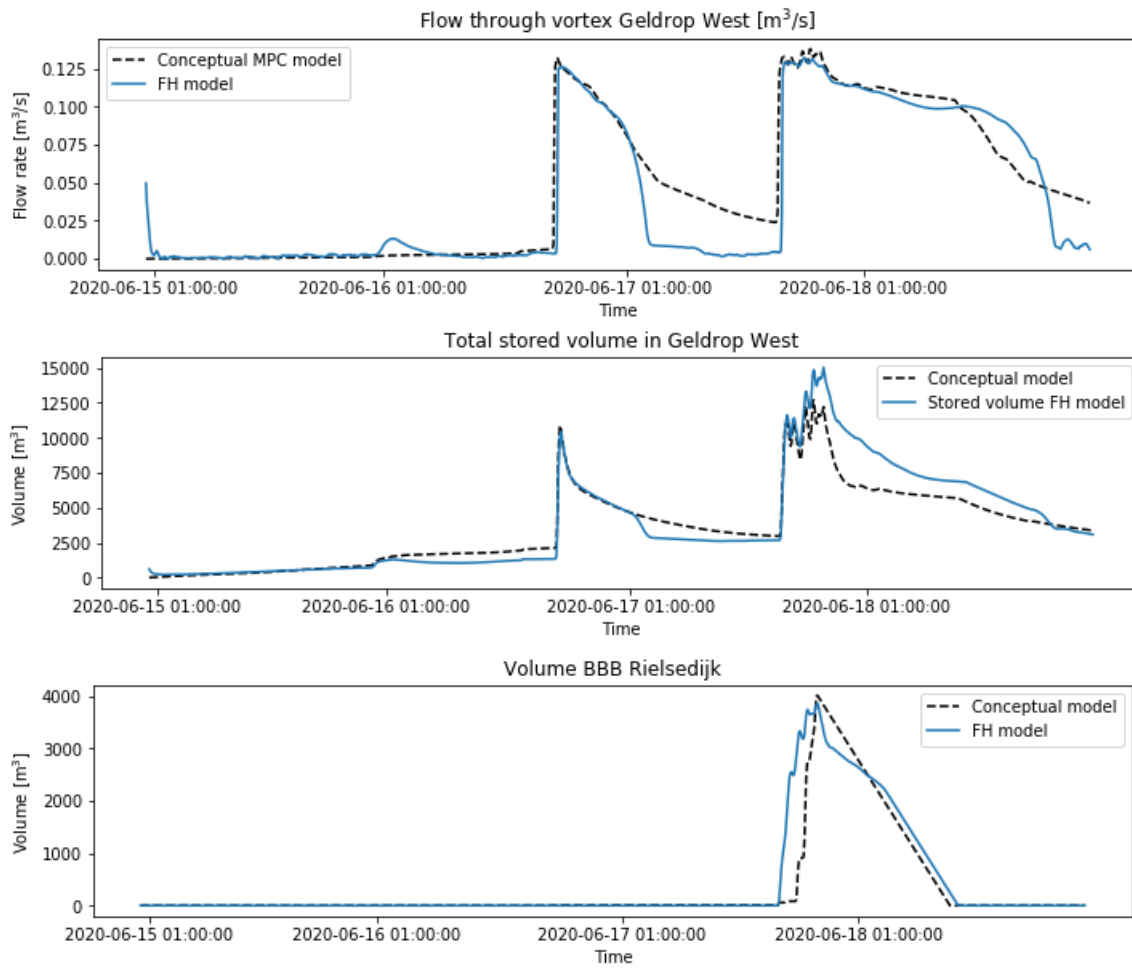
Event   **6**

Geldrop   **East**

Event   **6**

Mierlo

Volume Mierlo

Pump rate Mierlo

Event 7
Geldrop West

Head Geldrop West

Total stored volume in Geldrop West

Flow through vortex Geldrop West [m³/s]

Geldrop West total discharge through CSOs

Volume BBB Rielsedijk
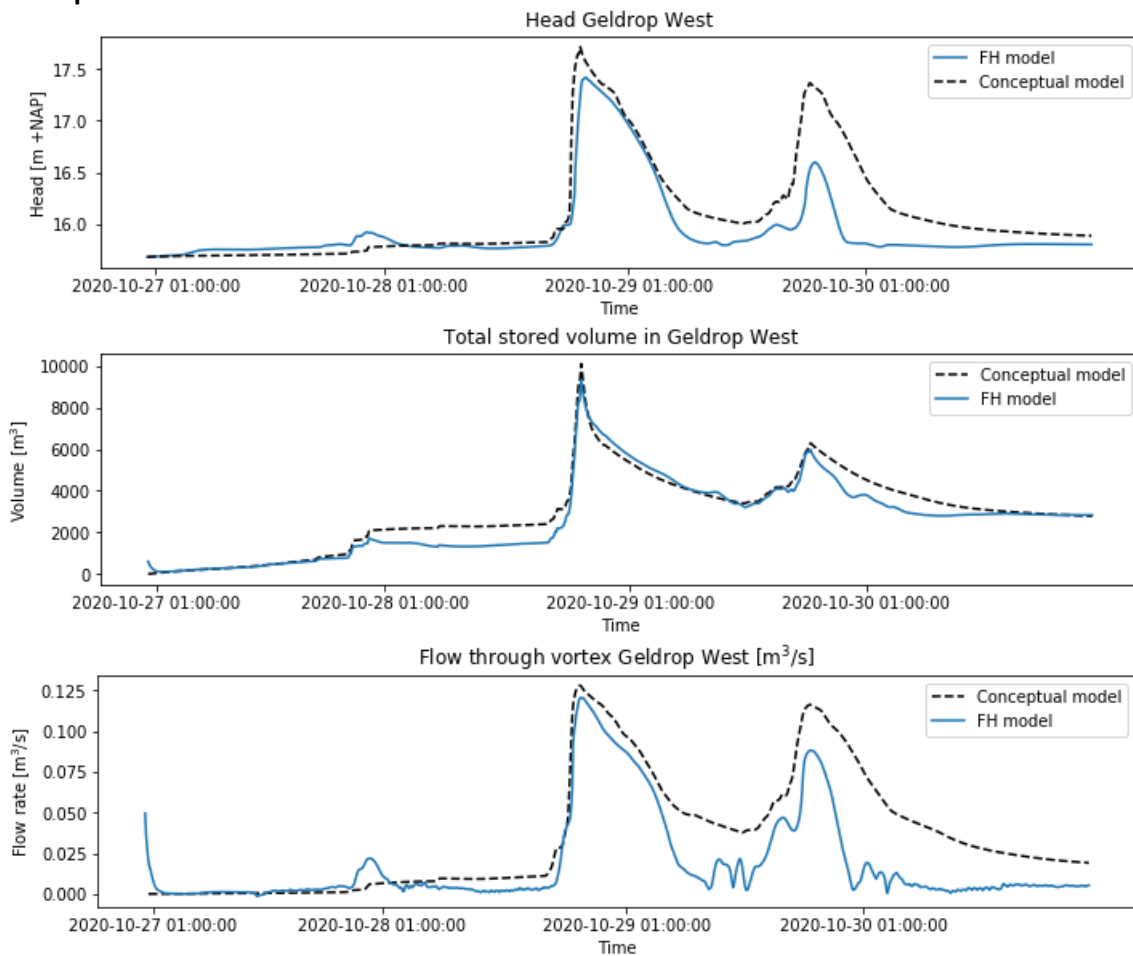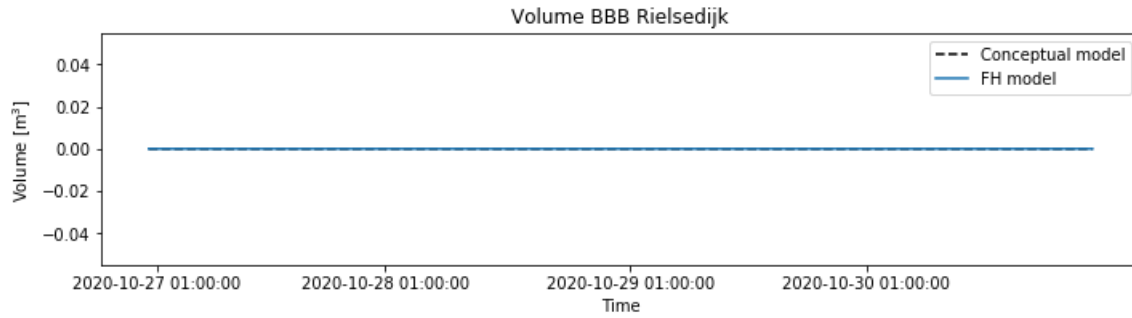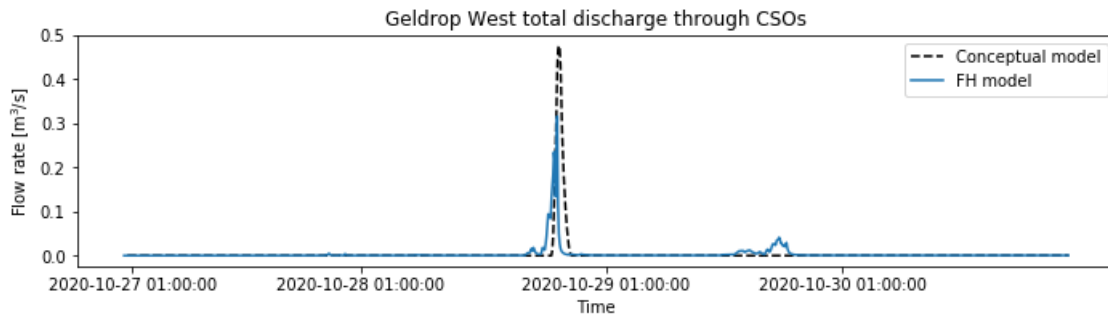
Evaluation validation Geldrop West	NSE value
Head	0.92
Total stored volume	0.3
Outflow	0.5
CSO discharge	-1
BBB stored volume	1

Geldrop   **East**

Head Geldrop East

Outflow Geldrop East
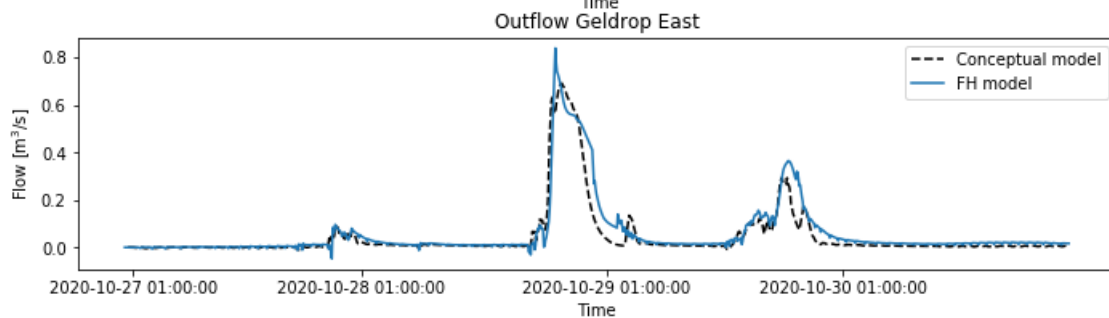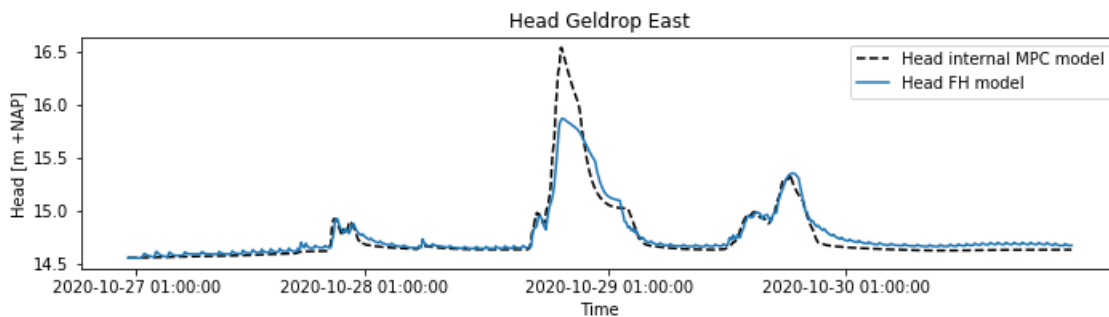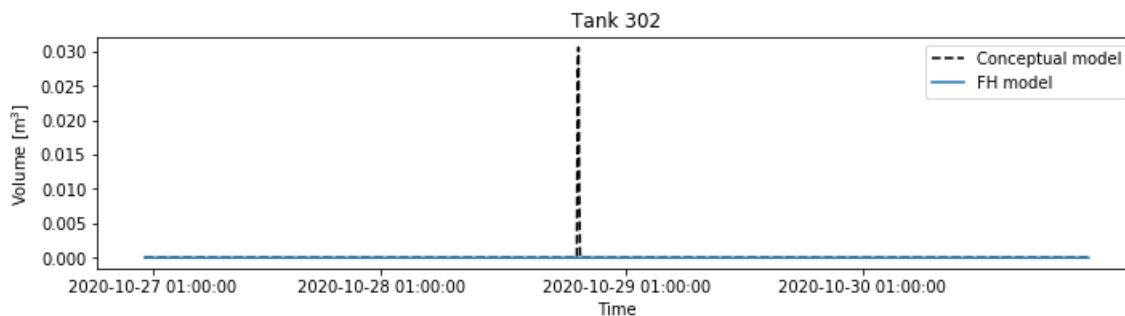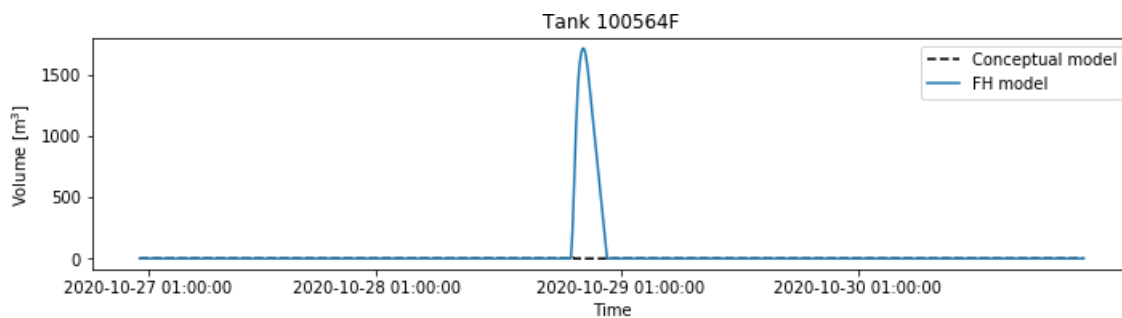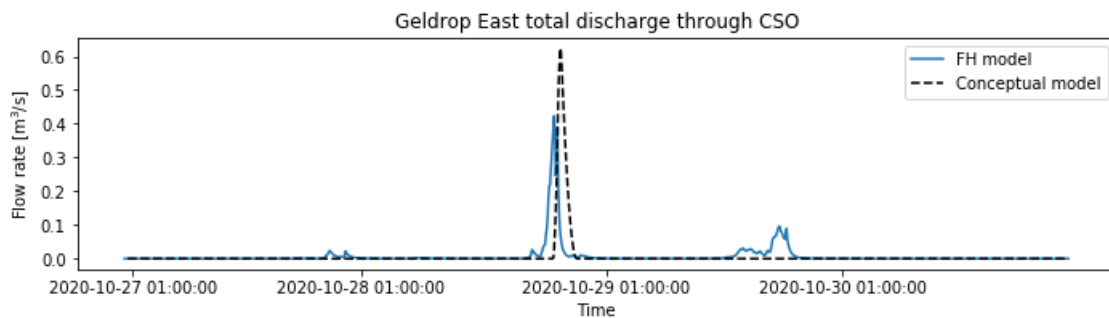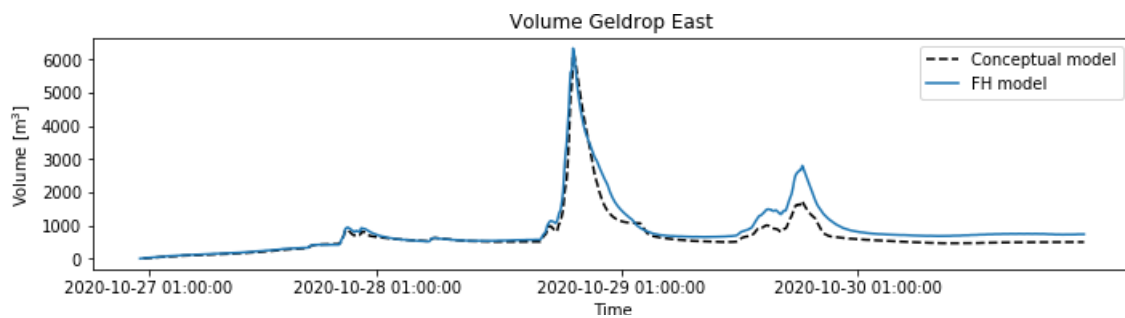
Evaluation validation Geldrop East	NSE value
Head	0.83
Total stored volume	0.87
Outflow	0.81
CSO discharge	-1
BBB stored volume	-0.03

Mierlo
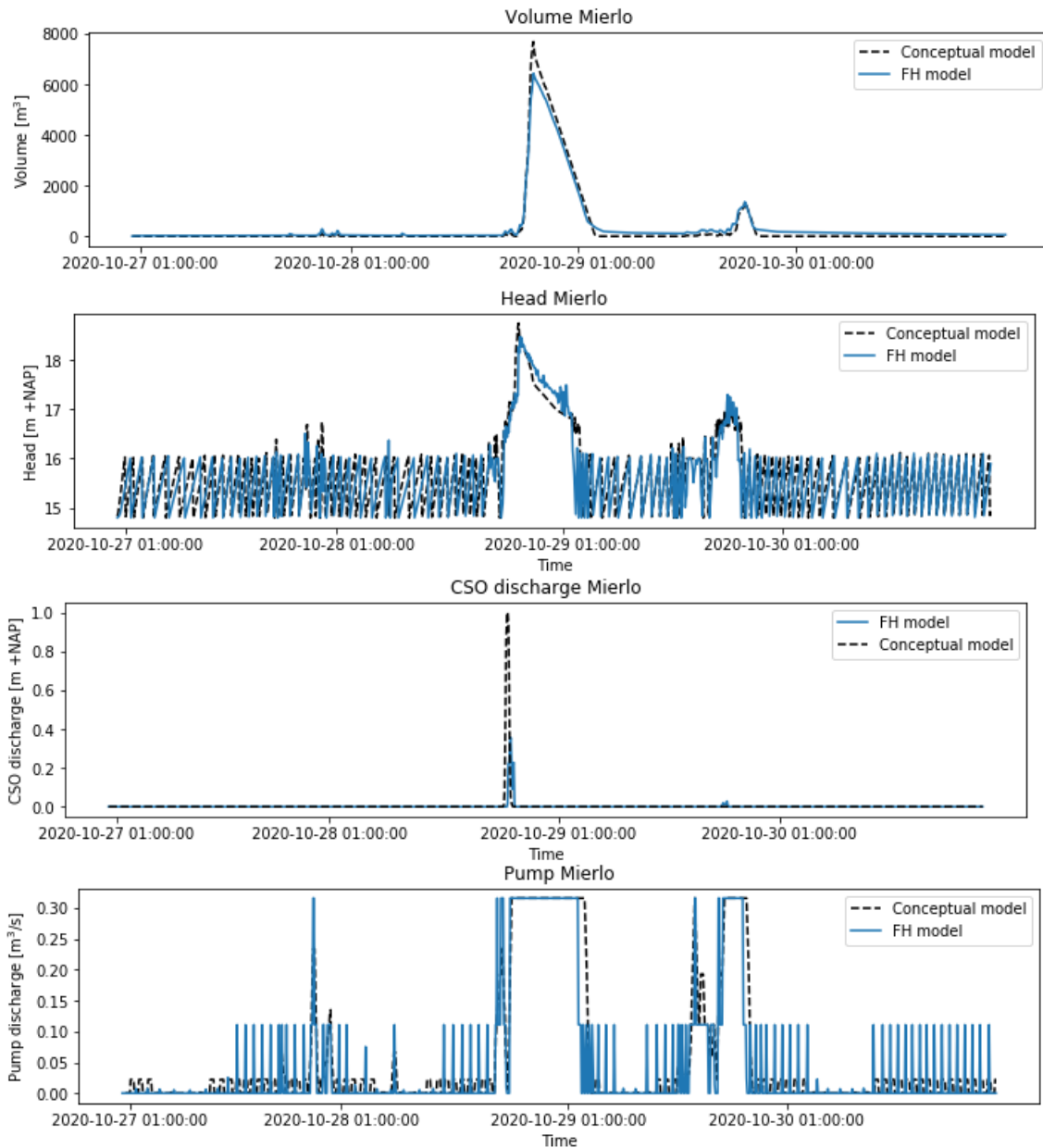
Evaluation validation Mierlo	NSE value
Head	0.8
Total stored volume	0.97
CSO discharge	-0.4
Pump discharge	0.8

Total stored volume in Geldrop West

Flow through vortex Geldrop West [m³/s]

Volume BBB Rielsedijk

Geldrop West total discharge through CSOs
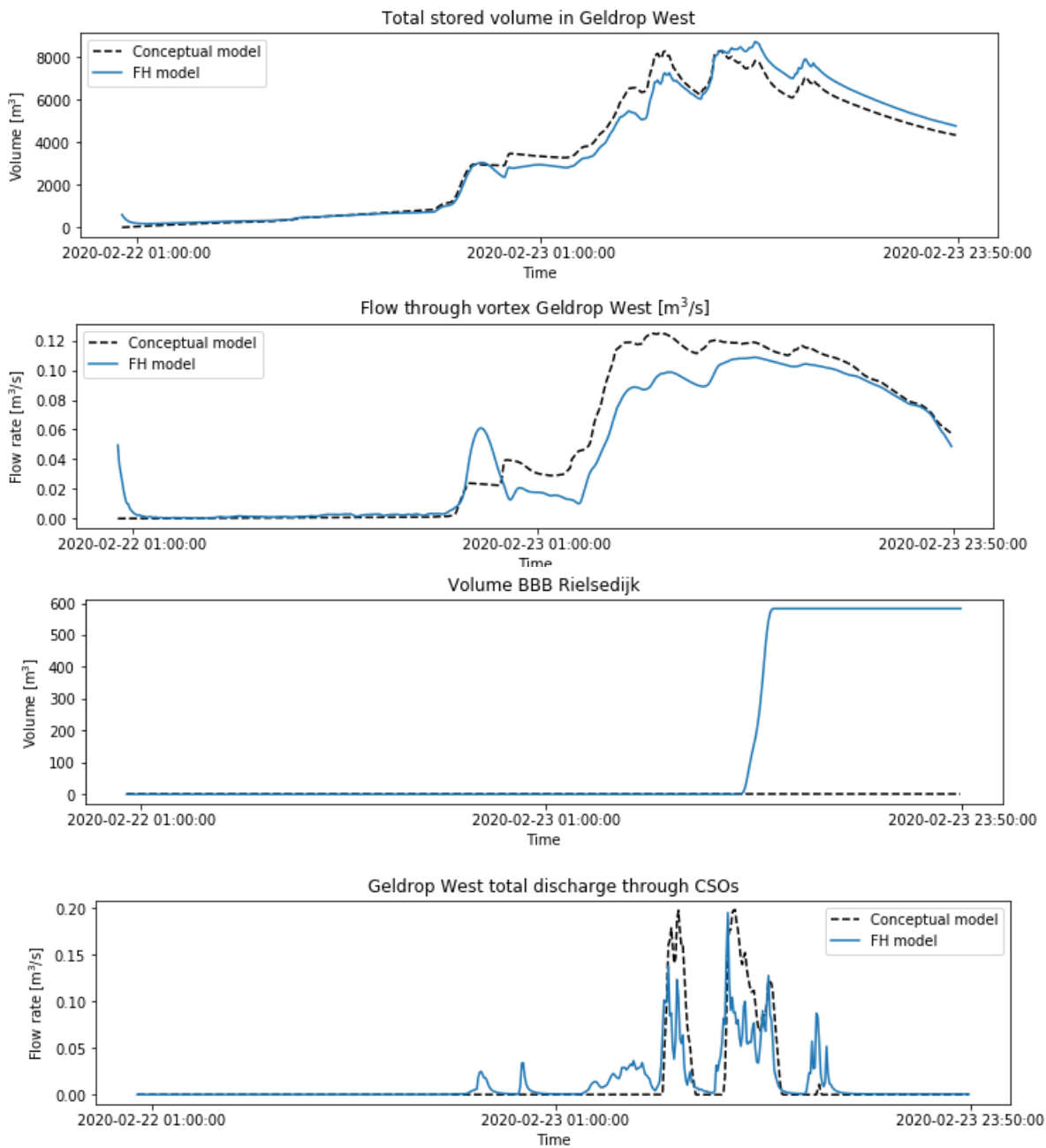
Evaluation validation Geldrop West	NSE value
Head	0.85
Total stored volume	0.97
Outflow	0.87
CSO discharge	0.1

Geldrop East

Head Geldrop East

Outflow Geldrop East

Volume Geldrop East

Tank 100564F

Tank 302

Geldrop East total discharge through CSO
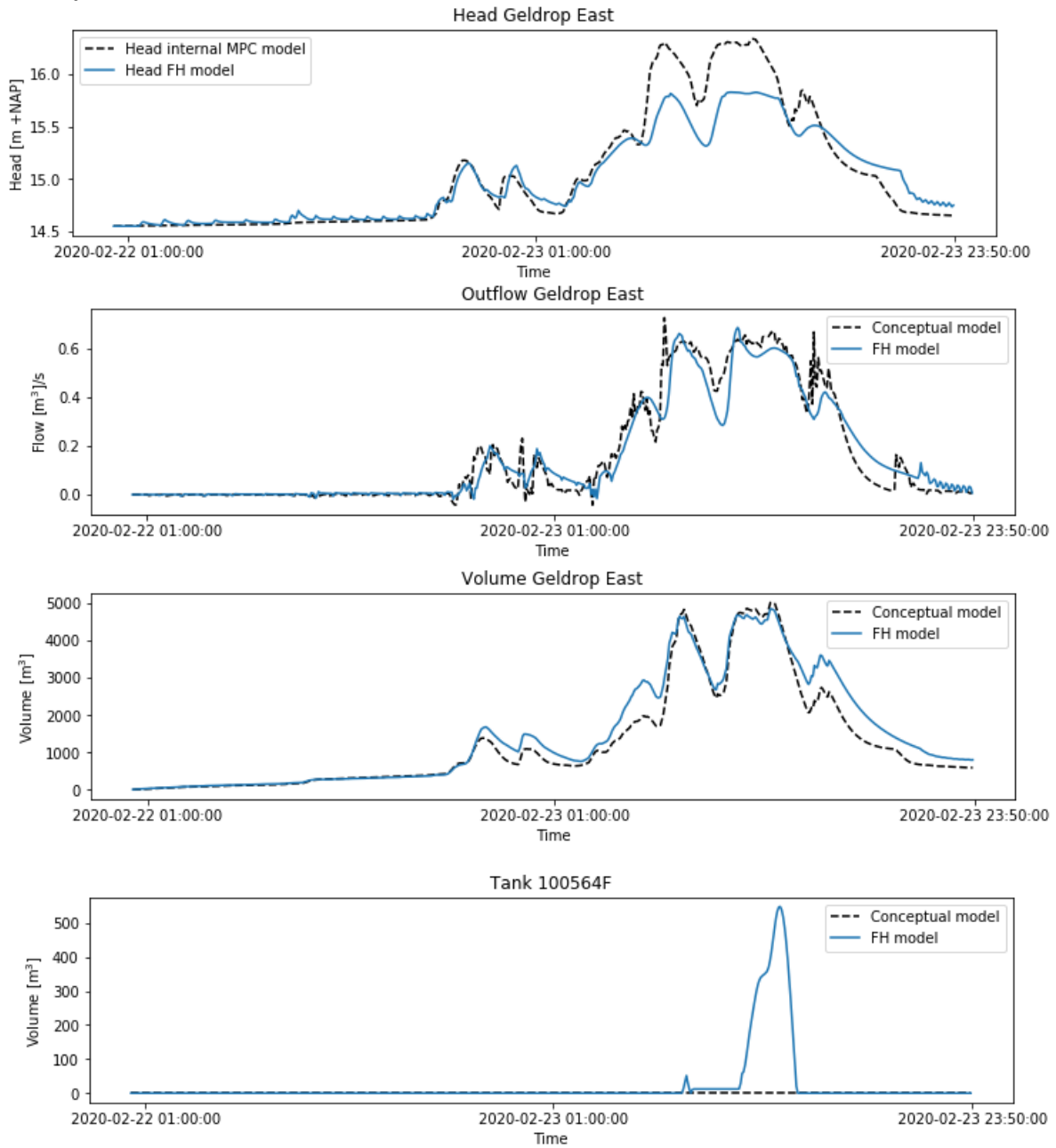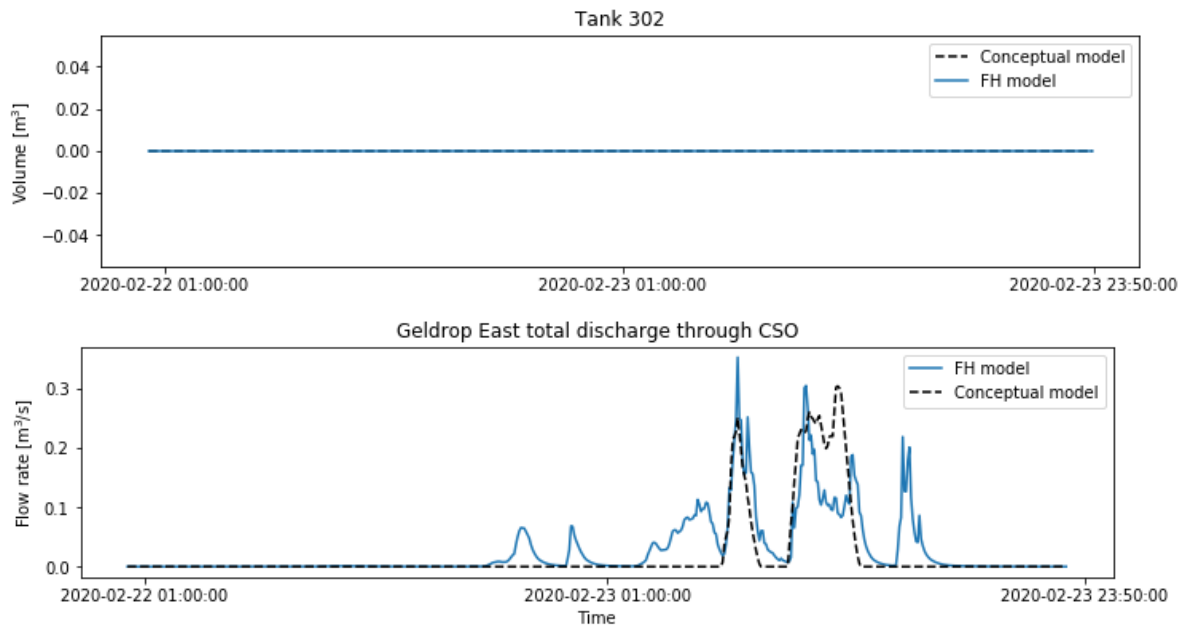
Evaluation validation Geldrop East	NSE value
Head	0.75
Total stored volume	0.96
Outflow	0.92
CSO discharge	0.35

Mierlo

Volume Mierlo

Head Mierlo

Pump discharge Mierlo

CSO discharge Mierlo
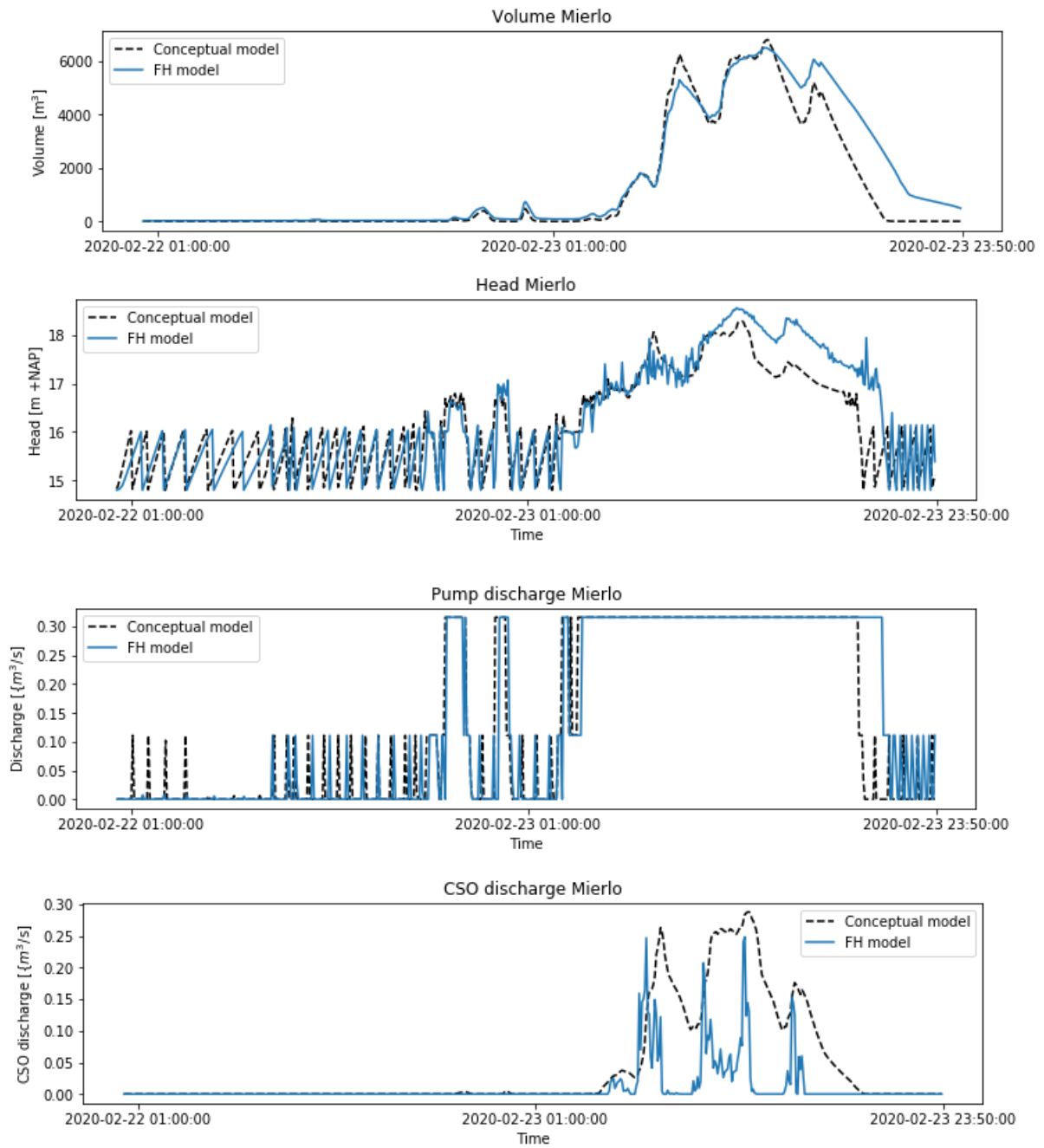
Evaluation validation Mierlo	NSE value
Head	0.78
Total stored volume	0.92
Outflow	0.83
CSO discharge	-7